A BACTERIAL SECRETED EFFECTOR PROTEIN DRIVES ABERRANT EUKARYOTIC MEMBRANE FUSION

by

NATHAN KYLE GLUECK

(Under the Direction of Vincent Starai)

ABSTRACT

Legionella pneumophila is a facultative intracellular bacterial pathogen, causing the severe form of pneumonia known as Legionnaires' disease. *Legionella* actively alters host organelle trafficking through the activities of 'effector' proteins secreted via a TypeIVB secretion system, in order to construct the bacteria-laden Legionella-containing vacuole (LCV) and prevent lysosomal degradation. The LCV is derived from membrane derived from host ER, secretory vesicles, and phagosomes, although the precise molecular mechanisms that drive its synthesis remain poorly understood. In characterizing the *in vivo* activity of the LegC7/YlfA SNARE-like effector protein from *Legionella* in the context of eukaryotic membrane trafficking in yeast, it was determined that LegC7 interacts with the Emp46p/Emp47p ER-to-Golgi glycoprotein cargo adapter complex, alters ER morphology, and induces aberrant ER:endosome fusion, as measured by visualization of ER cargo degradation, reconstitution of split-GFP proteins, and enhanced oxidation of the ER lumen. LegC7-dependent toxicity, disruption of ER morphology, and ER:endosome fusion events were dependent upon endosomal VPS class C tethering complexes and the endosomal t-SNARE, Pep12p.

This work establishes a model in which LegC7 functions to recruit host ER material to the bacterial phagosome during infection by inducing membrane fusion, potentially through interaction with host membrane tethering complexes and/or cargo adapters.

INDEX WORDS: *Legionella pneumophila*, LegC7, membrane trafficking, membrane fusion, *Saccharomyces cerevisiae*, SNARE, VPS class C tethering complex, Emp47p

A BACTERIAL SECRETED EFFECTOR PROTEIN DRIVES ABERRANT EUKARYOTIC MEMBRANE FUSION

by

NATHAN KYLE GLUECK

BS, Louisiana State University, 2013

BS, Louisiana State University, 2015

A Dissertation Submitted to the Graduate Faculty of The University of Georgia in Partial Fulfillment of the Requirements for the Degree

DOCTOR OF PHILOSOPHY

ATHENS, GEORGIA

2020

A BACTERIAL SECRETED EFFECTOR PROTEIN DRIVES ABERRANT EUKARYOTIC MEMBRANE FUSION

by

NATHAN KYLE GLUECK

Major Professor: Vincent Starai
Committee: Silvia Moreno
Michelle Momany
Zachary Lewis

Electronic Version Approved:

Ron Walcott
Dean of the Graduate School
The University of Georgia
December 2020

TABLE OF CONTENTS

LIST OF TABLES

Page

LIST OF FIGURES

Page

CHAPTER 1

INTRODUCTION

Legionella pneumophila is a Gram-negative aquatic bacterium that thrives intracellularly in protozoan hosts. The interest of researchers in *L. pneumophila* primarily stems from its ability to infect human alveolar macrophages, which can lead to the severe form of pneumonia termed Legionnaires' disease. In protozoa and macrophages, *L. pneumophila* secretes effector proteins into its host cell to change host cell biology in a manner that is conducive to the growth and survival of the bacterium. These effectors are critical for *L. pneumophila*'s intracellular survival and replication, and they have been the subject of intense study. Many of these secreted effectors modulate host membrane trafficking pathways such that the phagosome containing the bacterium acquires material from the host endoplasmic reticulum and avoids fusion with the host lysosome. This work focuses on the function of one such secreted effector, LegC7, during *L. pneumophila* infection.

Studying the functions of individual *L. pneumophila* secreted effectors is challenging. There are hundreds of effectors, there is a considerable amount of functional redundancy among them, and deletions of individual effectors most often do not produce readily observable phenotypes. An approach that has proven effective at avoiding these pitfalls is the heterologous expression of individual effectors in model organisms. This study utilizes heterologous expression of LegC7 in the model eukaryote *Saccharomyces cerevisiae* to gain insight into the function of LegC7 during *L.*

pneumophila infection, specifically its ability to alter canonical membrane trafficking pathways.

CHAPTER 2

LITERATURE REVIEW

LEGIONELLA TAXONOMY AND DISTRIBUTION

In 1976, the 58th annual convention of the American Legion was held in Philadelphia, PA. During the convention, there was an outbreak of an acute respiratory illness among attendees. Overall, 182 cases were identified, 29 of which were fatal. The root cause of the illness, termed Legionnaires' disease, was determined to be a bacterial lung infection, and the responsible bacterium was subsequently named *Legionella pneumophila*[1, 2].

Legionella are Gammaproteobacteria of the order Legionellales and family Legionellaceae. *Legionella* is the sole genus of the family Legionellaceae, and is most closely related to *Coxiella burnetii*, the intracellular parasite that causes Q fever[3, 4]. While *Legionella pneumophila* constitutes the overwhelming majority of clinical isolates, 60 species have been identified to date with over 20 associated with disease[3, 4]. *Legionella* spp. can be found in natural freshwater environments on every continent and can also colonize human-made aquatic structures[5-11]. *Legionella* spp. have also been isolated from marine environments, but freshwater environments serve as the main reservoir for the bacteria[12, 13]. *Legionella longbeachae* is an exception to this ecological niche in that it is primary found in soil[14, 15]. In natural environments, *Legionella* spp. parasitize or form commensal relationships with a wide variety of protozoa, predominately amoebae, which allows the bacteria to persist in harsh

environmental conditions[16-20]. *Legionella* are commonly associated with biofilms, which provide protection, nutrients, and access to protozoan hosts, and facilitate proliferation in warmer environments like human-made structures[21, 22].

LEGIONELLOSIS AND EPIDEMIOLOGY

Human infection by *Legionella*, or legionellosis, occurs when contaminated water droplets are inhaled into the lungs. Once in the lungs, *Legionella* can replicate within alveolar macrophages (see **Modulation of Host Cell Biology by *Legionella pneumophila***, page 15). This strategy for survival resembles *Legionella's* ability to replicate within single-celled, aquatic protozoa[23]. *Legionella* lung infections can cause either Legionnaires' disease, which presents as a severe case of pneumonia, or a milder illness called Pontiac fever involving fever and muscle aches[1, 24]. The mortality rate for Legionnaires' disease is ~1 in 10, with the highest rates of fatality occurring among individuals over 50 years old and individuals with weakened immune systems or pre-existing conditions such as emphysema or chronic obstructive pulmonary disease[25-27].

Legionella infections are often associated with improperly maintained water systems, particularly systems that tend to aerosolize water, such as heating and cooling systems for large buildings, plumbing, spa baths, and decorative fountains. In these systems, water temperature, flow conditions, lack of disinfection, scale, and corrosion are all contributing factors that can lead to bacterial growth and subsequent human infection. Hospitals harbor an exceptionally high risk of *Legionella* infection due to a combination of factors that include outdated or poorly managed water systems and large numbers of immunocompromised individuals[25, 26, 28-35]. It should be noted

that not all *Legionella* infections are associated with contaminated water. *Legionella longbeachae* is commonly associated with potting soil, and *L. longbeachae* infections generally result from the inhalation of dust particles carrying the bacterium[14, 15, 36, 37].

Legionella infections are viewed as dead-end infections, and indeed, only one report of probable human-to-human transmission has ever been reported[38]. The number of reported cases of legionellosis in the United States remained fairly consistent throughout the 1980's and 90's, but since 2000, the annual number of reported cases has steadily increased. Between 2000 and 2014, the number of reported cases rose from 0.42 per 100,000 persons to 1.62 per 100,000 persons[34, 39]. In 2018, nearly 10,000 cases were reported in the United States[40]. Furthermore, it is widely assumed that the reported number of *Legionella* infections doesn't accurately reflect the true number of clinical cases due to a lack of surveillance and the fact that symptoms of legionellosis aren't necessarily unique in comparison to those of other infections[39]. Due to the fact that the vast majority of reported cases of legionellosis are caused by *L. pneumophila*, it is the most studied *Legionella* species. While *L. pneumophila* and other virulent *Legionella* spp. presumably share many of the traits that make them infectious, the remainder of this literature review focuses exclusively on *L. pneumophila*.

THE HOST RANGE OF *LEGIONELLA PNEUMOPHILA*

Legionella pneumophila is capable of persisting in the environment in planktonic form and in sessile form by intercalating into existing biofilms to form synergistic relationships within the biofilm's complex microbial community[41-50]. The bacterium can even grow necrotrophically on dead cell masses within these biofilms[51]. However,

the overwhelming majority of *L. pneumophila* proliferation likely occurs within protozoan hosts that graze on these biofilms[23]. This strategy is particularly successful due to the vast range of hosts that support the intracellular multiplication of *L. pneumophila*. In some cases, protozoan hosts are restrictive of *L. pneumophila* intracellular growth but permissive to survival, which can still provide protection by insulating the bacterium against otherwise harmful environmental conditions, such as water disinfection methods or predation[19, 45, 52-64].

Since *L. pneumophila* was first discovered to be a pathogen of freshwater and soil amoebae[23], numerous co-culture studies have confirmed the capability of the bacterium to survive and/or multiply intracellularly in a litany of protozoan genera that spans three separate phyla[16, 52, 55-57, 59-62, 65-95]. With only two exceptions—*Balamuthia* and *Dictyostelium*—these protozoan genera have also been detected in *L. pneumophila*-containing samples taken from natural and human-made water systems and compost facilities, supporting the notion that they may be natural hosts for *L. pneumophila* in these systems[61, 64, 67, 73, 80, 88, 96-116]. Four protozoan species—*Acanthamoeba palestinensis*, *Naegleria lovaniensis*, *Vermamoeba vermiformis* (formally *Hartmannella vermiformis*), and *Acanthamoeba jacobsi*—have been isolated still harboring *L. pneumophila*, providing direct evidence of *L. pneumophila*'s diverse natural host range[80, 100].

While many elements of *L. pneumophila* infection remain consistent across hosts, the bacterium displays marked versatility in its pathogenesis, as evidenced by diverse "-omics" studies and observation of its pleomorphic nature[92, 117-124]. This versatility exacerbates the challenge of understanding *L. pneumophila* pathogenesis in

humans and highlights the need for caution when studying *L. pneumophila* in various mammalian tissue culture models.

MORPHOLOGICAL DIFFERENTIATION OF *LEGIONELLA PNEUMOPHILA*

Researchers began describing the exceptional pleomorphism of *L. pneumophila* shortly after its initial discovery as the Legionnaire's disease bacterium[125, 126]. To date, over a dozen distinct morphologies have been reported, but most of them tend to be intermediates on a spectrum that varies depending on whether *L. pneumophila* is growing intracellularly and depending on the host in which the bacterium is being studied. The exception to this is the relatively rare but pathologically relevant filamentous form[52, 68, 119, 126-133]. Generally, *L. pneumophila* oscillates between two phenotypes in response to its surroundings—an avirulent, replicative form and a virulent, non-replicative form. This biphasic nature is a hallmark of intracellular pathogens, because they must proliferate within hosts and then survive in a harsher extracellular environment after egress, prior to infecting a new host[134-136]. In 1998, Byrne and Swanson showed that *L. pneumophila* growing exponentially in broth culture does not maintain traits associated with virulence, but after transition to stationary phase as a result of amino acid depletion in the medium, the bacterium becomes sodium sensitive, cytotoxic, osmotically resistant, competent to evade macrophage lysosomes, infectious, and motile[128]. Since this discovery, the underlying mechanisms governing differentiation between *L. pneumophila*'s replicative and transmissive forms have been extensively studied. While *L. pneumophila* grown without a host is morphologically distinct when compared to intracellularly grown *L. pneumophila*, which also varies morphologically depending on the host organism,

findings reported on the topic of *L. pneumophila* differentiation have largely been validated across several growth media, including host-free culture, various mammalian and protozoan cell lines, mammalian model organisms, and natural environmental and lung tissue samples. This section describes the widely validated understanding of differentiation between the morphologically distinct replicative and transmissive forms of *L. pneumophila* but also briefly discusses the lesser understood filamentous form.

The Stringent Response

Central to the differentiation of *L. pneumophila* between the replicative and transmissive phenotypes is the stringent response (**Figure 2.1**). In bacteria, generally, the stringent response is induced in response to environmental conditions not conducive for replication. *L. pneumophila* in particular couples differentiation from its replicative form to its transmissive form with its stringent response[137, 138]. This ensures that the bacterium, upon exhaustion of its current host's nutrients, is equipped to escape, survive extracellularly, and infect a new host.

For bacteria, generally, the intracellular concentration of the alarmone (p)ppGpp (hereafter referred to as ppGpp) dictates the induction or repression of the stringent response. ppGpp synthetase RelA and ppGpp synthetase/hydrolase SpoT control ppGpp levels within the cell. RelA binds to ribosomes and synthesizes ppGpp in response to uncharged tRNAs, effectively increasing the ppGpp concentration in response to amino acid depletion. SpoT is bifunctional, hydrolyzing ppGpp during exponential growth and synthesizing ppGpp in response to a number of stresses including carbon, phosphate, iron, and fatty acid deprivation[139]. In *L. pneumophila*,

SpoT is required for differentiation from replicative to transmissive forms, and *spoT* mutants cannot survive entry into or exit from macrophages[140].

While elevated levels of ppGpp have been shown to modulate many cellular processes in various bacterial species, the classic and defining feature in all bacteria is manipulation of the transcription profile. At elevated concentrations, ppGpp directly interacts with RNA polymerase (RNAP) in concert with the DnaK suppressor, DksA, altering RNAP's affinity for certain promotors either positively or negatively, depending on the intrinsic properties of the promotors[139, 141]. This not only directly affects the transcription of operons under control of said promotors but also indirectly affects transcription through σ-factor competition[142]. During exponential growth, the vegetative σ-factor σ^{70} directs RNAP to operons essential for the synthesis of DNA, proteins, and lipids. However, elevated levels of ppGpp inhibit σ^{70}-associated RNAP binding to σ^{70} promotors, which allows other σ-factors that accumulate during the

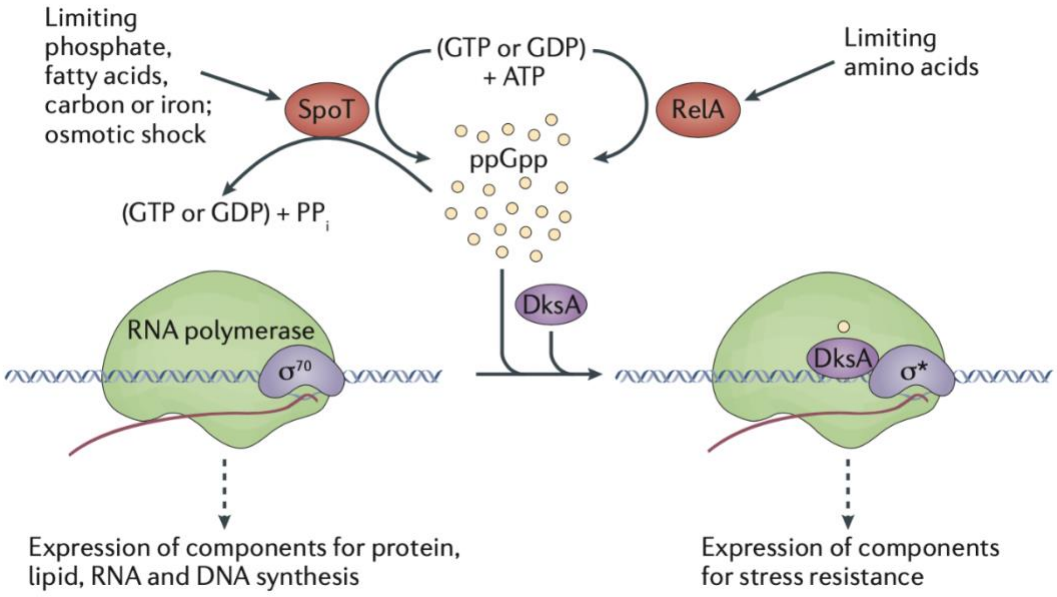

Figure 2.1. The bacterial stringent response. [143]

stringent response to compete for core RNAP[144]. Furthermore, ppGpp has been shown to inhibit the degradation or increase the activity of alternative σ-factors as well[145, 146].

In *L. pneumophila*, RpoS, FliA, and RpoN are all RNAP σ-factors that regulate the differentiation associated with elevated levels of ppGpp and the stringent response[138, 147-153]. During differentiation, RpoS promotes sodium sensitivity, evasion of the host cell lysosome, and motility, the latter of which is accomplished in part by the induced expression of FliA, the flagellar sigma factor. FliA also contributes to lysosome evasion, contact-mediated cytotoxicity, infectivity, and even biofilm formation[44, 147-149, 154]. RpoN (σ^{54}) and the transcription factor FleQ promote transcription of motility-related genes[151-153].

The LetA-RsmYZ-CsrA Regulatory Cascade

The LetAS-RsmYZ-CsrA regulatory cascade (**Figure 2.2**) is a central mechanism by which differentiation is initiated as a result of the stringent response in *L. pneumophila*. The stringent response activates the Legionella transmission activator—Legionella transmission sensor (LetA-LetS) phosphorelay system, which autophosphorylates the tripartite sensor kinase (LetS) and shuttles the phosphoryl group to the cognate response regulator (LetA).

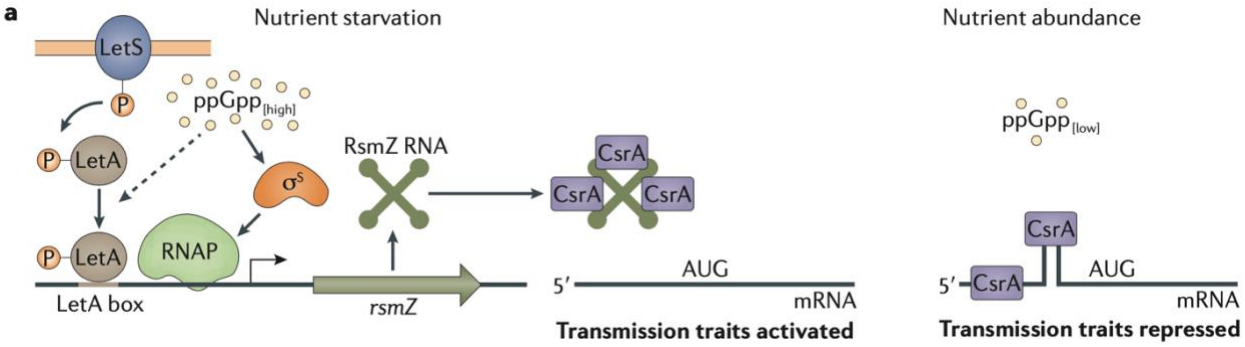

Figure 2.2. The LetA-RsmYZ-CsrA regulatory cascade. [143]

Once activated, LetA binds DNA upstream of *rsmY* and *rsmZ*, strongly promoting the expression of these two non-coding RNAs. Once transcribed, RsmY and RsmZ bind the global translation repressor CsrA, thereby relieving repression of genes associated with the transmissive form of the bacterium[149, 155-159]. Among the genes upregulated by this cascade are dozens of genes encoding substrates for the Type IVB Dot/Icm secretion system (see **The Dot/Icm Secretion System**, page 15), one of which is central to this thesis—*lpg2298*/*ylfA*/*legC7* (see **LegC7**, page 35)[157, 160]. Genetic studies have also shown that two other two-component regulator systems, PmrAB and CpxRA, also upregulate transmissive form genes, Dot/Icm substrates included, in *L. pneumophila* post-exponential growth[161-164].

Stringent response σ-factor RpoS and the LetAS-RsmYZ-CsrA regulatory cascade also regulate the *Legionella* quorum sensing (Lqs) system, which in turn helps to control the expression of transmissive form genes. In particular, RpoS directs RNAP to express the Lqs response regulator *lqsR*, and RsmYZ sequestration of CsrA relieves the repression of *lsqR*, whose gene product further contributes to replicative-to-transmissive differentiation[158, 165, 166]. Furthermore, treatment of *L. pneumophila* with synthetically produced Lqs signaling molecule LAI-1 (*Legionella* autoinducer-1) downregulates *csrA*, upregulates *rsmYZ*, and upregulates *lqsR*. This demonstrates that host nutrient exhaustion and *L. pneumophila* cell density compound to drive replicative-to-transmissive form differentiation[167, 168]. Other gene products implicated as regulators of *L. pneumophila* differentiation include the transcription and recombination regulator IHF (integration host factor), disulfide bond oxidoreductase/isomerase DsbA, and a host of proteins containing GGDEF and EAL motifs known to modulate

intracellular levels of secondary messenger di-GMP[123, 169-172]. The plethora of regulatory systems and the morphological fluidity as a result of differential expression of a substantial portion of the genome in response to environmental conditions and host identity demonstrate *L. pneumophila*'s exceptionally robust and adaptive strategy for survival through differentiation.

Filamentous Morphology

In contrast to the body of knowledge describing replicative and transmissive forms of *L. pneumophila* and how they fit into the bacterium's life cycle, the current understanding of its filamentous form remains quite limited. This is in spite of the fact that filamentous *L. pneumophila* can be found in environmental water samples as well as lung tissue and bronchial lavages taken from individuals with Legionnaire's disease[126, 173]. In fact, the first image of *L. pneumophila* ever published included the filamentous form[125].

Through various studies, filamentation has been linked to nutrient limitation, antibiotics, high temperature, and UV radiation, though the mechanisms by which filamentation is induced and carried out are poorly understood[131, 174-177]. Genetic studies suggest that CsrA, chaperonin HtpB, and putative spermidine transporter PotD are involved[178-180]. Filamentous *L. pneumophila* is capable of infecting lung epithelial cells and macrophages, though there is no evidence to suggest that filamentation confers increased virulence or fitness in the context of infection[173, 181]. Fragmentation of filamentous *L. pneumophila* into replicative form cells has been reported during both intracellular and extracellular growth, but the underlying mechanism is unknown[131, 181].

The benefits of filamentation in the environment or during infection are also unclear, though several possibilities have been suggested. These include improved biofilm formation and persistence within biofilms, improved defense against predation by protozoans, and even establishment of reservoirs within alveolar epithelial cells during infection, though there is limited evidence, if any, for these possibilities[68, 118, 131]. To conclude, the filamentation of *L. pneumophila* occurs in the environment and during lung infections, but more work needs to be done to elucidate the factors driving filamentation, the mechanisms governing it, and the benefits that filamentation provides for the bacterium.

HOST CELL ENTRY BY *LEGIONELLA PNEUMOPHILA*

L. pneumophila's amoeboid hosts rely on phagocytosis for food, and macrophages phagocytize microbes and cellular debris as part of the immune system. During conventional phagocytosis, receptors on the phagocytizing cell bind to surface molecules on the cell or object to be engulfed, and this binding continues outward from the initial point of contact as if the phagocytizing cell's membrane and the boundary of the phagocytized object are zippering together. As can often be observed during phagocytosis, actin-rich projections called pseudopods protrude out from the phagocytizing cell to contact and/or surround the phagocytosed object. Other mechanisms for internalization of extracellular content have been broadly referred to as pinocytosis but vary considerably and are employed to varying degrees based on cell identity. These mechanisms include (i) receptor-mediated endocytosis, for which there are several reported receptors and mechanisms of internalization, (ii) micropinocytosis, in which actin-rich pseudopods protrude from and then fuse to the plasma membrane,

engulfing extracellular fluid in a receptor-independent manner, and (iii) constitutive internalization of small vesicles of extracellular fluid, which is receptor- and actin-independent and is most commonly referred to simply as pinocytosis. [182, 183]

The phagocytosis of *L. pneumophila* by human phagocytes was originally described as proceeding through a novel mechanism termed coiling phagocytosis, whereby a pseudopod from a phagocyte (including human monocytes, polymorphonuclear leukocytes, and alveolar macrophages) contacts the bacterium, rolls the bacterium into a coil made by extension of the pseudopod, and pulls the bacterium into the cell[184]. This finding has since been validated and observed in protozoan hosts, but other forms of phagocytosis have been reported as well, including micropinocytosis and the classical zipper-like mechanism, indicating that *L. pneumophila* may gain entry into host cells through multiple mechanisms determined by any number of factors, such as host identity or bacterial morphology[65, 185-188].

Both the existence of an unusual (if not novel) mechanism of internalization and the ability of *L. pneumophila* to gain entry into nonprofessional phagocytes such as A549, CHO-K1, and HeLa epithelial cells provide evidence that entry into the host cell is a virulence-directed process rather than strictly host-mediated[129, 189-191]. In fact, it is unclear whether opsonin-dependent phagocytosis is relevant in the context of a lung infection. Human phagocytes routinely rely on cell surface receptor-binding to opsonin molecules such as antibodies and complement proteins that coat objects intended for phagocytosis. However, this mechanism for facilitating phagocytosis shouldn’t be assumed in the context of *L. pneumophila* infection, as (i) complement levels in the lungs are quite low, (ii) *L. pneumophila* is capable of infecting phagocytes in the

absence of serum, and (iii) blocking complement receptors does not affect *L. pneumophila*'s ability to gain entry into macrophages[192-195]. Furthermore, while phosphoinositide 3-kinases (PI3Ks; discussed in more detail in **Phosphoinositide Modification and Utilization** on page 18) are important for conventional phagocytosis, multiple studies have reported that PI3Ks are dispensable for the uptake of *L. pneumophila* by macrophages and model amoeba *Dictyostelium discoideum*[196, 197]. Nonetheless, one study indicated that *L. pneumophila* infection of macrophages stimulated the production of phosphatidylinositol 3-phosphate (presumably through the action of PI3Ks) and that the inhibition of macrophages' PI3Ks reduced the bacterium's ability to gain entry in a dose-dependent manner[198].

To conclude, our understanding of the mechanism by which *L. pneumophila* enters its host is relatively limited compared to our understanding of other areas of *L. pneumophila* pathogenesis. Regardless of how the bacterium gains entry, once inside the host cell, the compartment in which the bacterium resides undergoes a remodeling process that results in a unique compartment well conserved across its wide range of hosts[199]. This compartment has been termed the *Legionella*-containing vacuole (LCV), and the following sections discuss the tools and strategies employed by *L. pneumophila* to maintain this intracellular replicative niche.

MODULATION OF HOST CELL BIOLOGY BY *LEGIONELLA PNEUMOPHILA*

The Dot/Icm Secretion System

Within 5 minutes of internalization, *L. pneumophila* begins to subvert host cell function to avoid degradation and establish the compartment suitable and necessary for successful replication—the LCV (**Figure 2.3**)[200]. This is largely

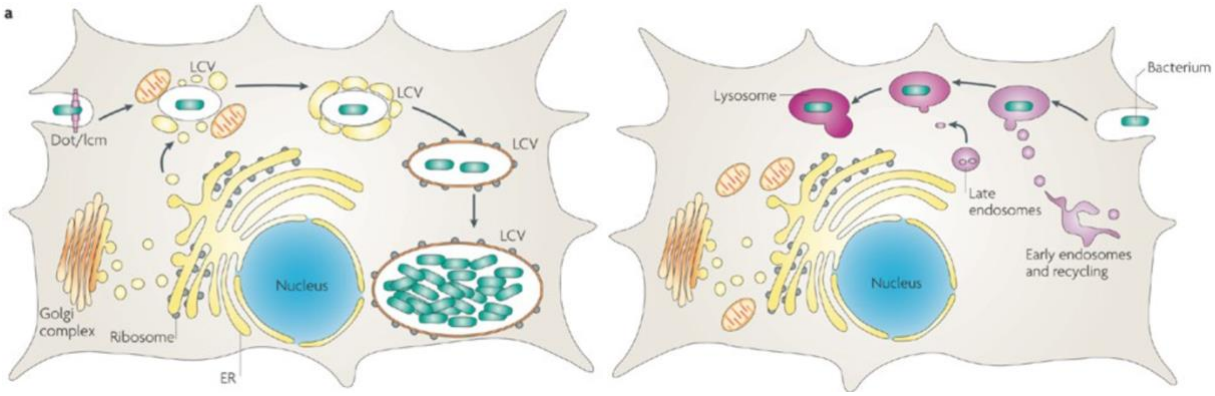

Figure 2.3. The intracellular fate of *Legionella pneumophila* in a mammalian macrophage (left) compared to that of an avirulent bacterium (right). [201]

accomplished through the activity of *L. pneumophila* effector proteins secreted through its type IVb Dot/Icm (Defective in organelle trafficking/Intracellular multiplication) secretion system (see **Table 2.1** for list of secreted substrates), the primary weapon system utilized to evade host defenses and multiply during infection[202]. Moreover, intimate contact between bacterium and host cell is essential for large-scale secretion of Dot/Icm substrates[203]. The Dot/Icm split nomenclature results from two separate, contemporaneous studies, which discovered regions of the *L. pneumophila* genome that were required for intracellular multiplication. In one case, a single genetic locus, designated *icm*, was able to complement an avirulent mutant defective in intracellular multiplication[204, 205]. This locus contained four putative genes – *icmWXYZ*. Another study designed to isolate mutants defective in intracellular multiplication discovered a single genetic locus containing one open reading frame designated *dotA*, which was essential for intracellular growth, organelle recruitment, and inhibition of phagosome—lysosome fusion[206, 207]. Since these initial discoveries, ~23 other *dot*/*icm* genes have been identified[208-214]. Most *L. pneumophila dot*/*icm* genes share sequence

homology with bacterial conjugative DNA transfer systems, most notably with the IncI plasmid conjugation systems of *Shigella flexneri* and *Salmonella enterica*[215]. While the Dot/Icm secretion system is ancestrally related to DNA conjugation systems and maintains the ability to transfer certain plasmids from one cell to another[216], its primary function is protein secretion during intracellular pathogenesis, secreting more than 300 proteins into the host cell. The secretion system localizes to the poles of the bacterial cell and consists of a hollow stalk that spans inner and outer membranes, forming a widened periplasmic “secretion chamber” that tapers towards each membrane[217, 218]. The exact mechanism of translocation of Dot/Icm substrates across the LCV membrane into the host cell has not been resolved. However, evidence suggests that IcmQ may permeabilize the membrane, with IcmR exerting regulatory function on IcmQ and cytoplasmic chaperones including IcmS and IcmW facilitating translocation of effector proteins into the host[219-221].

As mentioned in **Morphological Differentiation of *Legionella pneumophila*** on page 17, many Dot/Icm substrates are upregulated during *L. pneumophila*’s transition to its transmissive morphology, ensuring that they can be secreted into the host cell immediately upon internalization[157]. LCV biogenesis has been widely studied, revealing a remarkably robust process—a common theme in genetic studies of *L. pneumophila* is the bacterium’s ability to replicate within host cells despite deletions of genes encoding Dot/Icm-secreted effector proteins with demonstrable roles in LCV biogenesis[117, 222]. Host membrane dynamics are modulated in a variety of interconnected ways, including phosphoinositide modification, GTPase manipulation, recruitment of membrane tethering complexes and SNAREs (soluble *N*-ethylmaleimide-

sensitive attachment protein receptors), and exploitation of ubiquitin. Such membrane modulation results in a unique compartment that not only is tightly associated and probably fused with host rough ER but also displays traits of other organelles such as endosomes and Golgi[199, 223]. This modulation of host membrane dynamics by Dot/Icm effectors is discussed in further detail in following sections.

Phosphoinositide Modification and Utilization

The LCV acquires a distinct phosphoinositide profile to (i) facilitate recruitment of desirable host and bacterial machinery and (ii) avoid the endosomal maturation that is typical of phagosomes with contents meant for lysosomal degradation[188, 197]. Phosphoinositides are lipids derived from phosphatidylinositol, or PtdIns, which consists of two fatty acid chains attached to the first and second carbons of a glycerol backbone that is connected via a phosphodiester bond to an inositol ring[224]. These phospholipids comprise 10-20% of the phospholipids that make up eukaryotic organellar and plasma membranes[225, 226], and they are critically important for ensuring proper membrane trafficking and organelle maintenance in the cell. The inositol ring of PtdIns can be phosphorylated or dephosphorylated at the 3', 4', and 5' positions by PtdIns kinases or phosphatases (further abbreviated as PI kinases and PI phosphatases), respectively, and different phosphorylation patterns of this inositol ring confer differential affinities for interacting with membrane-binding proteins. Thus, organelle-specific PI kinases and PI phosphatases can modify local membrane PtdIns to affect the function of residential membrane molecules such as ion channels or transporters, induce activity of proximal cytosolic proteins, and recruit subgroups of proteins[224].

Researchers have used fluorescent markers that preferentially bind specific phosphoinositides to better understand phosphoinositide dynamics during *L. pneumophila* infection. At the site of *L. pneumophila* entry into the model protozoan host *D. discoideum*, PtdIns 3,4,5-triphosphate, or PI(3,4,5)P_3, transiently accumulates on the invagination containing the bacterium, but dissipates once the bacterium has been completely internalized. This is due to PI(3,4,5)P dephosphorylation at the 4' and 5' positions as demonstrated by the simultaneous accumulation of PI(3)P and the slightly longer persistence of PI(3,4)P_2 on the nascent LCV compared to PI(3,4,5)P_3. Approximately 30 minutes post-infection, PI(4)P begins to accumulate on the LCV and remains until egress, while the PI(3)P that has accumulated on the LCV starts to dissipate, with only 20% of LCVs remaining PI(3)P-positive 2 hours post-infection[188, 199]. The loss of PI(3)P from the LCV is likely important for evasion of lysosomal degradation, as PI(3)P accumulates on endosomes as they mature and plays an essential role in the maturation process[227-232]. Conversely, PI(4)P is primarily found on the Golgi, secretory vesicles, ER exit sites, and the plasma membrane in non-infected cells[224, 233, 234]. Given PI(4)P localization and the critical roles phosphoinositides play in non-infected cells, it isn't difficult to imagine the potential benefits of maintaining high PI(4)P levels on the LCV, and specific examples are discussed below. Notably, while the accumulation and immediate, successive loss of PI(3,4,5)P_3 at the site of entry is also observed for an avirulent, Dot/Icm-deficient *L. pneumophila* mutant, the Dot/Icm-deficient mutant does not accumulate PI(4)P on the LCV, but rather accumulates PI(3)P and undergoes eventual lysosomal degradation[188].

Several *L. pneumophila* Dot/Icm substrates have been shown to have phosphoinositide kinase/phosphatase activity or rely on phosphoinositides for membrane anchoring or activation. Effectors SidP and SidF both demonstrate PI 3-phosphatase activity. SidP converts PI(3,5)P to PI(5)P and PI(3)P to PtdIns in vitro and restores growth in a PI 3-deficient yeast strain[235], while SidF converts PI(3,4)P to PI(4)P in vitro and a Δ*sidF* mutant accumulates less SidC, a PI(4)P-binding effector, on the LCV[222]. LepB, a Rab1 GTPase-accelerating protein (discussed below), also has PI 4-kinase activity, converting PI(3)P to PI(3,4)P. A study of LepB revealed no significant difference in the reduction in SidC-positive LCVs among Δ*lepB*, Δ*sidF*, and Δ*lepB*/Δ*sidF* mutants, suggesting that LepB and SidF work in concert to convert PI(3)P to PI(4)P[236]. These Dot/Icm effectors with PI kinase/phosphatase activity likely comprise a small fraction of effectors with PI kinase/phosphatase activity—over 400 hypothetical proteins in the *L. pneumophila* genome have the CX_5R signature sequence of catalytic residues of PI phosphatases, 29 of which are confirmed Dot/Icm substrates[222, 237, 238].

Other Dot/Icm substrates utilize phosphoinositide-binding domains to exert their activity in areas enriched with specific phosphoinositides. Such phosphoinositide-binding domains are abundant in eukaryotes, and their presence in *L. pneumophila* effectors is one of many examples of Dot/Icm substrates having protein structures and functions that are common in eukaryotes but rare if not absent in prokaryotes. As mentioned previously, SidC binds specifically to PI(4)P in the LCV membrane, as does its paralog SdcA, allowing both to mediate recruitment of host ER to the LCV[197, 239, 240]. SidM/DrrA is a guanine nucleotide exchange factor (GEF, discussed in further

detail below) that specifically binds to PI(4)P with a remarkably high affinity[241-244]. LidA binds to both PI(3)P and PI(4)P and binds to GTP-bound Rab1, Rab8, and Rab6, protecting each from inactivation by host GTPase-accelerating proteins (GAPs, discussed in further detail below)[245-247]. RidL binds to PI(3)P as well as the host retromer complex, impeding endosome-to-Golgi retrograde transport machinery and thereby supporting bacterial replication[248]. LtpD, which is also thought to modulate endosomal trafficking, binds to PI(3)P in vitro and localizes to PI(3)P-positive membranes in vivo[249]. In addition to these examples, other Dot/Icm substrates have been shown to bind to PI(3)P or PI(4)P, including glucosyltransferase SetA, Lpg1101, and Lpg2603[250, 251].

Small GTPase Modulation and Utilization

Another prevalent strategy of *L. pneumophila* Dot/Icm substrates that contributes significantly to the remodeling of the LCV is the subversion or manipulation of host Ras superfamily small GTPases (hereafter referred to as small GTPases) during infection. The Ras super family contains over 150 human members, with highly conserved orthologs across *L. pneumophila*'s host range and across eukaryotes in general[252]. Eukaryotic small GTPases are critical for a variety of cellular processes, including signal transduction, cytoskeletal dynamics, and vesicular transport[253-256]. Small GTPases serve as molecular switches by alternating between active, GTP-bound and inactive, GDP-bound conformations, with the active forms exerting their function by interacting with other molecular partners[257]. Guanine nucleotide exchange factors (GEFs), GTPase-accelerating proteins (GAPs), and guanine dissociation inhibitors (GDIs) are diverse groups of proteins that participate in the activation, inactivation, and trafficking

of small GTPases[258]. GEFs catalyze the dissociation of tightly bound GDP from inactive GTPases, with the GDP being subsequently replaced by GTP, activating the small GTPase. While the term “GTPase” implies hydrolytic activity, the hydrolytic conversion of GTP to GDP when bound to small GTPases is relatively slow, and GAPs facilitate the hydrolysis of small GTPase-bound GTP to GDP, thereby inactivating the GTPase. Many small GTPases are prenylated with farnesyl or geranylgeranyl groups near their C-terminus, which anchors the GTPases to their target membranes. GDIs and GDI-like proteins bind these hydrophobic groups on inactive small GTPases, shielding them from the cytosol and solubilizing the small GTPases, allowing the cell to maintain cytosolic pools of inactive small GTPases.

While most bacterial pathogens target Rho family small GTPases[259], which regulate actin dynamics, cell cycle progression, and gene expression[253], *L. pneumophila* secreted effectors mainly target Arf, Rab, and Ran small GTPases[199]. Arf and Rab family GTPases regulate membrane dynamics and vesicular transport by controlling vesicular budding, coating, uncoating, sorting, transport, tethering, and fusion[260], while Ran GTPases control nucleocytoplasmic transport of RNA and proteins[261]. The first identified *L. pneumophila* Dot/Icm secreted effector, RalF, was shown to recruit the small GTPase ADP-ribosylation factor 1 (Arf1) to the LCV and exhibit Arf GEF activity[262]. In eukaryotes, Arf1 localizes to the Golgi and facilitates a variety of vesicle transport-related events through interactions with various molecular partners[263]. Arf1 controls coat protein complex I (COPI)-dependent Golgi-to-ER retrograde traffic by mediating assembly and disassembly of the COPI coatomer. Through association with various other Golgi-associated adapter proteins, Arf1 forms

cargo adapter complexes to mediate intra-Golgi and trans-Golgi cargo sorting and transport. In *L. pneumophila*-infected macrophages, recruitment of Arf1 to the LCV and activation by RalF promotes ER recruitment to and association with the LCV[262]. Furthermore, inhibition of Arf1 in the same macrophage infection model prevents ER recruitment to the LCV[264]. Perhaps unsurprisingly, nonfunctional or absent Arf GTPase Sar1, which mediates COPII-dependent ER-to-Golgi transport, results in a similar phenotype[264, 265]. *L. pneumophila* Dot/Icm secreted effectors also target several Rab GTPases. Rab GTPases are similar to Arf GTPases in that they perform a variety of functions involved in vesicle budding, sorting, coating, transport, tethering and fusion, with each specific function determined by and performed through interactions with binding partners[260]. The best understood Rab GTPase in terms of its targeted manipulation by *L. pneumophila* Dot/Icm substrates is Rab1[199]. In eukaryotes, Rab1 regulates ER-to-Golgi traffic. Rab1 is recruited to COPII-coated, ER-derived vesicles by its GEF, TRAPP I, where the activated Rab1-GTP assembles all of its accessory factors that allow tethering the ER-derived vesicles to the cis-Golgi for SNARE-mediated fusion[260]. During a *L. pneumophila* infection, Dot/Icm substrate SidM/DrrA acts as a Rab1 GEF, recruiting Rab1 to the LCV and activating it, thereby facilitating recruitment and possible fusion of ER-derived vesicles[241-245, 250, 266-268]. Furthermore, the N-terminal domain of SidM/DrrA catalyzes the adenosine monophosphorylation (AMPylation) of Rab1. This AMPylation is reportedly critical for Rab1 localization to the LCV[269] and prevents binding of Rab1 to human Rab1 effector MICAL-3[270]. However, it does not prevent binding by previously mentioned Dot/Icm secreted effector LidA, which shields Rab1 (as well as Rab6 and Rab8) from inactivation by host GAPs,

functioning as a GDI and rendering Rab1 constitutively active[245-247, 270]. During the late stages of infection, the Dot/Icm effector SidD deAMPylates Rab1[271-273], allowing another previously mentioned Dot/Icm effector, the bifunctional PI 4-kinase LepB to exert its GAP activity on Rab1, inactivating it[236, 241, 269, 274, 275]. LepB has also been shown to exhibit GAP activity for Rab3, Rab8, Rab13, and Rab35[274]. After inactivation, Rab1 is removed from the LCV through an unknown mechanism, presumably GDI-mediated. Inactive Rab1-GDP is also modulated by the Dot/Icm effectors AnkX and Lem3 through phosphocholination and dephosphocholination, respectively[276-279]. The addition of the phosphocholine moiety to Rab1-GDP leads to the reversible attachment of Rab1-GDP to the LCV membrane, possibly as a means of ensuring sequestration of Rab1 even in its inactive state. Lastly, previously mentioned Dot/Icm effectors SidC and SdcA facilitate mono- and poly-ubiquitination of Rab1, and SidC-mediated poly-ubiquitination of Rab1 was shown to be necessary for successful recruitment of ER to the LCV[280-282]. Ubiquitination by Dot/Icm effectors is discussed in further in the next section.

Though Rab1 seems to be the primary Rab GTPase targeted by *L. pneumophila*, other Rabs have been implicated in LCV maintenance as well. Proteomic analyses of LCVs isolated from *D. discoideum* and macrophages have revealed over a dozen host Rabs associated with the LCV[283, 284]. Notably, only late endosomal Rabs (Rab7 and Rab9) are enriched on the LCVs of Dot/Icm-deficient *L. pneumophila* in macrophages, while all other identified Rabs are drastically reduced[283]. This concurs with the fact that the LCVs of avirulent, Dot/Icm-deficient *L. pneumophila* undergo canonical endosomal maturation as they progress towards eventual fusion with host lysosomes.

Given that *L. pneumophila* relies on the recruitment of secretory vesicles and prevention of lysosomal degradation to proliferate within its host, it is unsurprising that RNAi knockdowns of secretory Rabs (Rab8a, Rab10, and Rab32) hinder intracellular growth while RNAi knockdowns of endocytic Rabs (Rab5a, Rab14, and Rab21) promote intracellular growth[283]. A study analyzing the SidE family of Dot/Icm-translocated ubiquitin ligases (SidE, SdeA, SdeB, and SdeC) found that these effectors could ubiquitinate other ER-associated Rabs in addition to Rab1 (Rab6a, Rab30, Rab33b), but they did not ubiquitinate endosomal Rab5 or cytoskeletal small GTPase Rac1[285]. Another gene in the *sidE*/*sde* gene cluster, *sidJ* encodes an effector with Rab deubiquitinase activity that, when deleted, impairs ER recruitment to the LCV and intracellular bacterial replication[286]. Finally, Dot/Icm secreted effector VipD has been shown to directly target activated Rab5 and Rab22 to interfere with endosomal trafficking[287].

In addition to Arf and Rab family small GTPases, nuclear transport small GTPase Ran, its effector RanBP1 (Ran-binding protein 1), and another host small GTPase Rap1 were also identified in LCV proteomes, confirmed to localize to the LCV during infection, and found to promote intracellular growth of *L. pneumophila*[284, 288]. Dot/Icm effector LegG1 was shown to activate Ran, supporting microtubule stabilization and LCV motility while stimulating host cell migration[288, 289].

Ubiquitin Signaling Manipulation

Recently, there has been a growing body of research documenting Dot/Icm-dependent curation of the host cell ubiquitin profile during *L. pneumophila* infection. Ubiquitination, as its name suggests, is a ubiquitous signaling system that is both

exclusive to and critical to the function of eukaryotic cells[290]. Ubiquitination refers to the covalent conjugation of ubiquitin (Ub)—this can be a Ub monomer or a polymeric chain—to an amino acid residue (generally lysine) of a target protein. Each 76-amio-acid Ub monomer contains seven lysines and an N-terminal methionine that can be ubiquitinated[290, 291]. This gives eukaryotes the ability to post-translationally modify proteins with mono-Ub or polyubiquitin chains of varying shapes and sizes. It is difficult to overstate the central role this system plays in eukaryotic cell biology—the human genome encodes >1000 genes encoding proteins involved in ubiquitination and deubiquitination, emphasizing the complexity and global nature of this signaling network[292, 293]. The best understood function of ubiquitination is the regulation of proteolytic turnover whereby endogenous proteins are marked for proteolytic degradation via ubiquitination[290, 291]. While degradation indirectly affects a wide variety of cellular processes by preventing the downstream functions of degraded proteins, ubiquitin has also been shown to recruit ubiquitin-binding partners, stabilize or inhibit protein interactions, allosterically alter protein activity, and change protein localization[290, 291].

Canonical ubiquitination is a highly conserved process that involves a three-enzyme cascade. First, a Ub-activating enzyme (E1) utilizes ATP to convert free Ub to a Ub-AMP intermediate before forming a thiol-ester linkage between the C-terminus of Ub and a cysteine residue on E1. Next, the Ub is transferred to a Ub-conjugating enzyme (E2). Lastly, a Ub-protein ligase catalyzes the formation of an isopeptide bond between the Ub molecule and a target protein[290]. In humans, there are two E1s, dozens of E2s, and over 1000 E3s, with the latter group providing a high level of substrate

specificity[292, 293]. Deubiquitinases (DUBs), of which there are nearly 100 in the human genome, are proteases that specifically cleave the isopeptide bonds between target proteins and conjugated Ub or within polyubiquitin chains, modifying substrates and providing free Ub to be used elsewhere[294].

Given the prevalence of ubiquitin signaling in eukaryotic organisms, it is unsurprising that genomes of bacterial intracellular pathogens encode a variety of proteins capable of utilizing host ubiquitin to promote bacterial survival and replication[292, 295-297]. For *L. pneumophila*, the first indication that host ubiquitin is important for bacterial virulence came from a study in which the authors found that RNA interference of host Cdc48/p97, an AAA-ATPase involved in multiple ubiquitin-dependent processes, reduced bacterial loads in *Drosophila* and mammalian cell models[298]. The authors established that LCVs were decorated with polyubiquitin and associated with Cdc48/p97 in a Dot/Icm-dependent manner[298]. Since that study, over a dozen Dot/Icm effectors have been implicated in the modulation of ubiquitin signaling[282, 285, 299-308]. Several of these effectors contain regions homologous to eukaryotic E3 ligase F-box and U-box domains[300, 302-304, 306]. F-box domain-containing proteins, or F-box proteins, are the substrate recognition components of the well-studied, multi-subunit SCF (SKP1-Cullin 1-F-box protein) complexes which are part of the broader CRL (Cullin RING E3 ubiquitin ligase) superfamily of RING-type E3 ligases, the latter of which constitutes the vast majority of E3 ligases in mammalian cells[309, 310]. CRLs like SCF complexes overwhelmingly exhibit the greatest range of substrate recognition due to interchangeable substrate recognition subunits like F-box proteins[309]. U-box proteins are functionally similar to RING-domain E3s—enough so

that these complexes are also considered RING-type E3 ligases[309]. Dot/Icm effectors with F-box and U-box domains are therefore attractive to researchers for their potential ability to harness ubiquitination machinery and affect change of host cell processes in a highly specific and cost-effective way.

To date, seven F-box-containing proteins and their orthologs have been described in *L. pneumophila*, all of which are Dot/Icm-secreted effectors[311]. One study showed that three of these—LegU1, LicA, and LegAU13/AnkB—interact with SCF complex components in vivo, with LegU1 and LegAU13 capable of forming a functional E3 ligase complexes with SKP1 and Cullin 1 in vitro[300]. This in vitro ubiquitination was specifically stimulated by UbcH5a and UbcH5c (and for LegU1, UbcH5b to a lesser extent) E2 enzymes, and LegU1 and LegAU13 also associated with polyubiquitinated proteins in vivo. As part of an SCF complex, LegU1 specifically interacts with and directs ubiquitination of host chaperone protein BAT3[300]. BAT3 is highly expressed in mammalian cells and has been implicated in a variety of cellular processes, including modulation of apoptosis, ER stress response, p53-regulated expression, and Hsp70 stability[312-315]. The authors of this study suggest that LegU1-directed ubiquitination of BAT3 could reduce the ER stress response or suppress apoptosis during infection[300]. A target of LegAU13-directed ubiquitination was not identified, but another study of LegAU13 ortholog AnkB showed that AnkB, specifically its F-box domain, is essential for intracellular bacterial proliferation and rapid recruitment of polyubiquitin to the LCV[306]. Intriguingly, LegAU13 and AnkB both localize to the cell periphery and ParvB, also associated with the cell periphery, was confirmed to be an AnkB-interaction partner[300, 305]. Unexpectedly, AnkB seems to reduce ubiquitination

of endogenous ParvB, raising the possibility that AnkB may compete with eukaryotic E3 ligase activity through its interaction with SCF complex members and/or ParvB. Notably, ParvB reportedly has pro-apoptotic effects[316]. Given that *L. pneumophila* infection suppresses host cell apoptosis (See **Inhibition of Host Apoptosis and Protein Synthesis**, page 34), modulation of ParvB activity by AnkB could contribute to suppression of apoptosis.

In addition to the F-box proteins, three Dot/Icm-secreted U-box-containing proteins—LubX, GobX, and RavN—have been described, all of which demonstrate E3 ligase activity[302-304, 317]. Notably, the U-box domains of GobX and RavN have limited primary sequence homology with eukaryotic U-box domains, but they maintain similar higher order structures, and key residues at the E2-binding sites of their respective U-boxes are conserved[303, 304]. In addition to GobX ubiquitin ligase activity, GobX exploits host cell *S*-palmitoylation at its Cys175 residue, targeting GobX to the Golgi[303]. LubX contains two U-box domains with remarkable similarity to eukaryotic counterparts[302]. However, the U-box closest to the C-terminus differs from eukaryotic U-boxes at key residues that are critical for U-box binding to E2 enzymes[318]. Consequently, the N-terminal U-box domain performs the role of a canonical E3 ligase U-box domain, while the second U-box domain appears to function in substrate recognition[302, 317, 318]. LubX was originally shown to facilitate ubiquitination of Clk1 (Cdc2-like kinase 1) in conjunction with UbcH5a and UbcH5c E2 enzymes. While inhibition of Clk kinases impairs intracellular growth of *L. pneumophila*, the mechanism by which Clk1 affects *L. pneumophila* and the consequences of LubX-mediated Clk1 ubiquitination are unclear[302]. Following the study discussing Clk1

ubiquitination by LubX, another study by the same group designated LubX as a "metaeffector" for its ability to target Dot/Icm-secreted effector SidH for ubiquitination, leading to its proteasomal degradation[317]. This study also found that *L. pneumophila* temporally regulates SidH levels within the host by delaying LubX delivery to the host cytosol, thereby depleting SidH during the later stages of infection. While the function of SidH is unclear, infection with a *lubx* mutant in *Drosophila* cells led to persistent SidH levels and a hyper-lethal phenotype, suggesting that SidH removal from the host cytosol is important to avoid premature host cell death[317].

In addition to proteins that resemble E3 ubiquitin ligases in both structure and activity, some Dot/Icm-secreted effectors contain noncanonical structures that still maintain ubiquitin ligase activity. Two of these effectors are previously mentioned SidC and its paralog SdcA. These proteins were originally described as effectors that localize to the LCV via PI(4)P-binding domains[239, 240] (See **Phosphoinositide Modulation and Utilization**, page 18). One study showed that Δ*sidC*Δ*sdcA* mutants were markedly worse at recruiting ER-derived vesicles to the LCV, and that the amount of SidC associated with isolated LCVs was directly proportional to the amount of associated host calnexin, a protein found on the ER[240]. Since then, it has been shown that SidC and SdcA exhibit E3 ligase activity[281, 282]. Sequence homology analysis of SidC homologs from different *Legionella* strains revealed two conserved clusters of residues that, when mapped to the crystal structure of SidC, form a continuous patch on the surface of the protein that contains a classical Cys-His-Asp catalytic triad found in cysteine-based proteases and deubiquitinases. Subsequent analysis revealed that, in fact, SidC and SdcA display E3 ubiquitin ligase activity that requires the catalytic triad.

Notably, the two effectors have differential preferences for host E2 enzymes, which likely contribute to a robust strategy for intracellular survival and replication[282]. Another group found that the small GTPase Rab1, a regulator of ER-to-Golgi transport, is mono-ubiquinated during *L. pneumophila* infection in a manner that requires SidC and SdcA[281]. Lastly, a structural analysis of SidC found that the PI(4)P-binding domain of SidC masks the active site of its E3 ligase domain and PI(4)P binding enhances ubiquitin ligase activity, revealing a mechanism of intramolecular regulation that can specifically target the ubiquitin ligase activity of SidC and its homologs to PI(4)P-containing membranes, most notably the LCV[319].

Another subset of Dot/Icm effectors exhibit ubiquitin ligase activity in a manner that departs even further from the traditional paradigm of ubiquitination. The SidE family of *L. pneumophila* effectors—including SidE, SdeA, SdeB, and SdeC—perform ubiquitination through a mechanism that is fundamentally different from the classical three-enzyme cascade described above. Bioinformatic analysis identified a putative mono-ADP-ribosyltransferase (mART) motif common among all SidE family members that is critical to their function[285]. Generally, mART-containing proteins catalyze mono-ADP-ribosylation of arginine residues at the expense of NAD^+[320]. While E1 enzymes activate Ub by expending ATP to form a Ub-AMP intermediate which is used to link Ub to the E1, SidE family proteins activate Ub through mono-ADP-ribosylation of Ub Arg42 ($Arg42^{Ub}$)[285]. The resultant ADP-ribosylated Ub (ADPR-Ub) is subsequently modified via phosphodiesterase activity embedded in the SidE family protein, releasing AMP and attaching phosphoribosylated Ub (PR-Ub) to serine residues of target proteins. This reaction can also occur in the absence of serine residues with a water

molecule as the acceptor, producing free PR-Ub[299, 321]. In addition to the ubiquitination of target proteins by SidE family proteins, ADPR-Ub and PR-Ub disrupt the classical three-enzyme cascade of ubiquitination by blocking activation of E1 and E2 enzymes, possibly affecting a wide range of ubiquitin-dependent processes[299]. A few targets for ubiquitination by SidE family proteins have been identified as well, including ER-associated small GTPases Rab1 and Rab33b and reticulon 4 (Rtn4), a protein that regulates tubular ER dynamics. Sde-dependent ubiquitination of Rab33b was shown to affect its activity rather than induce its proteasomal degradation[285], and Sde-dependent ubiquitination of Rtn4 causes rearrangement of tubular ER and enrichment of LCV-associated ER[321].

Most recently, Dot/Icm effector MavC has been shown to ubiquitinate E2 enzyme Ube2N, also in a noncanonical manner[301, 322]. MavC provides what seems to be the only known example of ubiquitination that does not require a nucleotide cofactor to activate Ub prior to substrate modification. MavC is a Ub-specific transglutaminase, catalyzing the covalent linkage between $Gln40^{Ub}$ and $Lys92^{Ube2N}$. This particular linkage abolishes UbeN2 activity, dampening NF-κB signaling and inhibiting apoptosis during the early stages of infection (See **Inhibition of Host Apoptosis and Protein Synthesis**, page 34)[301]. Given the prediction that E2s predominately exist as E2-Ub conjugates in the cell[323], one study aimed to determine whether or not MavC could use Ube2N-Ub as a substrate[322]. The study determined that MavC catalyzes an isopeptide cross-linkage between the Ube2N and Ub subunits of Ube2N-Ub, rendering the conjugate inactive. Moreover, MavC binds Ube2N and Ube2N-Ub with a much

higher affinity than free Ub, indicating that MavC exclusively modifies conjugated Ube2N-Ub under cellular conditions[322].

In addition to Dot/Icm effectors that ubiquitinate target proteins, *L. pneumophila* also secretes effectors that function as deubiquitinases (DUBs)[286, 307, 308]. In fact, the aforementioned SidE family proteins also possess DUB domains, characterized by a Cys-His-Asp catalytic triad that is common among proteases[307]. While this DUB activity does appear to regulate ubiquitin signaling at the LCV surface, SidE family DUB activity isn't important for intracellular bacterial multiplication in the way that mART and phosphodiesterase activities are. It has been suggested that the primary purpose served by a SidE family DUB domain may be to provide free ubiquitin for the rest of the protein to use[324]. This notion is supported by the fact that the active sites of SidE family DUB domains display remarkable conformational plasticity, allowing deubiquitination of three of the most abundant polyubiquitin chains[307]. The Dot/Icm-secreted DUB SidJ is encoded on a genetic locus shared by SidE family members SdeA, SdeB, and SdeC[325] and is uniquely capable of cleaving the phosphodiester bond linking ubiquitin to SidE family ubiquitin ligase targets[286]. In addition to this unique activity, SidJ is also capable hydrolyzing isopeptide bonds to deubiquitinate proteins modified via the canonical pathway. SidJ mutants lacking DUB activity cannot rescue SidE family-induced toxicity in eukaryotic cells, nor can they complement ***sidJ***Δ mutants during infection, demonstrating that DUB activity is central to the role SidJ plays in *L. pneumophila* infection[286]. SidJ also provides another example of how *L. pneumophila* temporally regulates other Dot/Icm effectors. During infection, the quantity of SidJ translocated into the host cytosol significantly increases over time. This

coincides with gradual deubiquitination of SidE family target Rab33b, a process that is significantly delayed during infection with a *sidJ*Δ mutant[286]. Lastly, another Dot/Icm "metaeffector" with seemingly high substrate specificity is LupA. LupA also contains the canonical Cys-His-Asp catalytic triad and appears to specifically regulate the stability or activity of LegC3, another Dot/Icm effector[308].

To conclude, ubiquitin signaling is a highly dynamic and versatile post-translational modification system that is critical to eukaryotic cell function. For that reason, intracellular bacterial pathogens have evolved means of manipulating ubiquitin signaling to aid in the acquisition of resources and evasion of host defenses. As researchers study Dot/Icm-secreted effector proteins, they continue to discover novel mechanisms through which *L. pneumophila* utilizes host ubiquitin to establish its replicative niche.

Inhibition of Host Apoptosis and Protein Synthesis

The majority of characterized Dot/Icm substrates promote LCV biogenesis and evasion of host defenses by manipulating host organelle trafficking through interaction with host phosphoinositides, small GTPases, and ubiquitin (Discussed in the previous three sections). Additionally, Dot/Icm substrates have been shown to inhibit host cell apoptosis and arrest protein synthesis. Despite initial reports that *L. pneumophila* induces apoptosis of host cells[326, 327], it is now apparent that apoptosis is inhibited until the late stages of infection[328]. This is consistent with the notion that host cell apoptosis would be detrimental to bacterial replication. One study demonstrated that anti-apoptotic genes positively controlled by the transcriptional factor NF-κB are upregulated in a Dot/Icm-dependent manner during *L. pneumophila* infection of

macrophages. Furthermore, infection triggers nuclear localization of NF-κB in a Dot/Icm-dependent manner, NF-κB activation occurs independent of known host activation pathways, and inhibition of (i) an anti-apoptotic protein and (ii) NF-κB translocation into the nucleus each result in premature host cell death and termination of bacterial replication[329]. Other studies have validated Dot/Icm-dependent NF-κB activation and inhibition of apoptosis during *L. pneumophila* infection. Dot/Icm substrate LegK1 apparently mimics host IκB kinases by phosphorylating IκB inhibitors, thereby stimulating NF-κB activation[330]. SdbA and LubX have also been implicated in the sustained activation of NF-κB during infection of A549 epithelial cells[331]. Lastly, SidF directly interacts with Bcl2 family proteins to inhibit apoptosis, and SdhA is anti-apoptotic, though its mechanism of action is unknown[332, 333].

LegC7

LegC7/YlfA is a *Legionella pneumophila* effector protein secreted by the Dot/Icm secretion system. LegC7 is conserved across all sequenced strains of *L. pneumophila*[1, 121, 334-337], and its expression is induced by the LetA-RsmYZ-CsrA regulatory cascade that occurs as part of the transition to a transmissive phenotype (See **The LetA-RsmYZ-CsrA Regulatory Cascade**, page 10)[157]. LegC7 was first characterized as a Dot/Icm substrate that is lethal when expressed in the budding yeast *S. cerevisiae*[338]. This original study identified via primary sequence analysis an N-terminal hydrophobic region large enough to be a transmembrane domain and two putative C-terminal coiled-coil regions. Both the transmembrane domain and the first coiled-coil region were determined to be required for the yeast lethality phenotype. Lastly, this study showed that LegC7 localizes to ER and ER-derived vesicles during

infection and when expressed ectopically in CHO cells and this localization is solely dependent upon the N-terminal portion that doesn't contain the coiled-coil regions.

A subsequent study established that LegC7 expression in yeast induces a vacuolar protein sorting defect and GFP-tagged LegC7 localizes to the yeast degradative vacuole, analogous to the eukaryotic lysosome[339]. The authors suggested that LegC7 interferes with endocytic maturation of the LCV during infection, thereby helping to prevent lysosomal degradation of the bacterial invader. More recently, an additional yeast study indicated that LegC7-induced disruption of vacuolar delivery of vacuole-directed cargo is specific to endocytic/vacuolar protein-sorting pathway, further supporting the hypothesis that LegC7 specifically interferes with endocytic maturation[340]. However, this notion does not easily reconcile with the finding that LegC7 localizes to ER and ER-derived vesicles, not endosomes or the LCV, during macrophage infection and when expressed ectopically in CHO cells[338, 339, 341]. Furthermore, it has now been shown that infection of macrophage-like U937 cells with a *L. pneumophila* double mutant containing deletions of *legC7* and its paralog *legC2* does not result in increased levels of endosomal marker LAMP-1 on the LCV, but these deletions do result in a significant reduction in LCV-associated host calnexin, an integral protein of the ER[341].

Born of the necessity to modulate host cell biology during pathogenesis, many Dot/Icm substrates, LegC7 included, have features that resemble proteins typically found in eukaryotes (hence the name LegC7—*Legionella* eukaryotic-like gene)[120, 339, 342, 343]. The primary sequence of LegC7 indicates potential structural similarity with eukaryotic SNARE proteins (See **SNARE proteins and SM proteins**, page

51)[338, 339, 341, 344]. Furthermore, recent work on *Chlamydia trachomatis* membrane inclusion protein IncA, a protein sharing significant sequence homology with LegC7, shows that IncA interacts with host SNAREs and is required for certain homotypic fusion events[345, 346]. These findings, combined with all the evidence of membrane trafficking alteration, have led researchers to label LegC7 and structurally related effectors LegC2 and LegC3 as SNARE-like while uncovering the extent to which they are functionally similar to eukaryotic SNAREs[341, 344]. One study showed that LegC7 and LegC2 form homo- and heterotypic dimers and trimers[341], though using these findings as evidence of SNARE function is dubious since oligomerization is a function of coiled-coil domains generally and homotypic oligomers of SNAREs are not biologically relevant[347, 348]. Another study discovered that synthetic liposomes containing LegC2, LegC3, and LegC7 fused with target liposomes containing mammalian R-SNARE VAMP4 and concluded that LegC2, LegC3, and LegC7 form a canonical 3Q-SNARE bundle that forms a *trans*-SNARE complex with the host R-SNARE VAMP4[344]. Notably, this SNARE complex was completely resistant to disassembly by the conserved SNARE chaperones NSF and α-SNAP. In light of these findings, it isn’t readily apparent why individual LegC proteins induce observable phenotypes in yeast, especially LegC7-mediated growth inhibition.

Table 2.1. A list of all referenced Dot/Icm substrates and their functions.

Dot/Icm Substrate	Putative Function(s)
AnkX	phosphocholination of Rab1-GDP, leads to attachment of Rab1 to the LCV
GobX	U-box-containing; E3 ubiquitin ligase activity; *S*-palmitoylation by host targets GobX to the Golgi
LegAU13/AnkB	F-box-containing; forms functional SCF complex; ParvB-interaction partner; anti-apoptotic
LegC2	SNARE-like; ER recruitment to LCV
LegC3	SNARE-like; inhibition of membrane fusion; regulated by LupA
LegC7	SNARE-like; ER recruitment to LCV
LegG1	Ran GTPase activation
LegK1	IκB kinase; anti-apoptotic
LegU1	F-box-containing; forms functional SCF complex
Lem3	dephosphocholination of Rab1-GDP, leads to detachment from LCV
LepB	Rab GAP activity; PI 4-kinase activity
LicA	F-box-containing
LidA	binds Rab1-GTP and PI(3)P/PI(4)P; Rab1 GDI
Lpg1101	PIP-binding
Lpg2603	PIP-binding
LtpD	PI(3)P-binding
LubX	U-box-containing; E3 ubiquitin ligase activity; ubiquitination of host Clk1; temporal regulation of Dot/Icm effector SidH via ubiquitination; anti-apoptotic
LupA	protease and/or DUB activity; regulates LegC3
MavC	Ube2N-Ub inactivation via intramolecular transglutamination; anti-apoptotic
RalF	Arf1 recruitment and Arf1 GEF activity
RavN	U-box-containing; E3 ubiquitin ligase activity
RidL	binds PI(3)P and host retromer complex; prevention of endosome-to-Golgi retrograde transport
SdbA	Anti-apoptotic
SdcA	PI(4)P-binding; E3 ubiquitin ligase activity; ubiquitination of Rab1; ER recruitment to LCV
SdeA	“all-in-one” ubiquitin ligase; Rab ubiquitination
SdeB	“all-in-one” ubiquitin ligase; Rab ubiquitination
SdeC	“all-in-one” ubiquitin ligase; Rab ubiquitination
SdhA	anti-apoptotic
SetA	glucosyltransferase; binds PIP
SidC	PI(4)P-binding; E3 ubiquitin ligase activity; ubiquitination of Rab1; ER recruitment to LCV
SidD	Rab1 deAMPylation
SidE	“all-in-one” ubiquitin ligase; Rab ubiquitination
SidF	PI 3-phosphatase activity; anti-apoptotic
SidH	targeted for proteasomal degradation by LubX
SidJ	DUB activity; ER recruitment to LCV
SidM/DrrA	PI(4)P-binding; Rab1 GEF; ER recruitment to LCV; Rab1 AMPylation
SidP	PI 3-phosphatase activity
VipD	Rab-targeting; inhibition of endosomal traffic

SACCHAROMYCES CEREVISIAE AS A MODEL EUKARYOTE

There are significant obstacles that hinder the study of *L. pneumophila* pathogenesis at the molecular level. For one, the bacterium and its natural hosts (protozoans and macrophages) have limited genetic tractability. Furthermore, the number of Dot/Icm substates that are translocated into the host cell (more than 300) compounds the issue. This group of proteins contains a considerable amount of redundancy, and the vast majority of these proteins are dispensable for successful infection [349]. This generally means that deletions of individual substrates or subsets of substrates don't lead to readily observable phenotypes in infection models.

One approach that has proven useful for studying effector proteins secreted by intracellular bacterial pathogens is heterologous expression of these proteins in the budding yeast *Saccharomyces cerevisiae* [350]. *S. cerevisiae* (from here on referred to as yeast) is an attractive model eukaryotic host for several reasons: (i) yeast cellular properties and processes are conserved in higher eukaryotes, which allows yeast to serve as a proxy for studying general eukaryotic cell biology; (ii) the yeast genome is minimally redundant, with over 75% of the open reading frames have known or predicted functions; (iii) yeast is easy and inexpensive to work with in a laboratory setting; and (iv) a wide variety of tools have been developed for studying yeast biology. Yeast has been employed to identify and study bacterial secreted effectors from a variety of intracellular pathogens of mammals, including *Chlamydia trachomatis* [351], *Legionella pneumophila* [338], *Salmonella typhimurium* [352], *Shigella flexneri* [353], *Vibrio parahaemolyticus* [354], and *Yersinia* species [352]. Yeast growth inhibition has served as a sensitive and specific reporter for effector proteins, with several high-

throughput studies finding that yeast growth inhibition by bacterial proteins that aren't secreted is very rare [338, 353, 355]. Other tools that have proven useful in the yeast model include observation of effector localization, observation of effector-induced alterations of yeast cytoskeletal and organellar morphology, and functional genomic and small molecule screens for suppression of growth inhibition or reversal of other effector-induced phenotypes [350].

MEMBRANE TRAFFICKING IN YEAST

Membrane trafficking is a highly controlled system that allows cells to direct newly synthesized cargo and material acquired from their surroundings to specific destinations within the cell (**Figure 2.4**). In addition to delivering proteins, lipids, and other molecules to destinations where they might exert a desired function, membrane trafficking is also integral to degradation, secretion, and recycling of cellular material. *S. cerevisiae* is one of the best-characterized eukaryotic models for membrane trafficking, and the pathways that have been described are conserved in higher eukaryotes, including mammals [356].

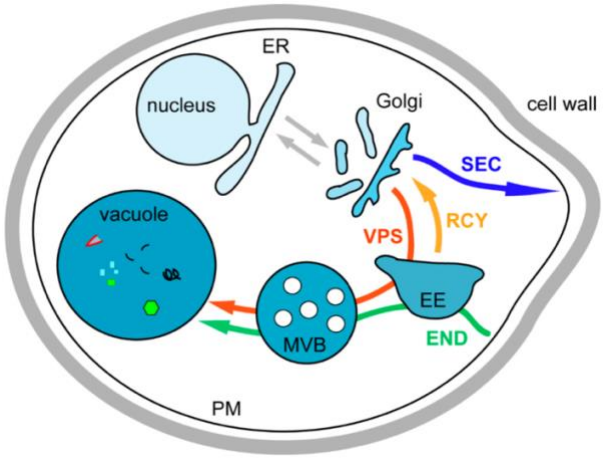

Figure 2.4. An overview of membrane trafficking pathways in yeast. [356]

Secretory (SEC) Pathway

The early secretory pathway is taken by all newly synthesized proteins that are exported from the endoplasmic reticulum (ER). In the ER, the newly synthesized proteins destined for ER export are sorted from ER resident proteins by a prebudding cargo complex. The prebudding complex then recruits an outer layer coat complex, together forming the COPII vesicle coatamer which facilitates membrane bending and subsequent COPII vesicle budding from the ER [357, 358]. In addition to excluding ER resident proteins, the prebudding complex, as well as other ER-sorting receptors, recognize and concentrate proteins based on their eventual destinations [359-364]. Once formed, COPII vesicles are specifically transported from the ER to the Golgi for further sorting. Conversely, vesicles transported from the Golgi to the ER or retrograde between Golgi cisternae are encapsulated by a COPI coat [365]. Once COPII vesicles are delivered to the Golgi, cargo is sorted into three distinct pathways: the vacuolar protein sorting (VPS) pathway, the alkaline phosphatase (ALP) pathway, and the exocytic (EXO) pathway, also referred to as the secretory pathway [356].

Vacuolar Protein Sorting (VPS) Pathway

Most vacuole-targeted proteins follow the vacuolar protein sorting (VPS) pathway. At the Golgi, these proteins are sorted through interactions with various cargo adapters, including the adapter AP-1 complex [366], Golgi-associated gamma-adaptin ear homology Arf-binging (GGA) proteins [367-369], and epsins Ent3p/Ent5p [370, 371], which concentrate the proteins and recruit the clathrin that coats vesicles that bud from the trans-Golgi network (TGN) [372]. In the VPS pathway, TGN-derived vesicles fuse with early endosomes, which undergo a maturation process to form late endosomes before finally fusing with the vacuole. This endosomal maturation involves endosome-

endosome fusion and intralumenal vesicle (ILV) formation [372]. Membrane fusion, endosome-endosome fusion in particular, is discussed in **Membrane Fusion** on page 47. ILV formation is the means by which vacuole-targeted integral membrane proteins can be delivered to the vacuolar lumen. This process is initiated by ubiquitination of membrane proteins destined for the vacuolar lumen [373]. Following ubiquitination, a series of five ESCRT (endosomal sorting complex required for transport) protein complexes (ESCRT-0 – IV) function in succession to concentrate ubiquitinated membrane proteins and bud the membrane into the endosomal lumen, creating an ILV containing vacuole-targeted proteins [374]. Due to the accumulation of ILVs, late endosomes are also referred to as multivesicular bodies (MVBs).

Alkaline phosphatase (ALP) pathway

The alkaline phosphatase (ALP) pathway is a Golgi-to-vacuole pathway that does not pass through endosomes [375]. Instead, cargo is recognized at the TGN by the AP-3 cargo adapter complex, specifically sorted into AP-3 clathrin-coated vesicles, and targeted directly to the vacuole [376, 377].

Exocytic (EXO) pathway

The exocytic (EXO) pathway refers to the transport of vesicles from the TGN to the plasma membrane. These vesicles travel along actin cables and are tethered to the plasma membrane by the octameric exocyst complex prior to fusion [378, 379]. The EXO pathway functions to secrete proteins out of the cell and deliver proteins to the plasma membrane.

Endocytic (END) pathway

The endocytic (END) pathway involves the internalization of plasma membrane and extracellular material, which are then directed either to the vacuole for degradation or to the TGN for recycling [380]. Endocytosis can be divided into two categories: (i) constitutive, non-specific endocytosis that provides a constant influx of extracellular material and (ii) receptor-mediated endocytosis, which requires binding of a ligand to a surface receptor to initiate internalization [356]. In both cases, the AP-2 adapter complex recruits clathrin to the site of endocytosis, forming an early coat [356]. Following early coat formation, the late coat Pan1p-Sla1p-End3p complex is recruited by ANTH- (AP180 *N*-terminal homology) and ENTH- (epsin *N*-terminal homology) domain containing proteins Sla2p and Ent1p/Ent2p, respectively. The late coat recruits the WASP (Wiskott-Aldrich syndrome protein) family protein Las17p and myosin, which form a WASP/myosin module that initiates invagination by activating the actin nucleating Arp2/3 complex. Actin filament formation drives invagination while myosin squeezes the plasma membrane together at the surface, and after sufficient invagination, scission completes formation of the endocytic vesicle [356, 381-383].

Autophagy

Autophagy is the process by which cells degrade cytosolic proteins and other macromolecules, as well as organelles, by delivering them to the vacuolar lumen. This is important for maintaining cell homeostasis, particularly in response to changes in nutrient availability or cell damage and provides the cell the ability to repurpose superfluous subcellular material [384]. For example, when yeast cells are transferred from a carbon source that requires peroxisomes, such as methanol or oleic acid, to a

preferred carbon source like glucose, the cells rapidly turn over the peroxisomes via autophagy [385, 386]. This is useful because organelles are expensive to maintain, and dysfunctional organelles can damage the cells in which they reside. Autophagy can be can divided into two categories, macroautophagy and microautophagy, both of which can be either selective or nonselective. Generally, microautophagy refers to inward budding or protrusion of the vacuolar membrane, while macroautophagy involves the formation of a double lipid bilayer around cytosolic contents followed by fusion of the outer bilayer with the vacuole, resulting in the delivery of the inner vesicle to the vacuolar lumen [384]. The distinctions between these processes are discussed in further detail below.

Nonselective microautophagy

During nonselective microautophagy, the vacuolar membrane invaginates to form a long, narrow tube-like structure, and vesicles bud off of the tip and/or sides of the tube [387, 388]. Since the membrane of the newly formed vesicles is indistinguishable from the vacuolar membrane, it is unclear how these vesicles can be degraded without the entire vacuolar membrane being subject to the same degradation.

Selective microautophagy

In selective microautophagy, cargo designated for autophagic degradation is sequestered at the vacuolar membrane. The mechanism by which invagination or protrusion/septation of the vacuolar membrane is induced is poorly understood. The process has been compared to the formation of ILVs in MVBs by ESCRT machinery, but ESCRT complexes do not appear to play a role in the process [389]. Rather, the overlap of autophagy machinery across different forms of autophagy suggests that this

protrusion of the vacuolar membrane more closely resembles the de novo generation of the macroautophagic phagophore (discussed below).

The best-studied case of selective microautophagy is micropexophagy in methylotrophic yeast such as *Pichia pastoris* and *Hansenula polymorpha* [390-392]. In this process, a unique structure called the micropexophagic apparatus (MIPA) appears to serve as a scaffold upon which the sequestering membrane is generated [390, 391]. The sequestering membrane wraps around the peroxisome and, upon completion, releases it into the vacuolar lumen, incased in vacuolar membrane [392]. Other examples of selective microautophagy include mitophagy (mitochondria) and micronucleophagy in which portions of the nucleus protrude into the vacuole and are pinched off [384].

Nonselective macroautophagy

Unlike microautophagy, macroautophagy refers to a process in which cytosolic contents are enclosed within a double lipid bilayer called an autophagosome prior to vacuolar delivery [393]. The necessity of a double bilayer as opposed to a single bilayer lies in the fact that it is less costly to the cell: unfolding proteins for translocation across a bilayer would require substantial investment of resources and exposing the hydrophobic interior of the bilayer to the cytosol is energetically unfavorable [384]. Macroautophagy begins at the phagophore assembly site (PAS), which is defined as site where the majority of autophagy-related (Atg) proteins localize [394-396]. The PAS and initiation of macroautophagy are poorly understood—it is unclear whether the PAS has a membrane structure, whether it is permanent, and whether it is converted into the phagophore or just plays a role in forming the phagophore. Regardless, phagophore

assembly begins at the PAS, and the phagophore is expanded through the addition of lipid bilayers from one or more donor sources. Presumably, these bilayers are supplied in the form of vesicles, but the possibility that bilayer may be donated from adjacent organelles has not been excluded. There is evidence suggesting that there are a variety of origins of these donor bilayers, including the ER, the trans-Golgi, and the plasma membrane [397-403]. Considering the membrane demands of autophagy, it is possible that the cell mobilizes membrane from multiple sources, easing the burden for any single source. Another issue that remains to be clarified is the mechanism through which the phagophore is curved onto itself in nonselective macroautophagy. Selective autophagy can utilize protein-protein interactions between autophagy machinery and the autophagic cargo, but nonselective autophagy cannot. Instead, membrane curvature may be induced by membrane proteins or unequal distribution of lipids. Lastly, the phagophore must be sealed to separate the inner and outer membranes prior to fusion with the vacuole. While this presumably occurs through fusion or scission, the mechanism is unknown. However, there is evidence suggesting that the release of Atg machinery from the autophagosome is a necessary regulatory step that allows autophagosome-vacuole fusion [404, 405].

Selective macroautophagy

The machinery involved in macroautophagy is largely conserved between selective and nonselective forms. The two are morphologically similar, with one key distinction: unlike nonselective macroautophagy, selective macroautophagy excludes bulk cytoplasm from the autophagosome. The expanding phagophore remains in close

apposition to the selective cargo, and the resulting autophagosome is generally smaller than that of nonselective macroautophagy [384].

Cytoplasm-to-vacuole targeting (Cvt) pathway

The cytoplasm-to-vacuole targeting (Cvt) pathway is a noncanonical autophagic pathway used to deliver resident hydolases to the vacuole [406]. Cvt is morphologically similar to selective macroautophagy. but specifically relies on precursor aminopeptidase I (prApe1p) [407, 408]. Cytosolic prApe1p dodecamers comprise the supra-order oligameric Ape1 complex that forms the larger Cvt complex together with Atg19p and alpha-mannosidase (Ams1p) oligomers. Atg19p then links the Cvt complex to autophagosome formation machinery through interaction with PAS proteins Atg8p and Atg11p [409].

MEMBRANE FUSION

Membrane fusion is a fundamental process in membrane trafficking in which two lipid bilayers merge to form a single continuous bilayer. While eukaryotes employ diverse fusion machineries, many elements of the fusion process are conserved: (i) small GTPases (usually Rab GTPases) that serve as membrane-bound anchors[260, 410], (ii) tethering proteins or protein complexes that bind these anchors on apposed donor and accepter membranes[411], (iii) SNARE (soluble NSF (N-ethylmaleimide-sensitive factor) attachment protein receptor) proteins which form helical bundles with SNAREs on apposed membranes, providing the force necessary to drive fusion[348], and (iv) SM (Sec1/Munc18 family) proteins that facilitate SNARE complex assembly[348]. The small GTPases undergo a conformational change when activated (GTP-bound), allowing them to bind both membrane lipids and specific effector proteins,

in this case tethering proteins and/or tethering complex subunits (for more information on small GTPases, see **Small GTPase Modulation and Utilization** on page 21). Other components of membrane fusion machinery are discussed in further detail below.

Membrane tethers

Membrane tethers are essential for the fidelity of intracellular trafficking of lipids and proteins. Indeed, the loss of membrane tethers blocks membrane traffic, often changes organelle morphology and identity, and can even be lethal[411]. Tethers are also evolutionarily conserved in eukaryotes, indicating the essential roles they have in membrane dynamics[412]. All tethers are cytosolic, which allows for dynamic, rapid targeting of these molecules to membranes in a manner that is independent of intracellular trafficking pathways. Tethers can be broadly divided into two categories: homodimeric coiled-coil tethers[413] and multi-subunit tethering complexes (MTCs)[414]. Coiled-coil tethers are generally larger, capable of spanning up to ~200 nm to link two membranes, while MTCs span less than 30 nm[411]. This review will only focus on vacuolar protein sorting (VPS) class C tethering complexes, specifically in *S. cerevisiae*, but an extensive list of tethers and their associated functions can be found below (**Table 2.2**).

Table 2.2. An extensive list of membrane tethers. [411]

Coiled-coil	Structure/composition	Proposed function
p115	115 kDa protein; homodimer	Tethering of COPI vesicles to Golgi; anterograde trafficking of newly synthesized cargo; Golgi ribbon formation
GM130	130 kDa protein; homodimer	Tripartite model of p115-dependent tethering
Giantin	400 kDa protein; homodimer	Tripartite model of p115-dependent tethering
CASP	160 kDa protein; homodimer	Retrograde transport within the Golgi
GMAP210	210 kDa protein; homodimer	Intra-Golgi trafficking and structural maintenance of Golgi
GCC185	185 kDa protein; homodimer	Endosome-to-TGN trafficking
GCC88	88 kDa protein; homodimer	Endosome-to-TGN trafficking
p230	245 kDa protein; homodimer	Anterograde transport from the TGN
Golgin97	97 kDa protein; homodimer	Anterograde transport from the TGN
EEA1	162 kDa protein; homodimer	Docking and fusion of vesicles at the early endosome
MTCs	**Structure/composition**	**Proposed function**
COG	8 subunits in yeast: Cog1-8	Intra-Golgi trafficking; endosome-to-Golgi retrograde transport
Dsl1	3 subunits in yeast: Dsl1, Dsl3(Sec39), and Tip20; in mammals: ZW10, RINT-1, and NAG	Golgi-to-ER retrograde transport
GARP	4 subunits: Vps51-54	Endosome-to-TGN trafficking
TRAPPI	7 subunits in yeast: Bet3A, Bet3B, Bet5, Trs20, Trs23, Trs31, and Trs33	Tethering of COPII-decorated vesicles from ER at the Golgi
TRAPPII	TRAPPI subunits and Trs65, Trs120, and Trs130	Intra-Golgi transport; binds COPI vesicles; retrograde trafficking from endosomes to Golgi
TRAPPIII	TRAPPI subunits and Trs85	Retrograde endosome-to-TGN transport, autophagy
HOPS	6 subunits in yeast: Vps11, Vps16, Vps18, Vps33, Vps39, and Vps41	Endolysosomal fusion, homotypic fusion of vacuoles in yeast
CORVET	6 subunits in yeast: Vps3, Vps8, Vps11, Vps16, Vps18, and Vps33	Acts upstream of HOPS and may tether vesicles or promote homotypic fusion of endosomes
Exocyst	8 subunits in yeast: Sec3, Sec5, Sec6, Sec8, Sec10, Sec15, Exo70, and Exo84	Tethering complex for transport carriers from recycling endosomes and the Golgi

VPS Class C Tethering Complexes

There are two hexameric VPS class C tethering complexes: the CORVET (class C core vacuole/endosome tethering) complex and the HOPS (Homotypic fusion and protein sorting) complex[415]. The CORVET complex tethers early endosomes, while the HOPS complex tethers late endosome and vacuolar membranes, as well as ALP vesicles and autophagosomes prior to vacuolar fusion. These complexes share a core complex composed of four subunits—Vps11p, Vps16p, Vps18p, and Vps33p—and each contain two unique subunits: Vps3p and Vps8p for CORVET and Vps39p and Vps41p for HOPS (**Figure 2.5**). Vps3p and Vps8p specifically bind to Rab5 homolog Vps21p[416] while Vps39p and Vps41p specifically bind to Rab7 homolog Ypt7p[417]. Early endosomal membranes are enriched with active Vps21p, and as endosomes mature, Vps21p is inactivated and replaced by active Ypt7p, which can be found on late endosomes and vacuoles[418]. This transition of Rab GTPases is what targets the

tethering complexes to their respective fusion sites, and the Rab-specific subunits of each complex are located at opposite ends of their respective complexes in order to bind Rabs on apposed membranes.

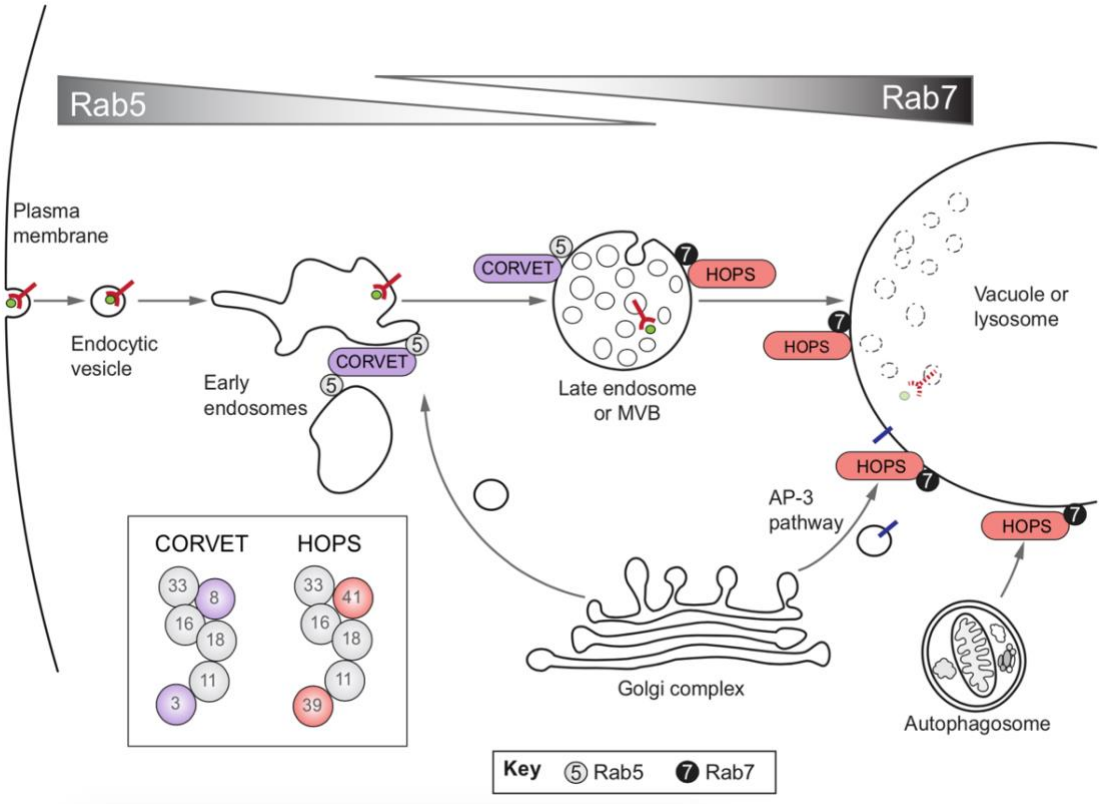

Figure 2.5. Class C tethering complexes. [415]

The core complex subunits have various functions. Vps11p and Vps18p have RING domains, which have been shown to be important for proper protein sorting[419]. RING domains can function as E3 ubiquitin ligases, and indeed mammalian Vps18 has been show to ubiquitinylate trans-Golgi clathrin adapter Gga3[420]. Vps16p is required for association of Vps33p with other complex members[421] and interacts with the vacuolar Q-SNARE Vam3[422]. Vps33p is an SM protein and seems to be the only SM protein that is an integral part of an MTC[415]. Vps33p function has been studied more

in the context of the HOPS complex, but presumably has similar functions in the CORVET complex. Vps33p interacts with SNAREs Vam3p and Nyv1p on apposed membranes as a chaperone to ensure correct trans-SNARE complex formation[423]. Vps33p also recruits the cytosolic SNARE Vam7p to the vacuole via the Vam7p PX (phox homology) domain[424-427]. In addition to ensuring correct trans-SNARE pairing, Vps33p also can act as a proofreader by inhibiting fusion in the event of mismatched or rotated SNARE assembly[428].

SNARE proteins and SM proteins

SNAREs generate the force required to destabilize apposed membranes at the site of fusion to generate a single, continuous lipid bilayer. These proteins typically contain a C-terminal transmembrane anchor and one ~70 residue, cytosolic, α-helical "SNARE motif" with heptad repeats, though there are examples of SNAREs with multiple SNARE motifs and/or no transmembrane domain. Upon their original discovery, SNAREs were categorized as t-SNAREs (target membrane) and v-SNAREs (transport vesicle) based on the membranes in which they reside. More recently, they have been classified as Q-SNAREs (typically t-SNAREs) and R-SNAREs (typically v-SNAREs) based on the highly conserved residue at the ionic layer (designated the 0-layer) of their respective SNARE motifs[347]. Q-SNAREs can be further divided in three types—Qa-, Qb-, and Qc-SNAREs—based on conserved C- and N-terminal regions[429]. Prior to fusion, one membrane contains 3Q-SNARE assemblies (Qabc) and the other membrane contains R-SNAREs. During fusion, an R-SNARE and a 3Q-SNARE form a four-helix bundle called a trans-SNARE complex or SNAREpin, beginning at the N-terminal ends of the SNARE motifs and "zipping" up toward the transmembrane

domains (**Figure 2.6**)[430, 431]. Simultaneously occurring in multiple SNAREpins per fusion event, this protein folding is a spontaneous, exergonic reaction that generates the force that pushes the membranes together. Notably, Qa-SNAREs have a three-helix Habc domain N-terminal to the SNARE motif which folds back onto the SNARE motif to form a “closed” four-helix conformation that interacts with SM proteins like Munc18 in the case of mammalian syntaxin-1[432, 433]. This domain is necessarily dissociated from the Qa-SNARE during complex assembly, though the mechanism by which this occurs is unclear. Potential functions of the Habc domain include inhibition of undesirable SNARE complex assembly and sequestration/transportation of SM family proteins.

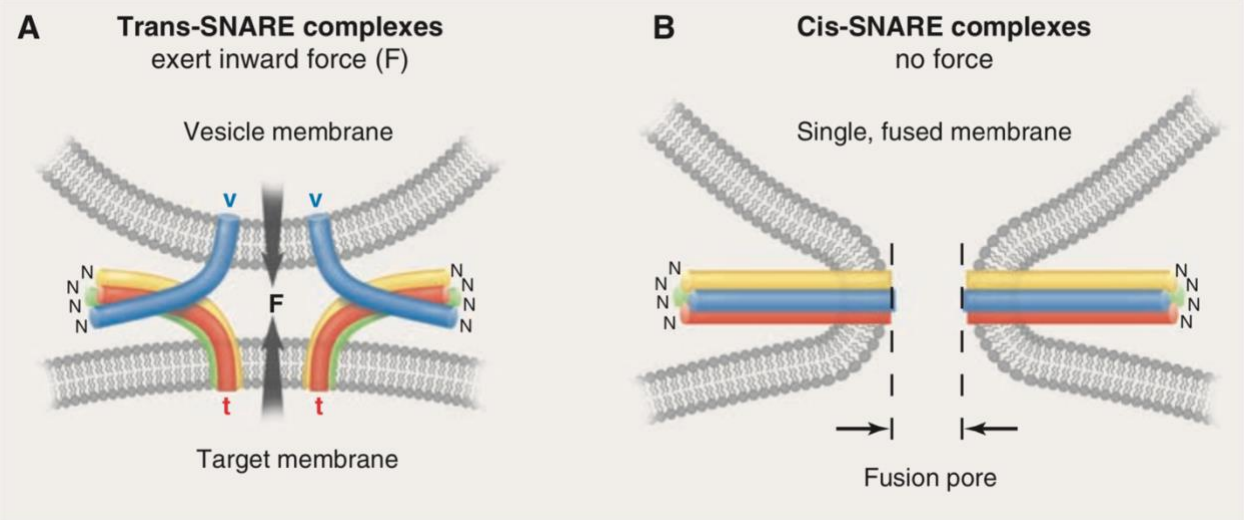

Figure 2.6. SNARE complex zippering to achieve membrane fusion. [348]

SM proteins, in addition to SNAREs, are essential for in vivo membrane fusion, though in vitro fusion can be achieved with SNAREs alone[348]. SM proteins function as arch-shaped clasps of the four helix bundles comprised of either (i) four SNARE motifs in a trans-SNARE assembly or (ii) the Habc domain and the SNARE motif of a Qa-

SNARE[432, 433]. All SM proteins probably ensure proper trans-SNARE assembly in a manner more or less similar to Vps33p, discussed in *VPS Class C Tethering Complexes* on page 49, and they likely stabilize the intramolecular bundle formed by Qa-SNAREs. A second mechanism of interaction between SM and SNARE proteins has been described for yeast Qa-SNAREs Ufe1p, Sed5p, and Tlg2p, and likely points to an intermediate step that allows for the dissociation of the Habc domain and the formation of the trans-SNARE complex[434, 435]. In this interaction, the N-terminal lobe of the SM protein is anchored to an evolutionarily conserved, N-terminal region of the Qa-SNARE. This interaction would allow for initiation of trans-SNARE assembly while also keeping the SM protein in position to clasp the nascent complex.

Following fusion, the participating SNAREs remain in remarkably stable cis-SNARE complexes (**Figure 2.6**). The endergonic unfolding of these complexes is performed by the AAA-type ATPase NSF (N-ethylmaleimide-sensitive factor) and its adapter SNAP (soluble NSF attachment protein), with the former providing the necessary energy and the latter coupling ATP hydrolysis with SNARE complex dissociation[436, 437]. This process is referred to as the priming stage of fusion, which presumes energy isn't expended to disassemble cis-SNARE complexes until the SNAREs are needed for another fusion event.

There are 24 SNAREs in *S. cerevisiae*, with each SNARE having compartment specific localization[438]. Despite the number of SNAREs, there are only a dozen or so combinations capable of forming fusogenic complexes, which provides another level of fidelity to membrane trafficking.

Emp47p, Emp46p, and Ssp120p

Emp47p, Emp46p (an Emp47p homolog), and possibly Ssp120p function in protein sorting in the early secretory pathway in yeast. As discussed in **Secretory Pathway** on page 41, nascent proteins that are translocated into the ER are sorted and packaged into COPII vesicles by various protein sorting cargo adapters to be sent to the Golgi, and Emp47p and Emp46p are two such cargo adapters (**Figure 2.7**). Each has a single C-terminal transmembrane domain and an N-terminal, lumenal carbohydrate recognition domain potentially to recognize glycoproteins intended for secretion[439, 440]. Emp47p forms homooligomeric complexes as well as heterooligomeric complexes with Emp46p, whereas Emp46p cannot form homooligomeric complexes. This oligomerization, combined with the binding of COPII machinery, is what facilitates COPII vesicle formation[441]. Indeed, Emp46p remains in the ER in an *emp47*Δ mutant,

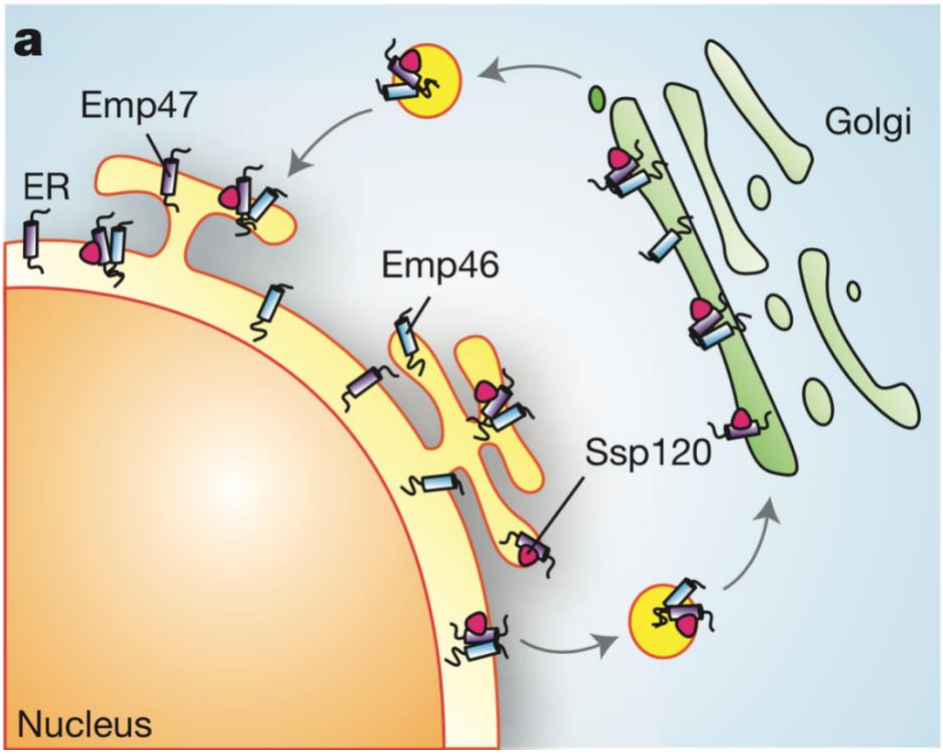

Figure 2.7. Emp46p/Emp47p/Ssp120p trafficking in yeast. [442]

potentially because of an inability to form homooligomers[441]. After reaching the Golgi, Emp46p and Emp47p are packaged into COPI vesicles and trafficked back to the ER.

Ssp120p contains no transmembrane domain and is translocated into the ER after synthesis[443]. In the ER, Ssp120p binds to Emp47p and is packaged into Emp47p-positive COPII vesicles[440, 442]. It has been proposed that the Emp47p-Ssp120p complex acts as a functional unit based on phenotypic similarities between *emp47*Δ and *ssp120*Δ mutants[440], but evidence to support this concept is limited. While Ssp120p is trafficked to the vacuole in an *emp47*Δ mutant, there is no apparent mislocalization of Emp47p or Emp46p in a *ssp120*Δ mutant[442], and since no specific targets of Emp47p/Emp46p/Ssp120p recognition have been confirmed, there has been no analysis of aberrant cargo trafficking.

The Emp47p-Ssp120p complex has also been compared to the mammalian ERGIC53-MCFD2 complex based on putative function and structural homology. MCFD2, homologous to Ssp120p, is thought to be a cargo specificity factor that ensures proper export of blood clotting factors V and VIII from the ER[444, 445]. However, other ERGIC-53 cargo doesn't require MCFD2[446] and studies have shown that oligosaccharides bind the carbohydrate recognition domain of ERGIC-53 independent of MCFD2[447-449]. More work needs to be done to define the role particularly of Ssp120p in cargo recognition but also of Emp47p/Emp46p/Ssp120p complexes more broadly.

CHAPTER 3

LEGIONELLA PNEUMOPHILA LEGC7 EFFECTOR PROTEIN DRIVES ABERRANT ER:ENDOSOME FUSION IN YEAST

Glueck, N.K., O'Brien, K.M., and Starai, V.J. Submitted to *Traffic*, November 19, 2020.

Introduction

Legionella pneumophila is a ubiquitous Gram-negative, facultatively intracellular bacterium, capable of invading and replicating within a broad range of freshwater protozoa[450, 451]. Upon aerosolization of contaminated water supplies and subsequent inhalation by susceptible individuals, *Lpn* is taken up into alveolar macrophages via coiling phagocytosis[452], where the bacterium persists and replicates within a modified membrane-bound compartment termed the *Legionella*-containing vacuole (LCV). Left untreated, this infection can lead to the severe form of pneumonia known as Legionnaires' disease, which can have a mortality rate of at least 10%[26]. Localized outbreaks of legionellosis continue to rise worldwide, and the number of reported cases in the United States in 2017 was ~7,500, an increase of more than 500% when compared to cases reported in 2000[453]. Like most intracellular bacteria, *L. pneumophila* actively manipulates host physiology in order to create its replicative niche. The *L. pneumophila* genome encodes for a Dot/Icm type-IVB secretion system, which secretes over 300 confirmed and predicted "effector" proteins into the host cell upon contact and internalization[454]. These effectors are known to modulate myriad host cell processes to ensure the survival of the bacterium, including: protein and membrane trafficking pathways[339, 455], autophagy[456], and actin dynamics[457]; these activities are coordinated to prevent the fusion of the *Legionella*-containing phagosome with endolysosomal degradative compartments and recruit ER-derived vesicles to the phagosome to generate the LCV[200]. Understanding the mechanisms by which these effectors can modulate eukaryotic physiology has been a focus of intense study[349, 454], but which has been complicated by the fact that activities of

these proteins are thought to be highly redundant, as few single effector gene disruptions lead to pathogenicity defects in model systems[349]. Therefore, the use of heterologous eukaryotic expression systems to dissect the activities of individual *Lpn* effectors has proven fruitful[339, 455, 458, 459].

LegC7/YlfA is a Dot/Icm protein substrate that was originally identified as a *L. pneumophila* effector that inhibits growth of *Saccharomyces cerevisiae* when expressed, although the mechanism of toxicity was not determined[459]. When expressed in CHO cells, it was found that LegC7/YlfA localized to ER and early secretory vesicles, and that this localization was dependent upon its N-terminal hydrophobic/transmembrane domain[459]. Furthermore, LegC7 expression in yeast resulted in general vacuolar protein sorting defects[339], and specifically inhibited endosomal cargo delivery to the degradative vacuole; other protein trafficking pathways to the vacuole were not affected[340]. Interestingly, LegC7/YlfA and two other *Lpn* effectors, LegC2/YlfB (a paralog of LegC7) and LegC3, have been described as eukaryotic “SNARE-like” proteins, as they have similar coiled-coil domain structures and can be found to engage in higher-order complexes, similar to the SNARE proteins responsible for catalyzing the majority of eukaryotic intracellular membrane fusion events[348]. Indeed, Δ*legC7* Δ*legC2* mutant strains of *Legionella* form aberrant LCVs during infection that less host ER-derived membrane, suggesting a role for LegC7 and/or LegC2 in ER membrane recruitment or fusion to the phagocytic membrane surrounding *Legionella*. Despite the reported importance of LegC7 and LegC2 in the synthesis of the LCV, these Δ*legC7*Δ*legC2* mutant strains do not display proliferation defects during pathogenesis[341]. Biochemical evidence of the SNARE-like membrane

fusion activity of complexes containing LegC2, LegC7, and LegC3 was discovered when synthetic liposomes harboring LegC2/LegC7/LegC3 “Q-SNARE” complexes were fused with target liposomes harboring a host endosomal R-SNARE, VAMP4[344]; this SNARE complex activity was also found to be completely resistant to the activity of the conserved SNARE complex remodeling complex, NSF/α-SNAP[344, 460]. Therefore, it is extremely likely that the LegC proteins are utilized by *L. pneumophila* to recruit host membrane compartments, including ER and VAMP4-containing vesicles to the LCV during pathogenesis via hijacking host SNARE machineries.

Based on these previous works, we set out to reconcile the observation that *L. pneumophila* LegC7 is toxic to yeast with its ability to both interact with ER and endosomal compartments in model host cells and alter endosomal membrane trafficking pathways in yeast. We now find that high-level expression of LegC7 induces strong ER morphology defects in yeast, creating aberrant ER membrane structures that also colocalize with Vps8p-containing endosomal compartments. Both the ER morphology defects and growth inhibition observed upon LegC7 expression are completely reversed by deletions in so-called “class C” complex core genes (*VPS11, VPS16, VPS18, VPS33*) which comprise the core subunits of two endolysosomal multisubunit tethering complexes, CORVET (class C core vacuole/endosome tethering) and HOPS (homotypic fusion and vacuole protein sorting). We also observe that LegC7 expression increases the oxidation state of the ER lumen and induces the reconstitution of split-GFP protein fragments contained within ER and endosomal compartments. Coupled with the finding that LegC7 induces the degradation of the ER lumenal Kar2p protein in a vacuolar protease-dependent manner, we now provide evidence that LegC7 directs

the fusion of ER-derived compartments with endosomes in a CORVET/HOPS-dependent manner, thereby bypassing normal ER:Golgi trafficking. These results provide additional evidence that LegC proteins from *Legionella* directly recruit ER membrane to the LCV during infection.

Results

LegC7 immunoprecipitates an ER:Golgi cargo adapter complex.

LegC7/YlfA expression in yeast is known to be toxic[459], although the expression of the similar coiled-coil secreted effectors from *Legionella* (LegC2/YlfB and LegC3) is not toxic under the same growth conditions[458, 459]; therefore LegC7 appears to have an in vivo activity distinct to that of LegC2/3. In an effort to elucidate the mechanism of LegC7-mediated growth inhibition, whole cell extracts were generated from cells expressing LegC7 or empty vector controls, incubated with Protein A:α-LegC7 resin (See **Reagent preparation** in **Materials and Methods**, page115), and resultant immunoprecipitates were subjected to LC-MS/MS for total protein identification. When

Table 3.1. Protein ID list from LegC7 immunoprecipitations (scores > 300).

Protein Name	Score	# of Peptides
Emp47	3050.32	32
Emp46	1277.74	22
Sro9	923.29	9
Atp2	821.02	9
Glycine tRNA ligase	800.08	13
Hsc82	737.75	8
Ils1	666.45	13
Ssp120	481.79	7
Idh2	474.07	6
Mir1	403.57	6
Crn1	389.80	9
Ilv2	381.30	6
Adt2	362.39	5
YHR020W	317.44	7

eliminating proteins identified across both pulldown conditions, we noted a strong enrichment of the ER:Golgi glycoprotein cargo adapters, Emp47p and Emp46p (**Table 3.1**)[439, 441]. In addition, we noted the enrichment of the Emp47p-interacting protein, Ssp120p, suggesting a possible interaction of LegC7 with, or enrichment within, ER-derived COPII-coated vesicles.

As LegC7 appears to interact with an Emp47p-containing complex, we considered the possibility that LegC7 was glycosylated in vivo. To address this, we purified LegC7 from yeast extracts using the same Protein A:α-LegC7 resin used previously. SDS-PAGE bands containing LegC7 were excised and submitted to the University of Georgia Complex Carbohydrates Research Center for *N*-glycan analysis via nano-LC-MS/MS (Supplemental Materials and Methods). While peptides from LegC7 were clearly detected (**Fig. 3.9, Table 3.4**), no glycosylations or other post-translational modifications on any LegC7 peptide were discovered (**Fig. 3.10A-R**). Therefore, while LegC7 appears to interact with a known glycoprotein cargo receptor, this interaction either does not require glycosylation of LegC7, or this interaction is an indirect one.

***EMP46/47* deletions mimic the LegC7-induced inhibition of carboxypeptidase S trafficking.**

Given the apparent interaction between the Emp47p complex and LegC7, as well as our previous observation that LegC7 expression inhibits the delivery of GFP-tagged carboxypeptidase S (CPS-GFP) to vacuoles[340], we considered the possibility that LegC7 may interfere with Emp47p complex function, which then results in the

previously-observed CPS-GFP trafficking defects. Therefore, we observed the CPS-GFP trafficking phenotypes of *emp47*Δ *emp46*Δ strains and compared them to wild type strains expressing LegC7. Wild type yeast cells expressing CPS-GFP show a vacuolar lumenal distribution with few cytosolic punctae in each cell, likely representing endosomes containing CPS-GFP (**Fig. 3.1A, C, and D**). Expression of LegC7 results in the accumulation of punctate structures and far fewer cells containing vacuolar CPS-GFP, as seen previously[340] (**Fig. 3.1C and D**). When CPS-GFP localization is observed in an *emp46*Δ *emp47*Δ strain, we noted that fewer cells showed vacuolar localization of CPS-GFP, with a corresponding increase in cytosolic punctae, similar to that observed in LegC7-expressing strains (**Fig. 3.1B-D**). As the cellular distribution of

CPS-GFP is overall similar between LegC7-expressing and Emp-deficient strains, it is likely that LegC7 expression interferes with Emp47 complex function in some manner. Interestingly, however, *emp46*Δ *emp47*Δ deletion strains do not strongly reduce the LegC7-mediated growth inhibition (**Fig. 3.11**), suggesting that LegC7 does not absolutely depend upon the presence of Emp46/47 for function in vivo. Given the fact that Emp47 and Emp46 form an important cargo adapter complex residing in the ER and on COPII vesicles, however, we next decided to observe the effects of LegC7 expression on ER morphology.

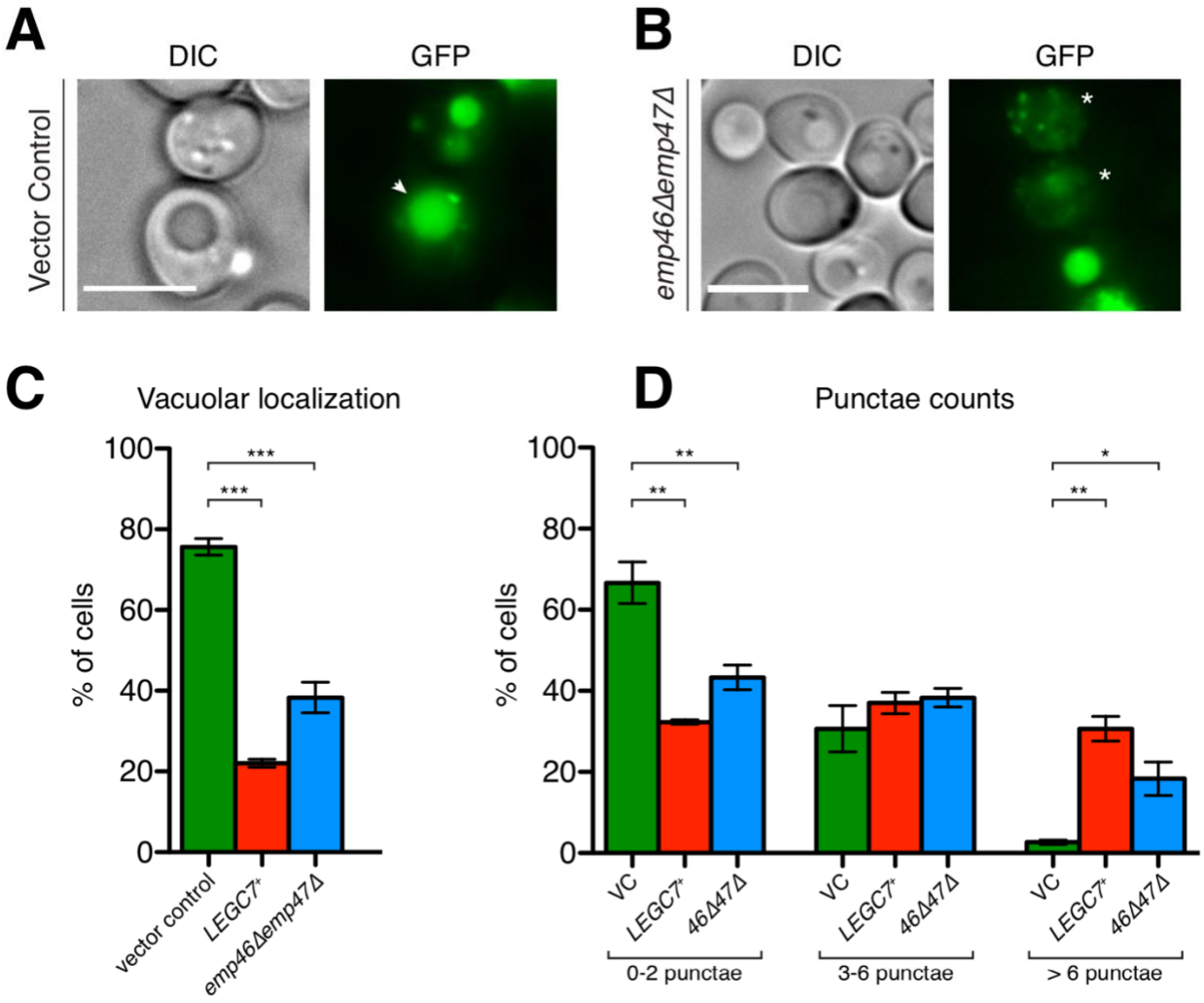

Figure 3.1. An *emp46*Δ*emp47*Δ double mutation and LegC7 expression both alter localization of Carboxypeptidase S. Yeast strains harboring GFP-CPS were visualized to determine vacuolar localization and number of punctae. All strains were grown to saturation in CSM medium at 30°C, harvested via centrifugation, resuspended in an equal volume of fresh CSM containing 1% raffinose and 1% galactose, and grown for an additional 18 h at 30°C before imaging. (**A**) and (**B**) are representative images of cells with and without vacuolar localization, respectively. The white arrow indicates vacuolar localization and the white astrisks indication cells without vacuolar localization. Scale bars = 5 μ. Individual cells were analyzed to determine vacuolar localization of GFP (**C**) and number of punctae (**D**). ≥ 100 cells each per three independent experiments were analyzed; error bars represent ± the standard deviation between experiments; (*) = $P < 0.05$; (**) = $P < 0.005$; (***) = $P < 0.0005$.

LegC7 expression alters normal ER morphology.

Based upon the discovery that LegC7 immunoprecipitates proteins known to reside in COPII-coated vesicles (Emp46p, Emp47p, and Ssp120p) involved in ER:Golgi protein transport, we decided to observe the effects of LegC7 expression on gross ER and Golgi morphologies. Yeast strains expressing GFP fusions of an ER translocon subunit, Sec63p, show the expected distribution of perinuclear and cortical ER membrane (**Fig. 3.2A**)[461]. Expression of a fluorescently-tagged LegC7, LegC7-mRuby2, however, induces a drastic redistribution of perinuclear ER membrane in cells which clearly express LegC7-mRuby (**Fig. 3.2A**). Strikingly, LegC7-mRuby2 appeared to accumulate in large punctate structures that overlapped with large accumulations of Sec63-positive membranes (**Fig. 3.2A, arrowheads**); these large Sec63-GFP accumulations were not observed in vector control strains. To ensure that the LegC7-mRuby2 fusion protein was still active in vivo, we confirmed that strains expressing LegC7-mRuby2 were inhibited for growth to the same extent as untagged LegC7 (**Fig. 3.12A**); N-terminal, GFP-tagged LegC7 was no longer toxic (**Fig. 3.12A**), even when strains expressed nearly equivalent levels of LegC7 (**Fig. 3.12B**). Therefore, we concluded that LegC7-mRuby2 still maintained LegC7 activity, and this activity results in ER morphology defects upon expression. To determine whether LegC7 expression also disrupts Golgi morphology, we performed similar experiments in strains expressing GFP-Vrg4, a *cis*-Golgi GDP-mannose transporter[462]. In control cells, *cis*-Golgi structures were observed to be generally punctate, with some perinuclear localizations (**Fig. 3.2B**), in agreement with previously reported structures[462]. In the presence of LegC7-mRuby2 expression, we noted similar punctate and perinuclear structures, and

LegC7-mRuby2 did not strongly colocalize with any Vrg4-GFP-positive membranes (**Fig. 3.2B**). Taken together, these images suggest that LegC7 expression does not strongly alter normal cis-Golgi morphology, while having strong effects on normal ER morphology.

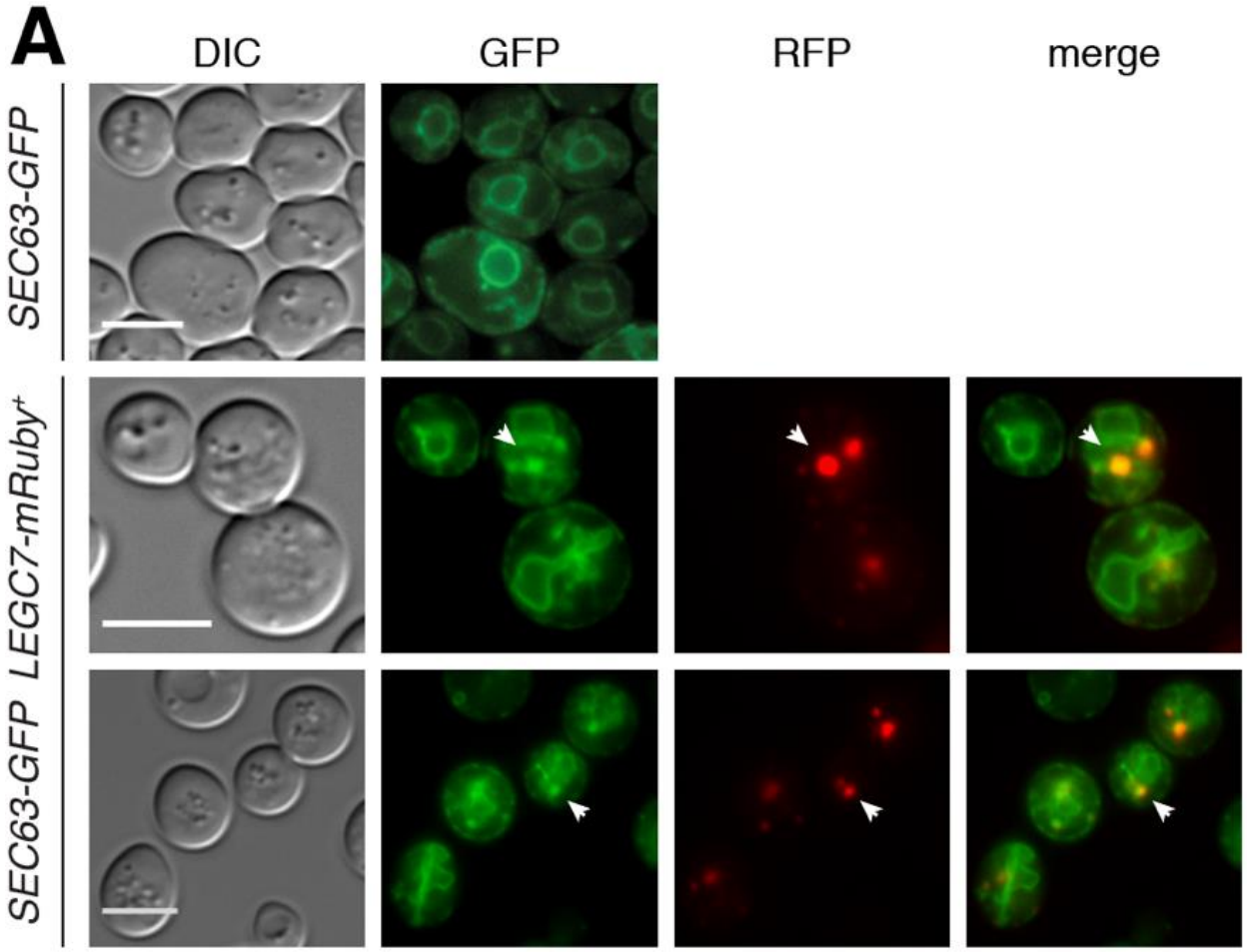

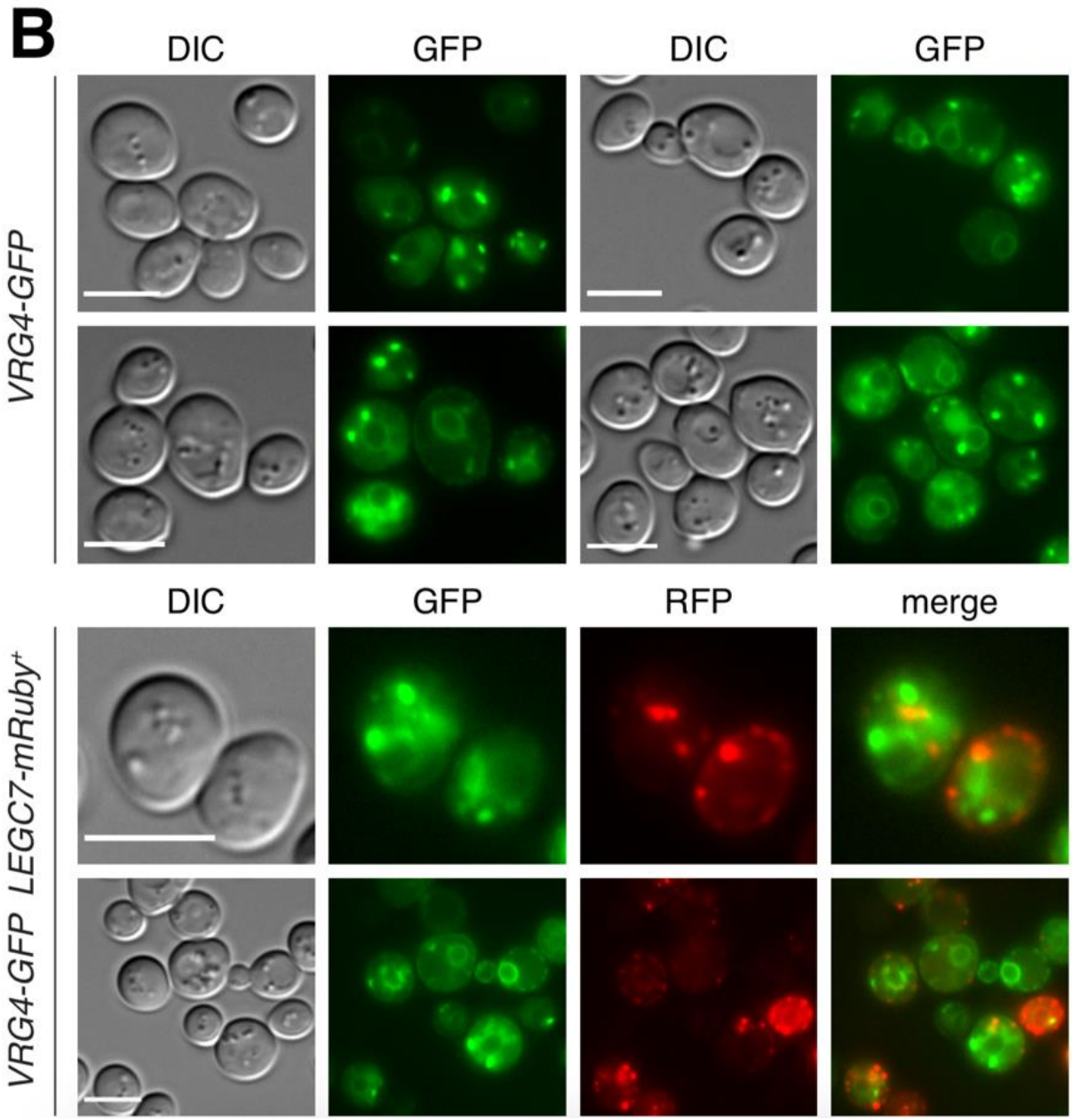

Figure 3.2. LegC7 alters ER morphology but doesn't affect Golgi morphology in a discernable manner. Yeast strains expressing LegC7-mRuby2 and GFP fusions of ER translocon subunit Sec63p (**A**) or cis-Golgi GDP-mannose transporter Vrg4p (**B**) were visualized. All strains were grown to saturation in CSM medium at 30°C, harvested via centrifugation, resuspended in an equal volume of fresh CSM containing 1% raffinose and 1% galactose, and grown for an additional 18 h at 30°C before imaging. Arrows indicate patches where LegC7-mRuby2 and Sec63-GFP colocalize. Scale bars = 5 μ.

Deletion of the class C tethering complex subunits suppresses LegC7-mediated growth inhibition.

In parallel to observing the effects of LegC7 expression on ER membrane structure, we also considered that LegC7 expression was previously shown to inhibit the delivery of proteins to the degradative vacuole via both biosynthetic and endocytic pathways[340]. To identify the potential targets of LegC7 activity on potential endolysosomal or protein trafficking targets, we performed a directed screen of 86 gene deletions that focused on general membrane trafficking mechanisms to identify strains that continued to grow in the presence of LegC7 expression**.** Among all gene deletions screened, deletions of the CORVET and HOPS tethering core complex subunits (Vps11p, Vps16p, Vps18p, Vps33p) resulted in nearly complete restoration of growth in the presence of LegC7 expression (**Fig. 3.3A**). CORVET (class C core vacuole/endosome tethering) and HOPS (homotypic fusion and protein sorting) are hexameric tethering complexes that facilitate the SNARE-dependent fusion of endolysosomal compartments through direct interactions with Rab-family GTPases, SNARE complexes, and membrane lipids across apposed organelles[415, 418].

In addition to the shared core subunits listed above, each distinct tethering complex contains two unique and interchangeable subunits, which mediate binding specificity to Rab-family GTPases (**Fig. 3.3B**). CORVET contains Vps3p and Vps8p, which bind to the Rab5 homolog, Vps21p, found on early endosomal membranes[463, 464]. HOPS complex contains Vps39p and Vps41p, which bind to the Rab7 homolog, Ypt7p, found on late endosomal and vacuolar membrane compartments[465-467]. As both HOPS and CORVET complexes are disrupted in class C core mutant strains, we

individually deleted each of the Rab-specific subunits of these complexes to determine the effects of CORVET- or HOPS-specific disruptions on LegC7 activity. Unlike what we observed with the core subunit deletions, however, deletions of the Rab-specific subunits resulted in varying degrees of restored growth in the presence of LegC7 expression **(Fig. 3.3A)**. It was interesting to note that, of the four interchangeable subunits, deletions of the CORVET-specific *VPS8* gene provided the strongest restoration of growth to LegC7-expressing strains under these conditions. As Vps8p interacts directly with the endosomal Rab GTPase, Vps21p, as a part of the CORVET complex[463, 464], it raised the possibility that proper endosomal fusion dynamics is required for the *in vivo* toxicity of LegC7 in yeast.

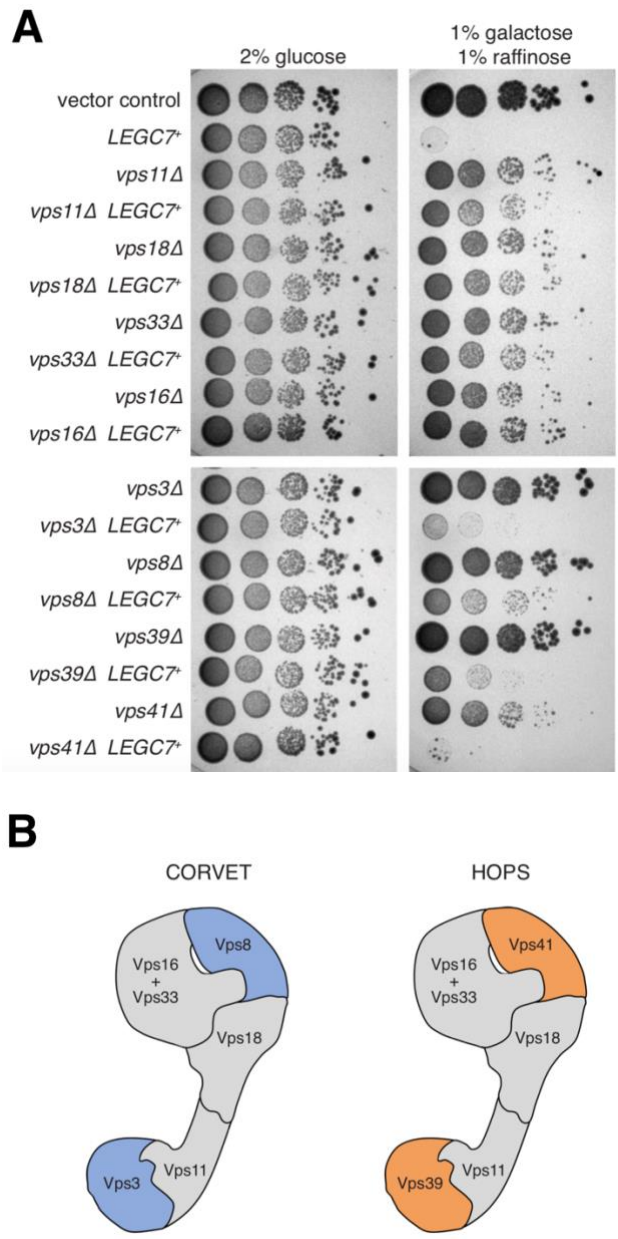

Figure 3.3. Deletion of class C tethering complex subunits suppresses LegC7-mediated growth inhibition. (**A**) Yeast deletion mutants harboring either pYES2NT C or pYES2-LEGC7+ were grown to saturation in CSM at 30°C. For each strain, 1 OD600 unit was harvested via centrifugation, resuspended in 1 mL of 0.9% NaCl, and serially diluted 1:10 four times. 5 µL of each dilution was plated onto CSM containing 2% glucose and CSM containing 1% galactose and 1% raffinose to induce LegC7 expression. (**B**) Models of the class C tethering complexes are displayed, with the core complex in gray and the Rab-specific subunits in blue and orange.

LegC7 induces colocalization of Vps8p and ER.

As class C core gene deletions and *VPS8* deletions appeared to suppress the toxicity of LegC7 expression, we decided to visualize the localization of some representative CORVET/HOPS complex subunits in the presence of LegC7. Vps8-GFP (CORVET) normally forms a punctate pattern in the cell (**Fig. 3.4A**), as expected[468]. Upon co-expression of LegC7-mRuby, however, we find Vps8-GFP punctae that strongly colocalize with LegC7-mRuby (**Fig. 3.4A and F**). Expression of LegC7 in strains harboring Vps33-GFP, representative of the class C core complex, does not dramatically alter the localization of Vps33-GFP, nor does LegC7 appreciably colocalize with Vps33-GFP/class C core (**Fig. 3.4B and F**). Also, in contrast to the colocalization observed between LegC7 and Vps8p, LegC7-mRuby2 did not colocalize with the Vps21 effector of the CORVET complex (**Fig. 3.4D**).

Because LegC7-mRuby colocalized with both Vps8-GFP and Sec63-GFP punctae (**Fig. 3.2A**), we then considered the possibility that these Vps8p-positive and Sec63-positive structures also colocalized in response to LegC7. In strains lacking LegC7, Vps8-GFP and Sec63-RFP form expected morphologies and do not colocalize (**Fig. 3.5A**). In the presence of LegC7, however, we noted both defective ER morphology coupled with a strong recruitment of Vps8-GFP to the Sec63-RFP punctae (**Fig. 3.5A**); these structures may therefore represent accumulation of endosomal material on the ER membrane. Due to the requirements of CORVET/HOPS subunits for LegC7 toxicity, coupled with the observation that endosomal material accumulates on the ER in a LegC7-dependent manner, we sought to determine if CORVET/HOPS complex activity was required for the LegC7-dependent disruption of ER morphology.

To address this possibility, both LegC7-mRuby2 and Sec63-GFP were expressed in a *vps33*Δ mutant strain, which lacks functional CORVET/HOPS complexes. Strikingly, the aberrant ER phenotype normally observed in strains expressing LegC7 (**Fig. 3.5C**) was not present, and the ER morphology of these cells appeared to be completely wild type. Therefore, these data suggest that the function of endosomal tethering complexes plays a role in the aberration of the ER observed with LegC7 expression, despite the fact that CORVET/HOPS complexes function exclusively in endolysosomal membrane dynamics and play no known role in ER-to-Golgi transport[415, 418].

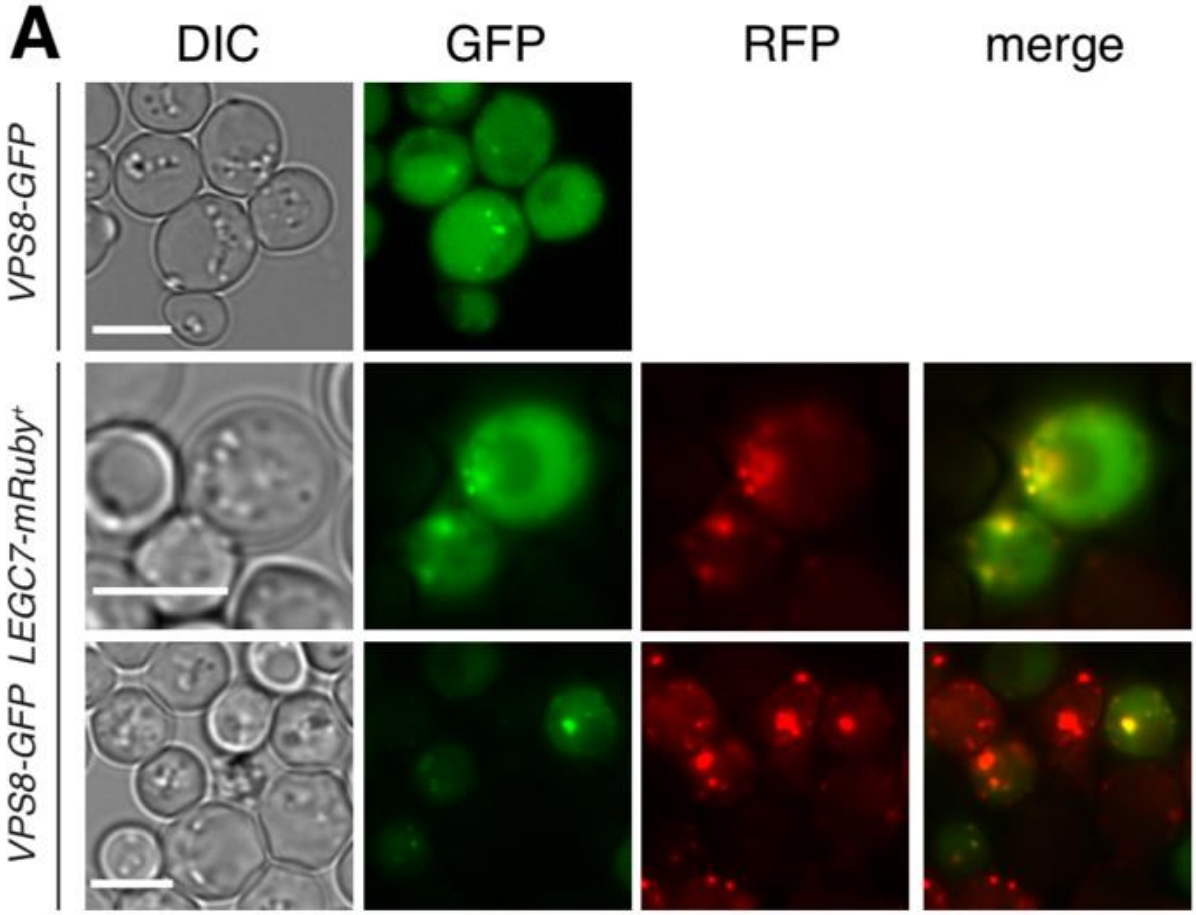
A
DIC
GFP
RFP
merge
VPS8-GFP
VPS8-GFP LEGC7-mRuby+

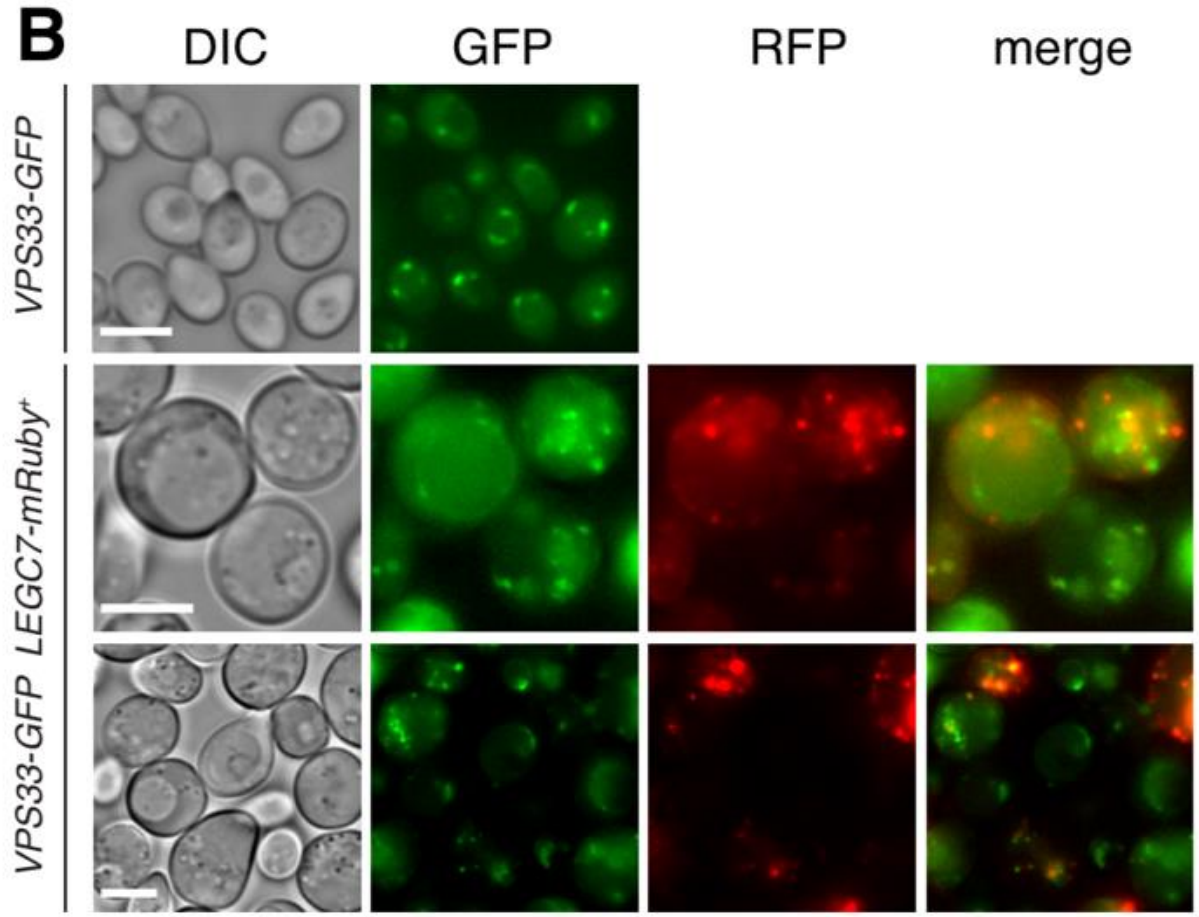
B
DIC
GFP
RFP
merge
VPS33-GFP
VPS33-GFP LEGC7-mRuby+

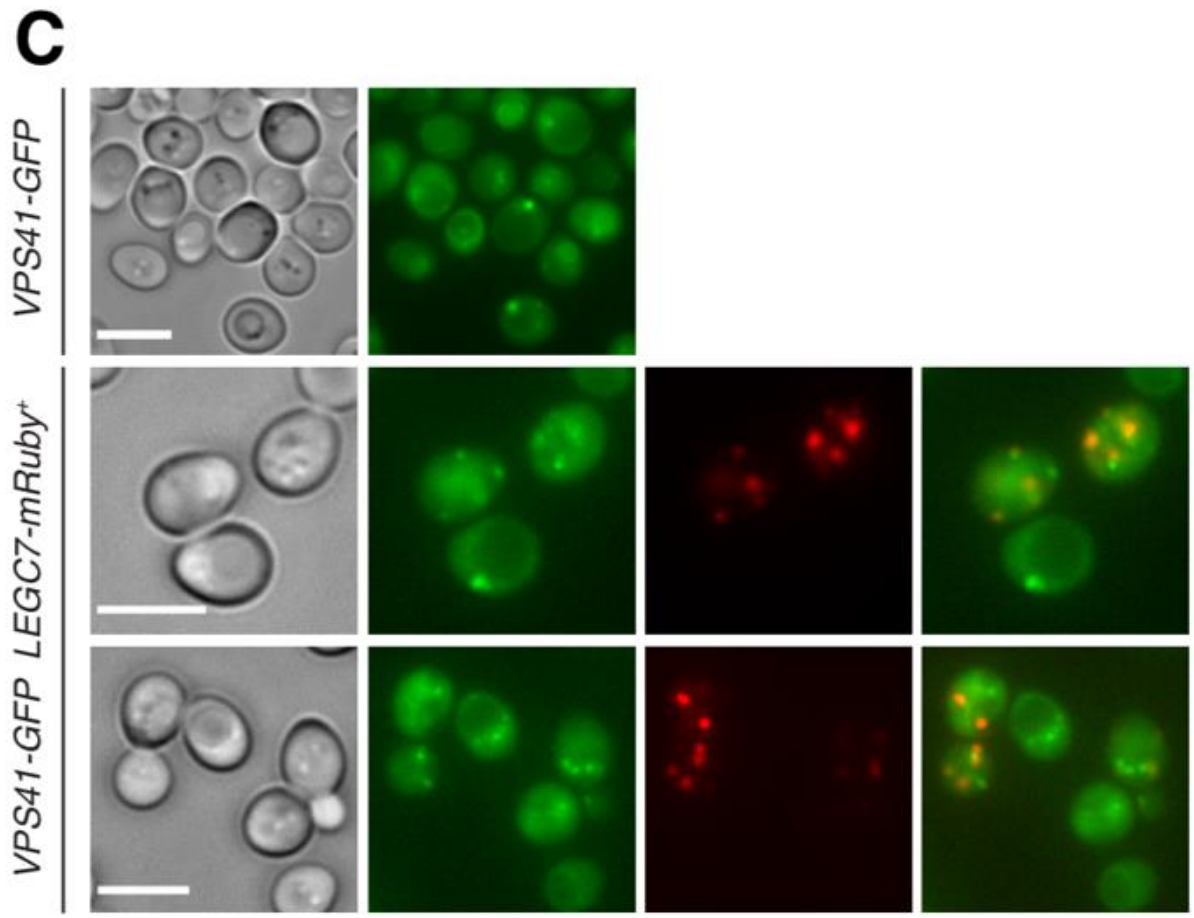
C
VPS41-GFP
VPS41-GFP LEGC7-mRuby+

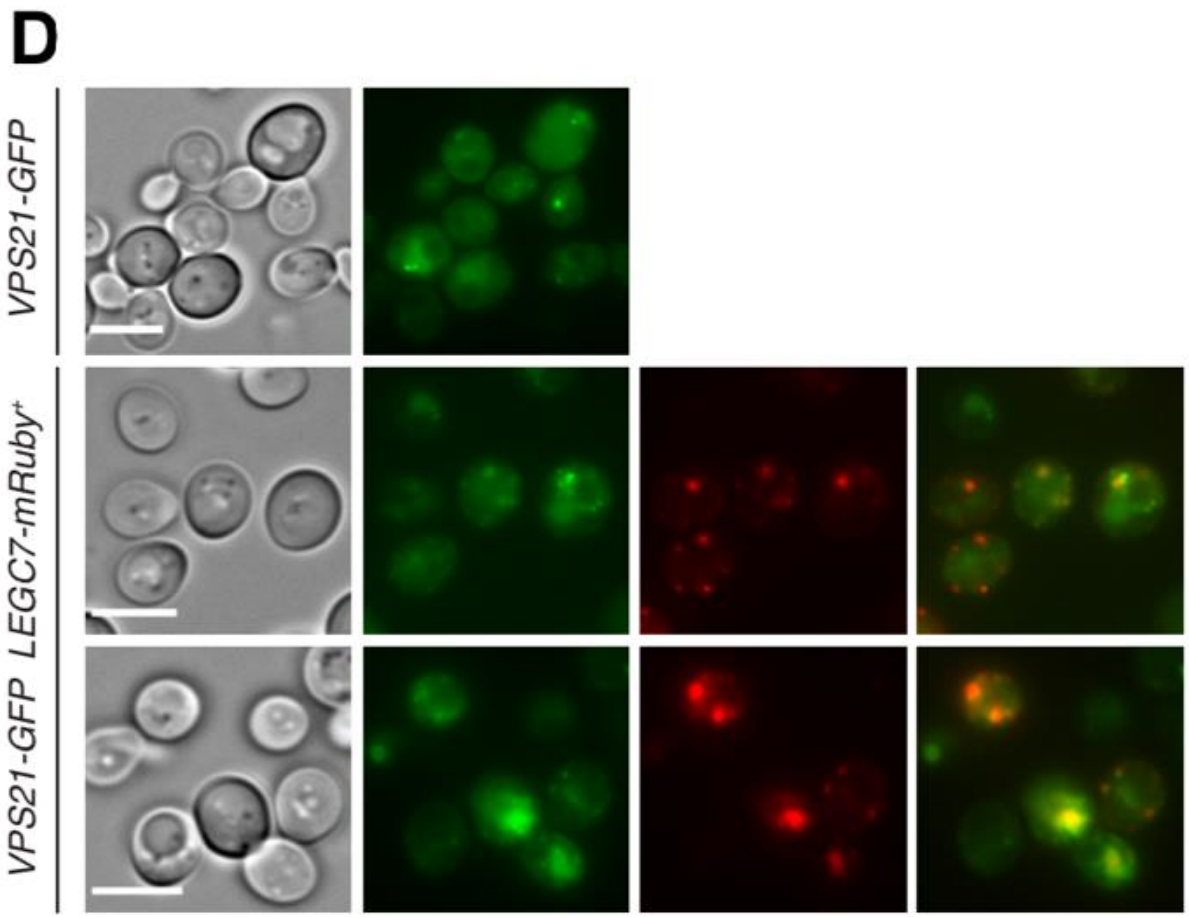
D
VPS21-GFP
VPS21-GFP LEGC7-mRuby+

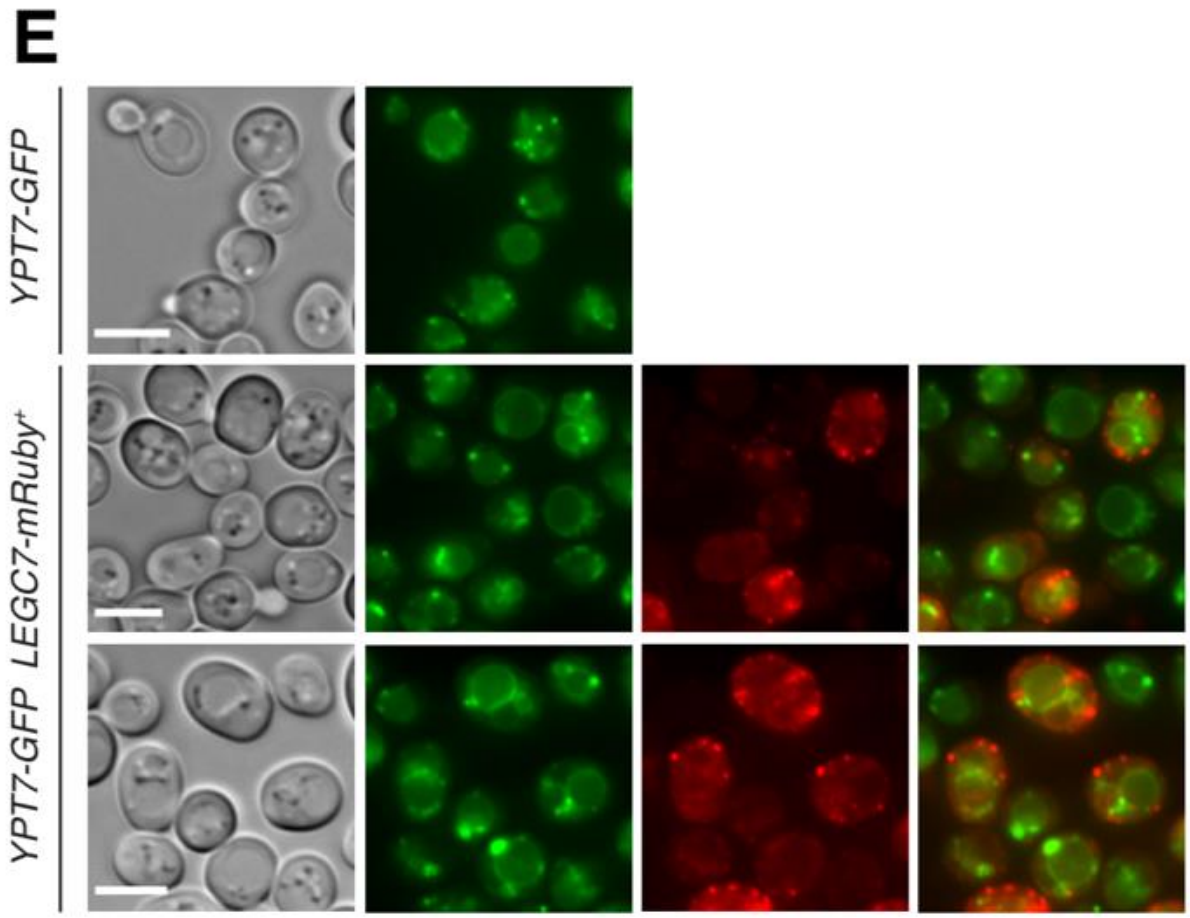
E
YPT7-GFP
YPT7-GFP LEGC7-mRuby+

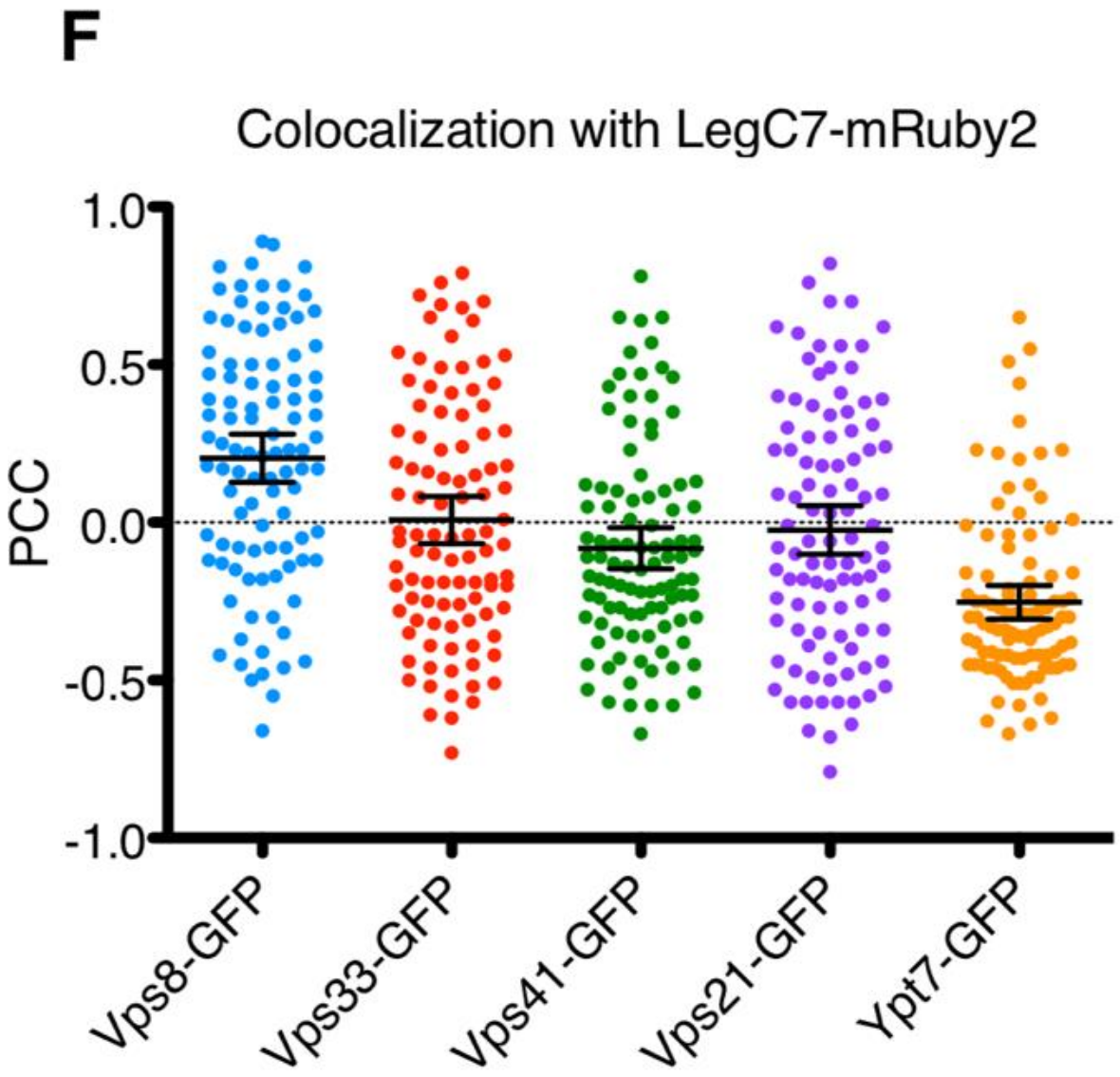

Figure 3.4. LegC7 colocalizes with early endosomal fusion machinery more than that of late endosomes. Yeast strains expressing LegC7-mRuby2 and GFP fusions CORVET-specific subunit Vps8p (**A**), class C core complex subunit Vps33p (**B**), HOPS-specific subunit Vps41p (**C**), early endosomal Rab5 homolog Vps21p (**D**), and late endosomal Rab7 homolog Ypt7p (**E**) were visualized. All strains were grown to saturation in CSM medium at 30°C, harvested via centrifugation, resuspended in an equal volume of fresh CSM containing 1% raffinose and 1% galactose, and grown for an additional 18 h at 30°C before imaging. Scale bars = 5 μ. (**F**) Colocalization of GFP and mRuby2 was quantified in the form of Pearson correlation coefficients (PCCs) for 100 cells per strain using the Coloc2 plugin in Fiji (ImageJ). Error bars represent 95% confidence intervals of the average PCC.

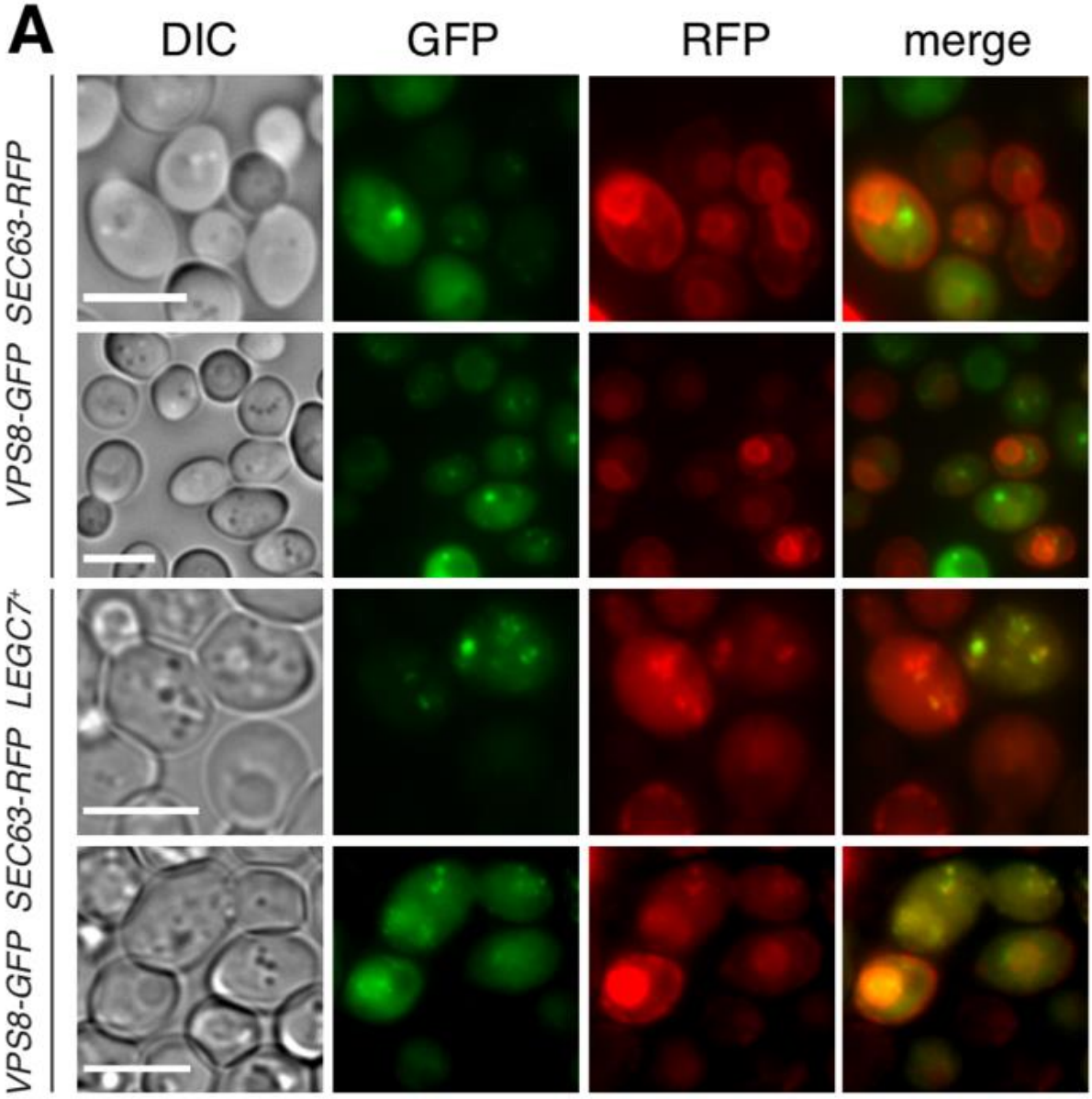
A
DIC
GFP
RFP
merge
VPS8-GFP SEC63-RFP
VPS8-GFP SEC63-RFP LEGC7+

B

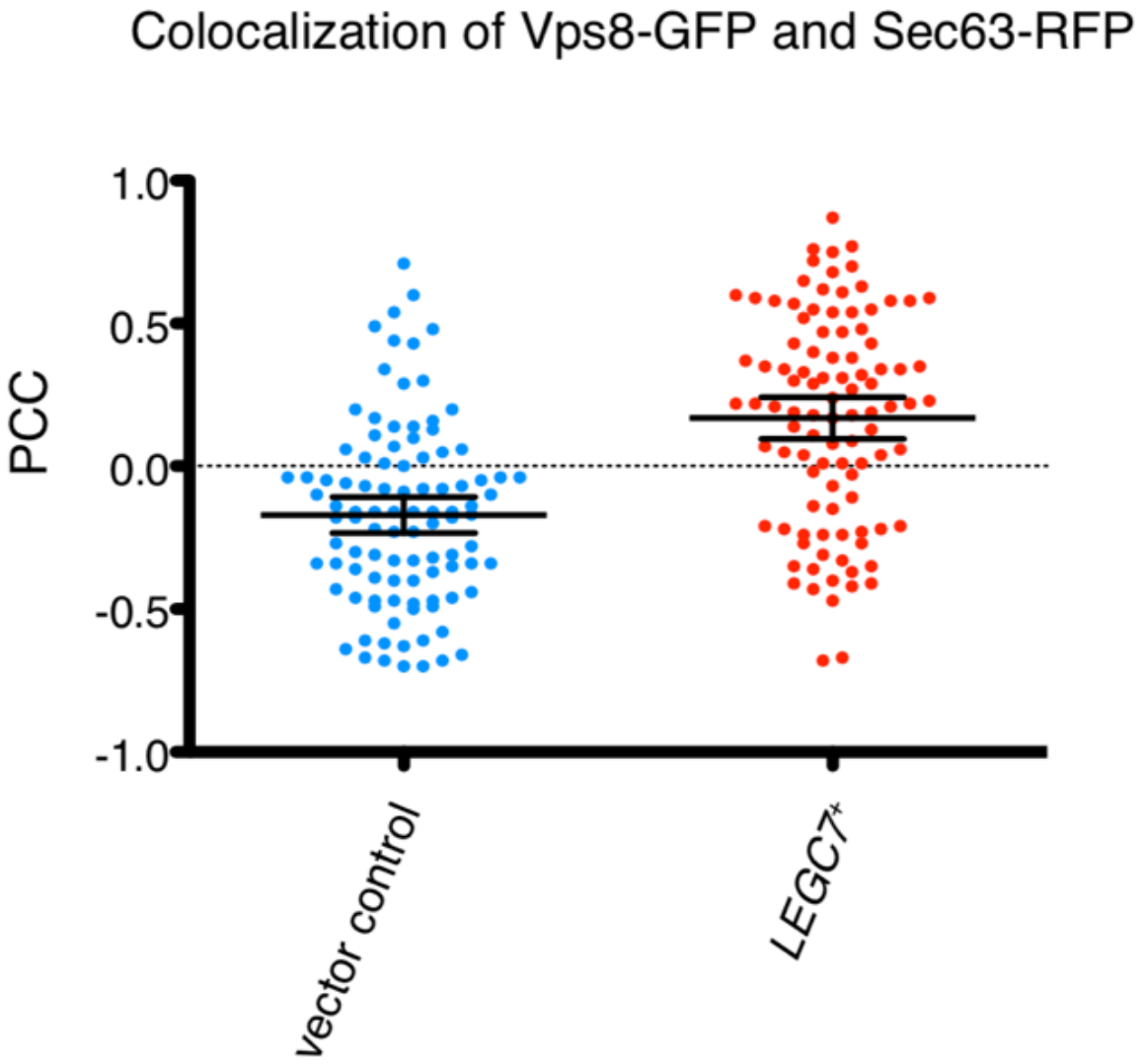
Colocalization of Vps8-GFP and Sec63-RFP
PCC
1.0
0.5
0.0
-0.5
-1.0
vector control
LEGC7*

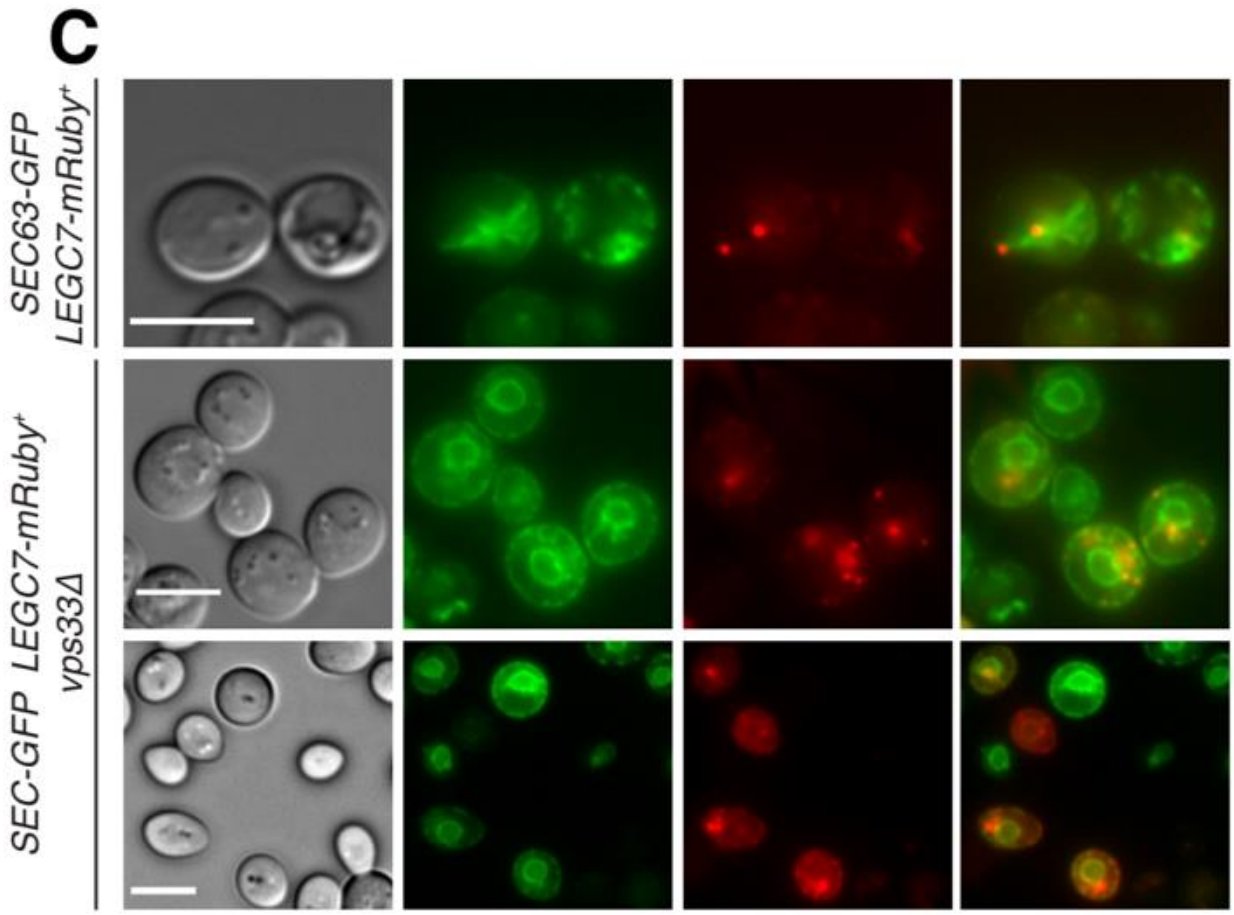

Figure 3.5. CORVET subunit Vps8p localizes to the ER during LegC7 expression, and endosomal tethering machinery is required for LegC7-induced alteration of ER morphology. (**A**)Yeast strains containing Vps8-GFP, Sec63-RFP, and pYES2NT C or pYES2-*LEGC7*+ were visualized. (**B**) Colocalization of GFP and RFP was quantified in the form of Pearson correlation coefficients (PCCs) for 100 cells per strain in (**A**) using the Coloc2 plugin in Fiji (ImageJ). Error bars represent 95% confidence intervals of the average PCC. (**C**) Yeast strains containing Sec63-GFP and expressing LegC7-mRuby2 were visualized to observe the effect of a vps33Δ deletion on ER morphology during LegC7 expression. All strains were grown to saturation in CSM medium at 30°C, harvested via centrifugation, resuspended in an equal volume of fresh CSM containing 1% raffinose and 1% galactose, and grown for an additional 18 h at 30°C before imaging. Scale bars = 5 μ.

LegC7 causes the degradation of ER lumenal content.

As LegC7 has an N-terminal transmembrane domain[459] and induced abnormal ER and endolysosomal structures upon expression, we attempted to identify the membrane compartment to which LegC7 localized via subcellular fractionation. Total membranes from yeast strains expressing LegC7 were fractionated in a density-dependent manner. Each fraction from the gradient was TCA precipitated and probed via western blotting for ER and Golgi marker proteins and LegC7. While LegC7 appeared to localize to membranes with a density between ER (Kar2p) and Golgi (Och1p) (**Fig. 3.6A**), we also noted a faint degradation product of the ER lumenal protein Kar2p in the low-density fractions of the LegC7-expressing strain; this product was never observed in any fractions of the control strain (**Fig. 3.6A**). With this finding, we considered the possibility that this degradation results from the fusion of endolysosomal compartments and ER facilitated by LegC7, thereby exposing Kar2p to vacuolar proteases.

To test whether LegC7-dependent degradation of Kar2p requires vacuolar proteases, whole cell extracts of a vacuolar protease-deficient *pep4*Δ mutant expressing LegC7 were probed for the Kar2p degradation product. The degradation product does not appear in a *pep4*Δ mutant, demonstrating a requirement for vacuolar proteases for LegC7-dependent Kar2p degradation (**Fig. 3.6B**). This Kar2p degradation is also absent in both a CORVET/HOPS-deficient *vps33*Δ mutant and an endosomal t-SNARE-deficient *pep12*Δ mutant, demonstrating that endosomal fusion machinery is necessary for this degradation event as well. Notably, LegC7-dependent Kar2p degradation does

appear in an *atg1*Δ mutant, confirming that this degradation event is independent of cellular autophagic processes, including ER-phagy[469, 470].

Given that LegC7 causes vacuolar protease-dependent degradation of Kar2p, mutants screened for Kar2p degradation were also screened for LegC7-induced growth inhibition to determine if growth inhibition is a direct result of degradation of ER lumenal contents. Aside from the complete restoration of growth in the *vps33*Δ strain (**Fig. 3.3A**), *pep12*Δ provides suppression of LegC7 toxicity, while *pep4*Δ does not (**Fig. 3.6C**), strongly supporting the hypothesis that while endosomal fusion machinery is required for vacuolar protease-dependent degradation of Kar2p, simple degradation of ER lumenal contents by vacuolar proteases is not the reason for the LegC7-mediated growth inhibition.

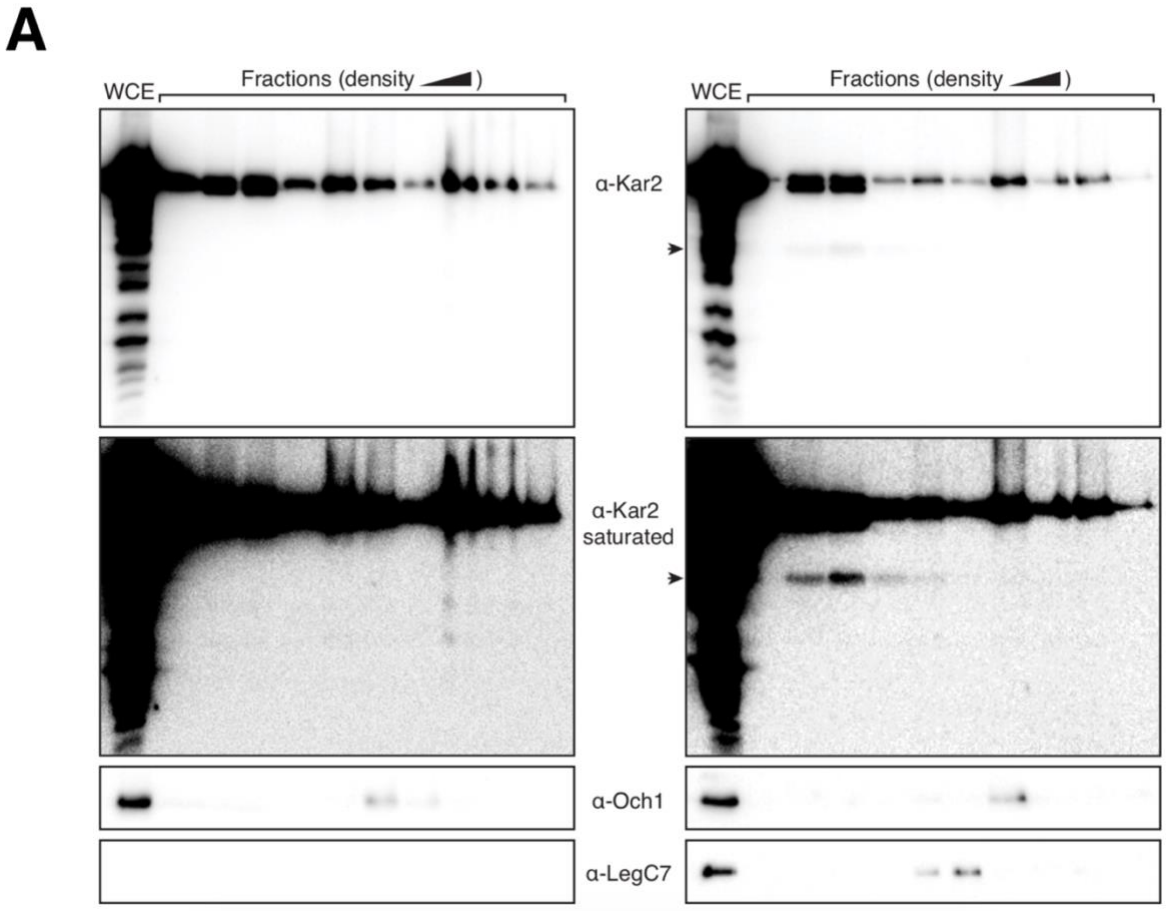

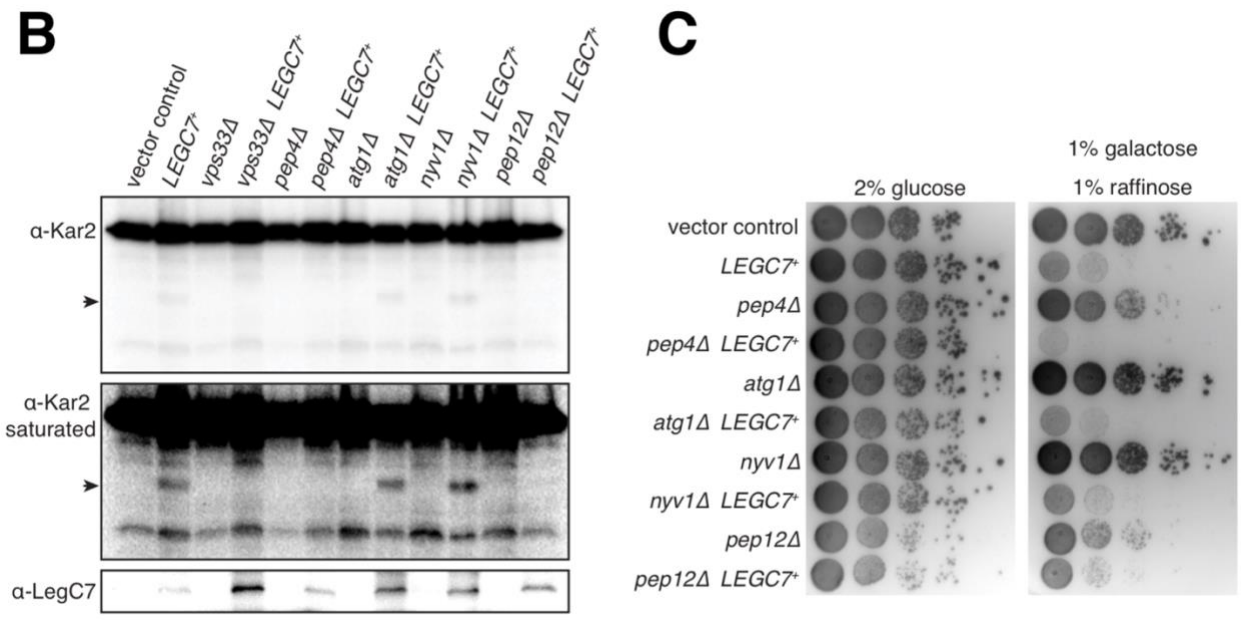

Figure 3.6. LegC7 causes the degradation of ER lumenal ATPase Kar2p, dependent upon endosomal fusion machinery and vacuolar proteases. (**A**) Yeast strains containing pYES2NT C or pYES2-*LEGC7*+ were grown to saturation in CSM medium at 30°C, harvested via centrifugation, resuspended in an equal volume of fresh CSM containing 1% raffinose and 1% galactose, and grown for an additional 18 h at 30°C. Equal amounts of each strain were harvested via centrifugation, dounced, fractionated into 10 fractions, and fractions were TCA precipitated (**Materials and Methods**). Equal volumes of each fraction were separated via SDS-PAGE and immunoblotted for the ER lumenal ATPase Kar2p, the cis-Golgi mannosyltransferase Och1p, and LegC7. (B) Strains were treated as in (A) but not fractionated. Equal volumes of whole cell extracts were separated via SDS-PAGE and immunoblotted for Kar2 and LegC7. The black arrows in (A) and (B) indicate Kar2 degradation product caused by LegC7. (C) Yeast deletion mutants harboring either pYES2NT C or pYES2-LEGC7+ were grown to saturation in CSM at 30°C. For each strain, 1 OD600 unit was harvested via centrifugation, resuspended in 0.9% NaCl, and serially diluted 1:10 four times. 5 µL of each dilution was plated onto CSM containing 2% glucose and CSM containing 1% galactose and 1% raffinose to induce LegC7 expression.

LegC7 expression alters the redox state of the ER lumen.

To determine whether LegC7 expression altered the general physiology of the ER through a potential ER:endosome fusion event, we employed a redox-sensitive, ER-targeted GFP (eroGFP) to observe the redox state of the ER lumen during LegC7 expression. EroGFP contains a pair of cysteine residues that form a disulfide bond under oxidizing conditions, which reorients the chromophore. This reorientation decreases excitation at a 488 nm, and increases excitation at a 405 nm; the ratio of fluorescence from these two maxima serves as a measurement for the redox state of the ER lumen in vivo[471]; addition of either DTT (reducing) or H_2O_2 (oxidizing) to cells expressing eroGFP changes this ratio, as expected (**Fig. 3.13**) . To determine the effects of LegC7 expression on the ER redox state, cells (n=10^5) were passed through a flow cytometer 6 hours post-induction of LegC7 expression, and fluorescence from excitation at 405 nm and 488 nm was measured. Fluorescence from cells without eroGFP (**Fig. 3.7A**) and heat-killed, eroGFP-expressing cells (**Fig. 3.7B**) was measured to define populations of low-fluorescence cells and dead eroGFP-expressing cells, respectively. These populations were removed from data sets for each other strain (**Fig. 3.7C-F**) to isolate the populations used to determine the ratio of fluorescence (Ex_{405}/Ex_{488}) as a measure of ER redox state (**Fig. 3.7G-J**).

Typically, the ER maintains an oxidizing environment to facilitate the oxidative folding of nascent proteins[472]. After 6 hours of LegC7 expression, the ratio of fluorescence (Ex_{405}/Ex_{488}) increases ~10% compared to the vector control, corresponding to a higher percentage of oxidized eroGFP molecules (**Fig. 3.7K**), similar to the observed response to 10 mM H_2O_2 (**Fig. 3.13**). However, LegC7 expression in a

*vps33*Δ strain does not change the ratio of fluorescence compared to the vector control (**Fig. 3.7I, J, and K**); suggesting that further oxidation of the ER lumen during LegC7 expression is dependent upon functional endosomal tethering complexes.

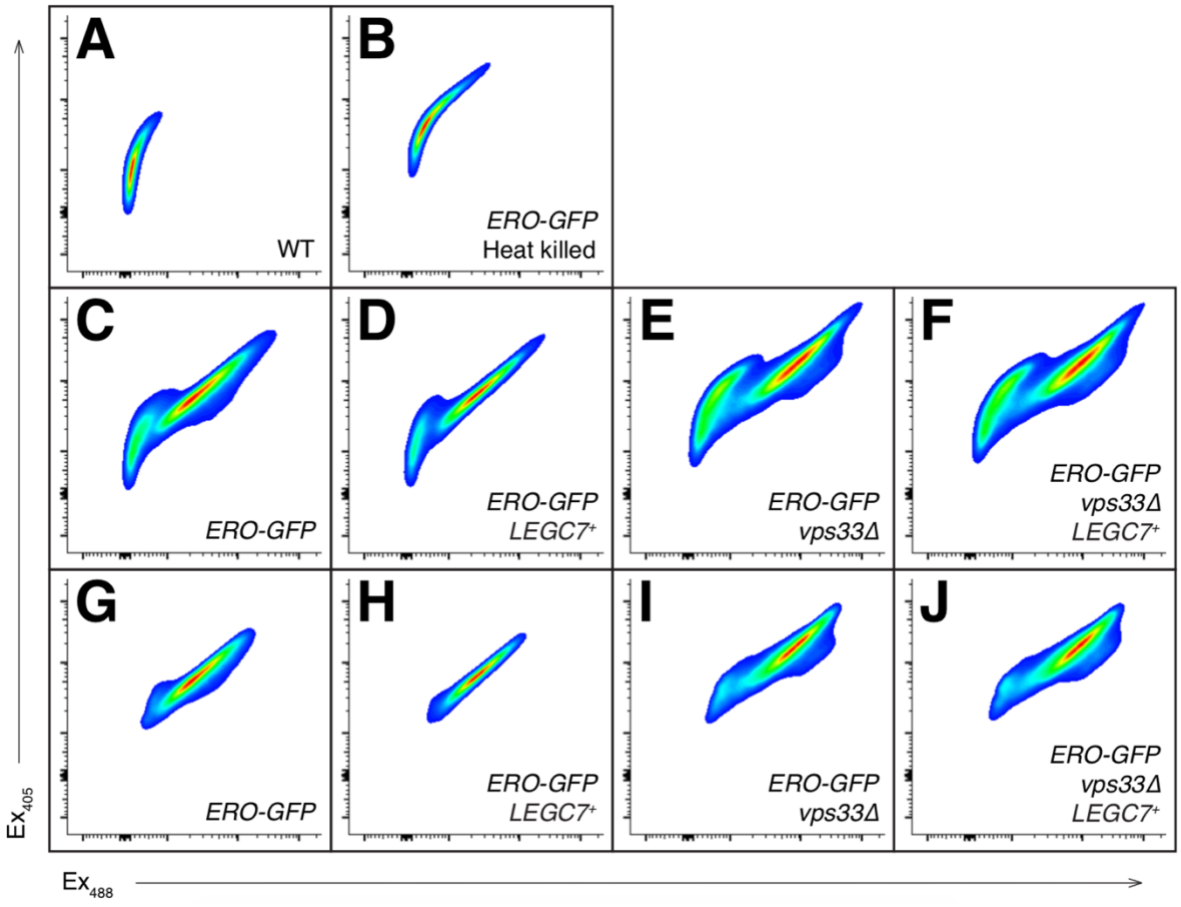

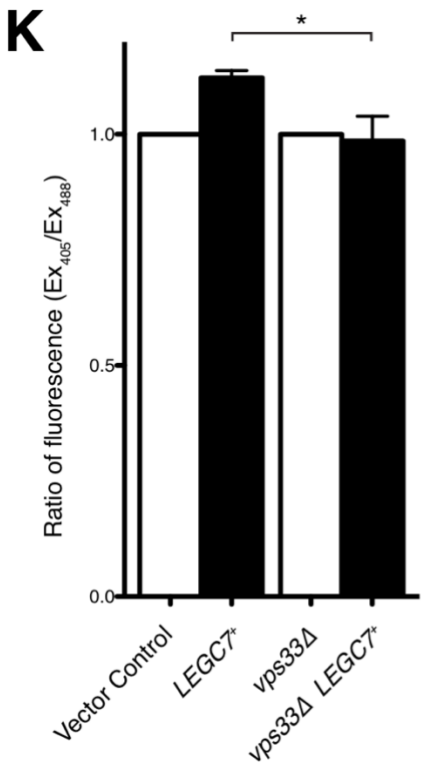

Figure 3.7. LegC7 expression oxidizes the ER lumen, but not in a *vps33*Δ mutant. Yeast strains containing ER-targeted redox-sensitive eroGFP were grown to saturation in CSM medium at 30°C, harvested via centrifugation, resuspended in an equal volume of fresh CSM containing 1% raffinose and 1% galactose, and grown for an additional 6 h at 30°C. Cells were then analyzed via flow cytometry (n = 105). Gates for cells without eroGFP (**A**) and heat-killed cells containing eroGFP (**B**) were used to eliminate low fluorescence and dead cell populations, respectively, from strains in panels (**C – F**) to generate panels (**G – J**). (**K**) Ratios of GFP fluorescence (Ex405/Ex488) were calculated, and ratios for (**G**) and (**H**) were normalized by the same factor such that the ratio for (**G**) = 1. ratios for (**I**) and (**J**) were normalized such that the ratio for (**I**) = 1. Three independent experiments were performed to generate ratios displayed in (**K**); error bars represent ± the standard deviation between experiments; (*) = $P < 0.05$. Panels (**A – J**) are representative plots, taken from one experiment.

LegC7 may induce ER:endosome fusion events.

Based on our evidence suggesting LegC7 induces fusion of ER and endosomal compartments, we designed a split-GFP bimolecular complementation system to assess this possibility in vivo (**Fig. 3.8A**). It is known that the GFP chromophore can be divided into two separate, non-fluorescent domains (GFP_{1-10} and GFP_{11})[473]. However, upon being brought into close proximity to each other, the GFP_{11} helix can interact with GFP_{1-10}, thereby reconstituting functional and fluorescent GFP[473]. Therefore, by directing these individual domains of GFP to the lumen of distinct membrane-bound compartments, we can measure reconstituted GFP fluorescence as a proxy for a fusion event. To measure the possibility of ER fusing to endosomal compartments, GFP_{1-10} was fused to the first 50 amino acids of the vacuolar carboxypeptidase Y protein (CPYss), which is known to be responsible for the targeting of CPY to the vacuole via endosomes[474]. In addition, the GFP_{11} helix was fused to the C-terminus of the transmembrane domain of integral ER membrane protein Scs2p (Scs2TM) to direct it to the lumenal side of the ER [473]. In order to confirm proper localization of these constructs, mRuby2 was fused to the N-terminus of Scs2TM-GFP_{11}. CPYss-mRuby2-GFP_{11} was also constructed as a control to confirm the delivery of CPYss-GFP_{1-10} to endosomes and to control for endosomal compartment density during LegC7 expression (**Fig. 3.8A**).

Cells harboring CPYss-GFP_{1-10} (endosomes), mRuby2-Scs2TM-GFP_{11} (ER), and a vector control were grown to mid-log, lysed, and membrane-bound compartments were subjected to density-dependent fractionation. Following fractionation, GFP fluorescence of each fraction collected was measured and plotted as a percentage of

the total fluorescence across all fractions (**Fig. 3.8B**). The remainder of each fraction was TCA precipitated and probed for organelle markers and LegC7. In strains expressing LegC7, the maximum GFP fluorescence ratio peak shifts towards more dense compartments; this shift was highly reproducible across experiments (**Figs. 3.8B and C**). LegC7 expression had no effects on the fractionated GFP fluorescence from strains expressing CPYss-GFP_{1-10} and CPYss-mRuby2-GFP_{11} (both endosomal, **Fig. 3.14**). Interestingly, the two fractions with significantly higher GFP fluorescence during LegC7 expression, fractions 19 and 20 (**Fig. 3.8C**), were the most dense fractions in which Kar2p degradation was first detected (**Fig. 3.8B, bracket**).

While LegC7 protein did not colocalize with compartments containing the Kar2p degradation product, LegC7 induced an apparent enrichment of early endosomal t-SNARE Pep12p in more dense fractions also containing ER membrane (Kar2p) and LegC7 (**Fig. 3.8B,** right panel), suggesting a shift of endosomal membranes to ER densities. Taken together, these results show that LegC7 expression causes the mixing of some ER and endosomal compartments, resulting in the reconstitution of a split-GFP protein and causing aberrant degradation of ER content by endosomal/vacuolar proteases.

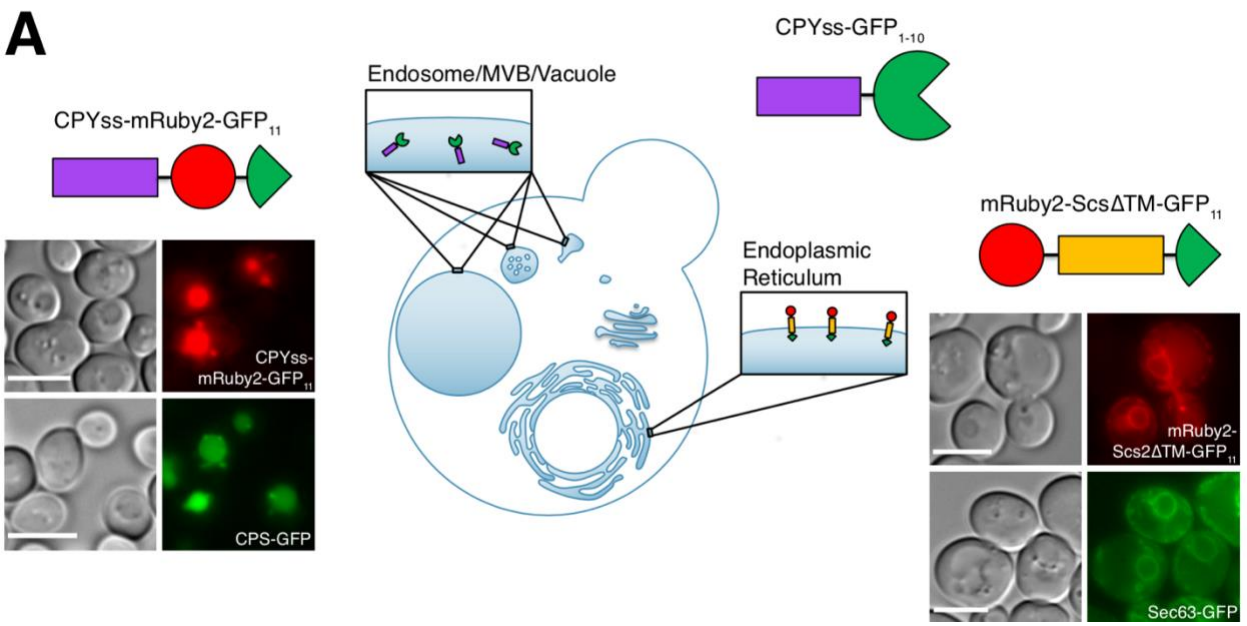
A
CPYss-mRuby2-GFP11
CPYss-GFP1-10
Endosome/MVB/Vacuole
Endoplasmic Reticulum
mRuby2-ScsΔTM-GFP11
CPYss-mRuby2-GFP11
CPS-GFP
mRuby2-Scs2ΔTM-GFP11
Sec63-GFP

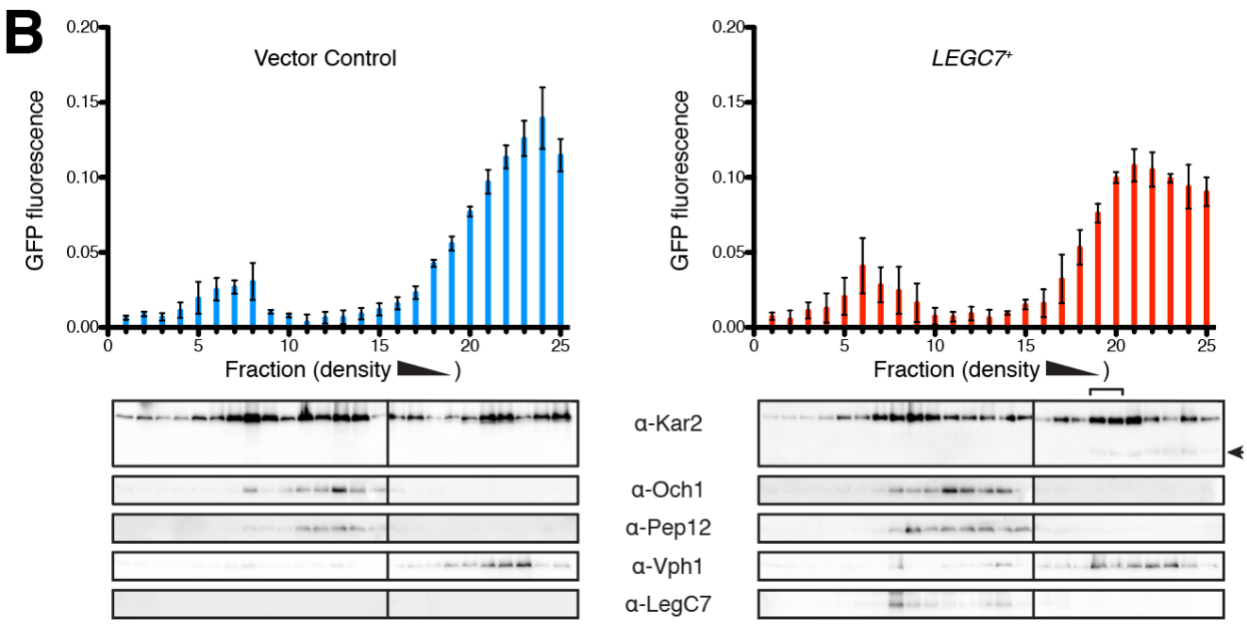
B
Vector Control
LEGC7+
GFP fluorescence
Fraction (density)
α-Kar2
α-Och1
α-Pep12
α-Vph1
α-LegC7

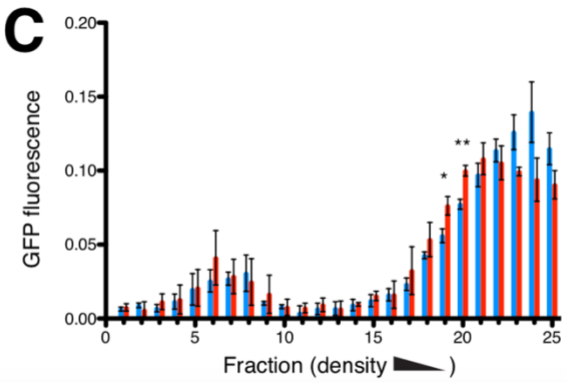

Figure 3.8. LegC7 may cause fusion of ER-derived and endosomal compartments. (**A**) Model of the split-GFP system constructed for this study. Strains containing individual constructs were grown to saturation in CSM medium at 30°C for imaging. Scale bars = 5 µ. (**B**) Strains containing ER-targeted mRuby2-ScsΔTM-GFP11 and endosome-targeted CPYss-GFP1-10 and either pYES2NT C (left) or pYES2-LEGC7+ (right) were grown to saturation in CSM medium at 30°C, harvested via centrifugation, resuspended in an equal volume of fresh CSM containing 1% raffinose and 1% galactose, and grown for an additional 18 h at 30°C. Equal amounts of each strain were fractionated into 25 fractions (**Materials and Methods**), and 20 µL volumes of each fraction were measured in triplicate for GFP fluorescence and averaged. Error bars represent ± the standard deviation across three independent experiments. The remainder of each fraction was TCA precipitated, and equal volumes were separated via SDS-PAGE and immunoblotted for the ER lumenal ATPase Kar2p, the cis-Golgi mannosyltransferase Och1p, the early endosomal t-SNARE Pep12p, the vacuolar ATPase subunit Vph1p, and LegC7. The black arrow indicates Kar2 degradation product and the bracket indicates fractions 19 and 20 where we see Kar2p degradation and a shifted fluorescence peak. (**C**) GFP fluorescence plots were combined for comparison; (*) = $P < 0.05$; (**) = $P < 0.005$.

Table 3.2. Primers used in this study[a].

RSG F1	5’-CGACTCACTATAGGGCGAATTGGGTACCGGGCCCCCCCTCGAGCAGCCACCAGCCGC	pRS415-*KAR2* promoter-mRuby2
RSG R1	5’-GGACACCATGGTATGTTTGATACGCTTTTTCCC	
RSG F2	5’-GCGTATCAAACATACCATGGTGTCCAAAGGAGAGG	mRuby2-G_3AS
RSG R2	5’-GCTAGCACCACCACCCTTATACAATTCATCCATACCAC	
RSG F3	5’-GGTGGTGGTGCTAGCTCATCCAGCATGGGTATATTC	G_3AS-*SCS2*TM-PWG_3SM
RSG R3	5’-CATAGAACCACCACCCCATGGTCTGTAGAACCATCCTAAAACC	
RSG F4	5’-CCATGGGGTGGTGGTTCTATGAGAGATCATATGGTTTTGCATG	PWG_3SM-GFP_{11}-pRS415
RSG R4	5’-GAGCTCCACCGCGGTGGCGGCCGCTCTAGAACTAGTTTAAGTAATACCAGCAGCATTAAC	
CRG F1	5’-CTCACTATAGGGCGAATTGGGTACCGGGCCCCCCCTCGAGCATAGCGATGTTGGTCATCC	pRS425-CPY promoter + ss-mRuby2
CRG R1	5’-GGACACCATGGAGAGATGATCCAGGTCGAG	
CRG F2	5’-GGATCATCTCTCCATGGTGTCCAAAGGAGAGGAG	mRuby2-$[G_3S]_2$LE
CRG R2	5’-CCATATGATCTCTCTCGAGAGAACCACCACCAGAACCACCACCCTTATACAATTCATCCATACCACC	
CRG F3	5’-GTATAAGGGTGGTGGTTCTGGTGGTGGTTCTCTCGAGAGAGATCATATGGTTTTGCATG	$[G_3S]_2$LE-GFP_{11}-pRS425 (with RSG R4)
CG R1	5’-CACCTTTAGACATGGAGAGATGATCCAGGTCGAG	pRS423-CPY promoter- + ss GFP_{11} (with CRG F1)
CG F2	5’-CTCGACCTGGATCATCTCTCCATGTCTAAAGGTGAAGAATTGTTTAC	GFP_{11}-pRS425
CG R2	5’-GAGCTCCACCGCGGTGGCGGCCGCTCTAGAACTAGTTCATCGATGAGAACCACC	

[a]G_3As, PWG_3SM, and $[G_3S]_2$LE are single-letter amino acid codes for linker sequences added. ss = first 50 amino acids encoding the signal sequence of CPY (*PRC1*).

Table 3.3. Complete protein ID list from LegC7 immunoprecipitations

Protein Name	Score	# of Peptides
Emp47	3050.32	32
Emp46	1277.74	22
Sro9	923.29	9
Atp2	821.02	9
Glycine tRNA ligase	800.08	13
Hsc82	737.75	8
Ils1	666.45	13
Ssp120	481.79	7
Idh2	474.07	6
Mir1	403.57	6
Crn1	389.80	9
Ilv2	381.30	6
Adt2	362.39	5
YHR020W	317.44	7
Hrk1	298.80	8
Tub2	270.01	4
Rna1	223.91	5
Sam1	207.93	2
Pma1	194.12	4
Srp40	190.52	4
Gus1	174.56	2
Rpl3	166.36	2
Boi1	148.85	3
Atp1	148.04	1
Lys12	134.47	3
Faa1	132.03	2
Rps20	119.97	2
Fas1	113.02	1
Cpn60 (*Legionella*)	109.51	2
Gpp1	108.84	1
Tub1	100.28	2
Dbp3	88.61	2
Gfa1	79.46	2
Kap123	78.26	1
Nsr1	75.33	1
Rps0A	74.93	1
Ade5,7	73.31	2
Nop58	70.61	1
Rps11B	62.67	1
Hfa1	62.53	1
Sdd3	55.40	2
Lp12_1736 (*Legionella*)	53.54	1
Rpl21B	48.80	1
Ggc1	44.62	1
Cps1	44.59	2
Tef4	43.64	1

Table 3.4. Predicted tryptic peptide sequences of LegC7.

Position of cleavage site	Amino acid sequence[a]	No of Amino acid residues	Figure #
17	MATNETELQVLIQHDSK	17	A
33	STITTSSLDSTDKDPK	16	B
54	ASTGTPEIESASLAQIVDTQK	21	C
60	QLSQVK	6	
79	ESLESIVDSIAENPSLITR	19	D
92	AASAWGELPMWQK	13	E
145	VTGGLVLTAPTLAVGLFAHIGVLLVIGGVTGLTYTAGAIVLDD HHTCNVNIAK	53	
169	EGLFGLADLLQITIEALDAIR	21	F
178	FAEEIEK	7	G
185	NENLR	5	
192	LTDNIDR	7	H
212	LGNEVESLSAQVELYMEIEK	20	I
226	DTNEMEQTVK	10	J
234	LQESTTK	7	
241	QTDLLEK	7	K
263	SQLQLAEK	8	L
271	IAELHEVR	8	M
280	LSLGLEVQK	9	N
306	TLEGTVQTLTGTVIADEEQR	20	O
311	VSFQK	5	
320	KLDGFLNDK	8	P
330	QLSFDQVAER	10	Q
339	AEEELK	6	
351	QSNDR	5	
357	YSELLK	6	
365	QEQQVER	7	
373	LGLHK	5	
404	ENVKPSNDPVHSGLLSHGIYSTPK	24	
411	VTQPK	5	
418	VEVVEDR	7	R
425	QTIALVN	7	

[a]LegC7 Peptides detected via LC-MS/MS highlighted in green; underlined sequences are predicted possible *N*-glycosylation sites (http://www.cbs.dtu.dk/services/NetNGlyc/)

~~M~~ATNETELQVLIQHDSKSTITTSSLDSTDKDPKASTGTPEIESASLAQIVDTQKQLSQVK

ESLESIVDSIAENPSLITRAASAWGELPMWQKVTGGLVLTAPTLAVGLFAHIGVLLVIGG

VTGLTYTAGAIVLDDHHTCNVNIAKRLKEGLFGLADLLQITIEALDAIRKKFAEEIEKFKNE

NLRLTDNIDRLGNEVESLSAQVELYMEIEKMLRKDTNEMEQTVKKLQESTTKQTDLLEK

NQKELSKIRKEYEKSQLQLAEKIAELHEVRLSLGLEVQKAKTVAKTLEGTVQTLTGTVIA

DEEQRVSFQKKLDGFLNDKQLSFDQVAERICKAEEELKKVKEELRQSNDRYSELLKRQ

EQQVERLEKLGLHKLERIVDKENVKPSNDPVHSGLLSHGIYSTPKGKVTQPKVEVVED

RQTIALVN

Figure 3.9. Identification of LegC7 peptides by LC-MS/MS. Amino acid sequence coverage obtained by the LC-MS/MS analysis of tryptic digest of LegC7 (highlighted in green). Sites of *N*-glycosylation predicted by Net-N-glyc web tool are underscored and no evidence for *N*-glycosylation was observed. Based on the LC-MS/MS data amino acid at the first position (M – Methionine) either might not be present in the protein sample or had undergone non-specific cleavage.

A

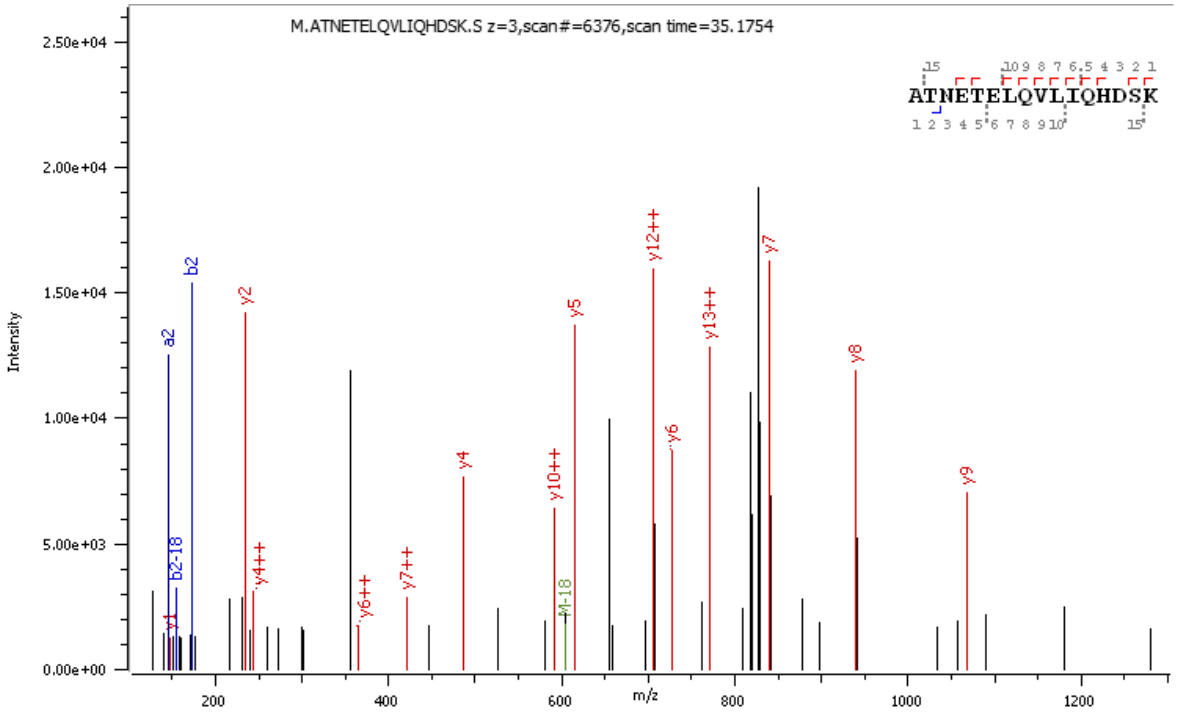
M.ATNETELQVLIQHDSK.S z=3,scan#=6376,scan time=35.1754
ATNETELQVLIQHDSK
Intensity
m/z
2.50e+04
2.00e+04
1.50e+04
1.00e+04
5.00e+03
0.00e+00
200
400
600
800
1000
1200
b2
a2
y2
y1
b2-18
y4++
y6++
y7++
y4
y10++
y5
M-18
y12++
y6
y13++
y7
y8
y9

B

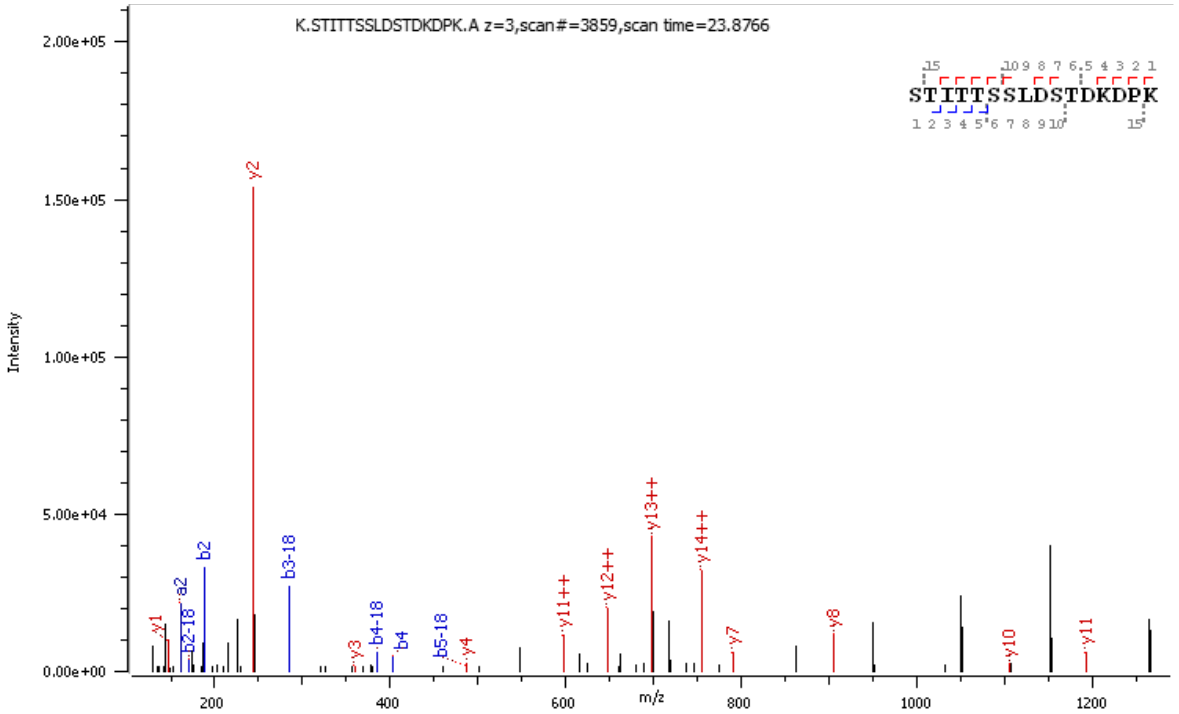
K.STITTSSLDSTDKDPK.A z=3,scan#=3859,scan time=23.8766
STITTSSLDSTDKDPK
Intensity
m/z
2.00e+05
1.50e+05
1.00e+05
5.00e+04
0.00e+00
200
400
600
800
1000
1200
y2
b2
a2
y1
b2-18
b3-18
b4-18
b4
y3
b5-18
y4
y11++
y12++
y13++
y14++
y7
y8
y10
y11

C

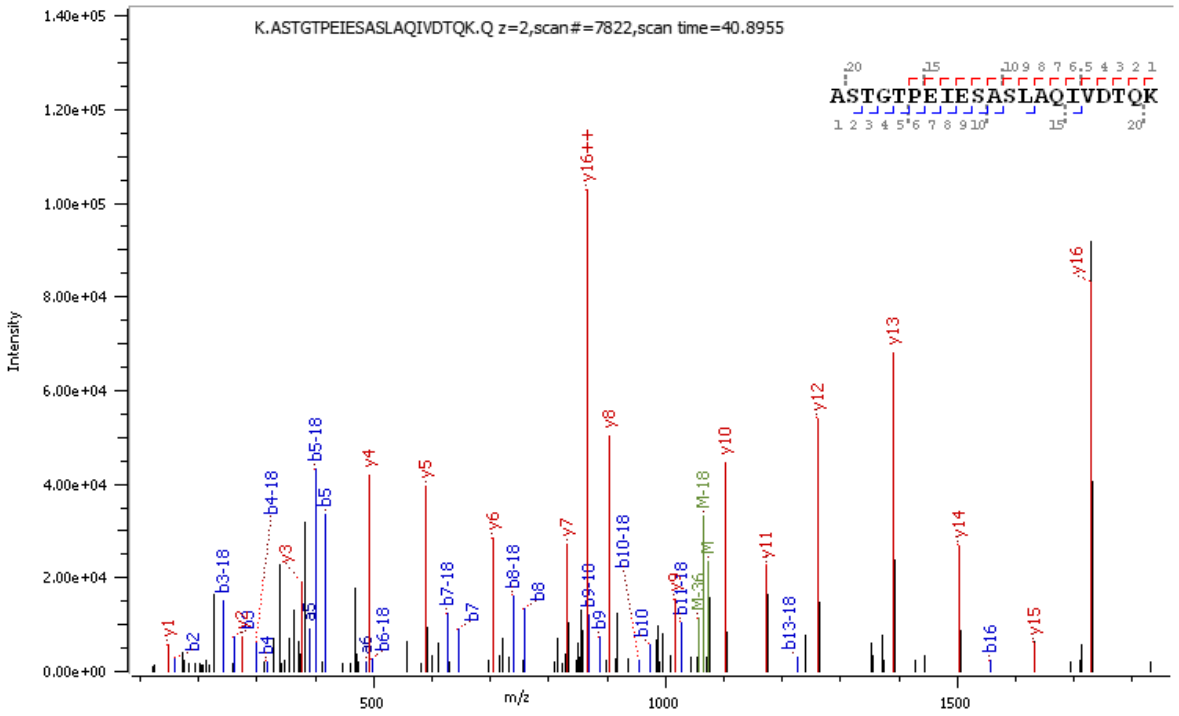
K.ASTGTPEIESASLAQIVDTQK.Q z=2,scan#=7822,scan time=40.8955
ASTGTPEIESASLAQIVDTQK
Intensity
m/z

D

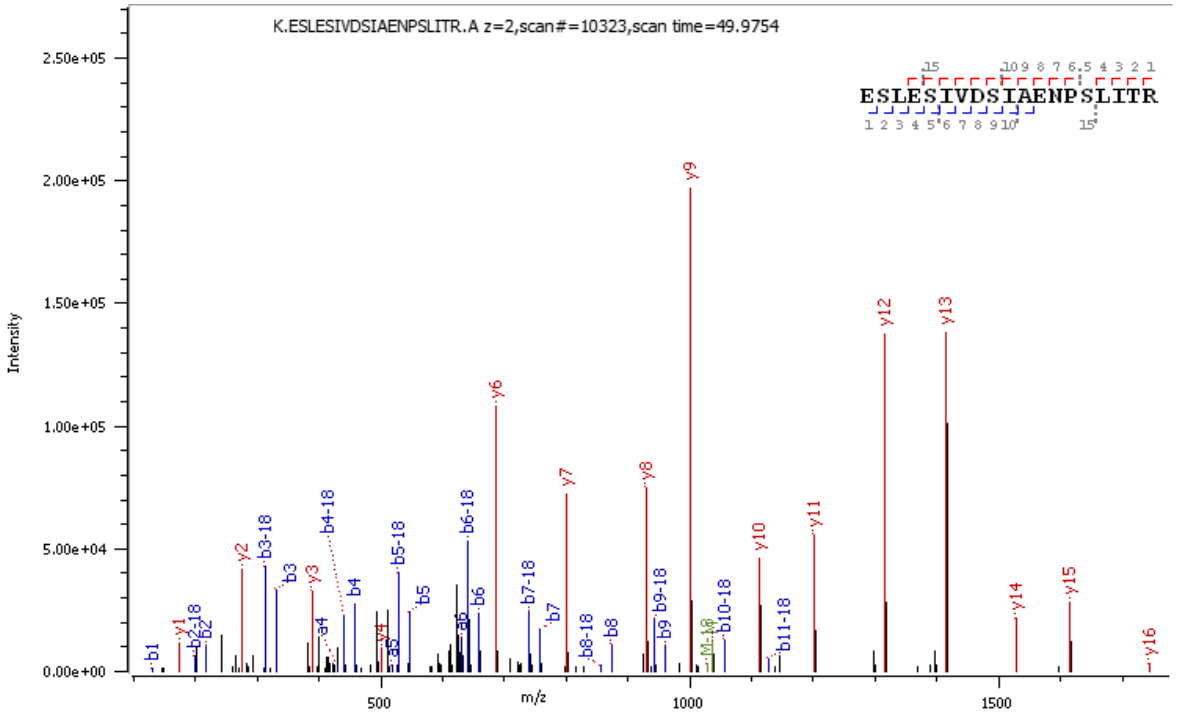
K.ESLESIVDSIAENPSLITR.A z=2,scan#=10323,scan time=49.9754
ESLESIVDSIAENPSLITR
Intensity
m/z

E

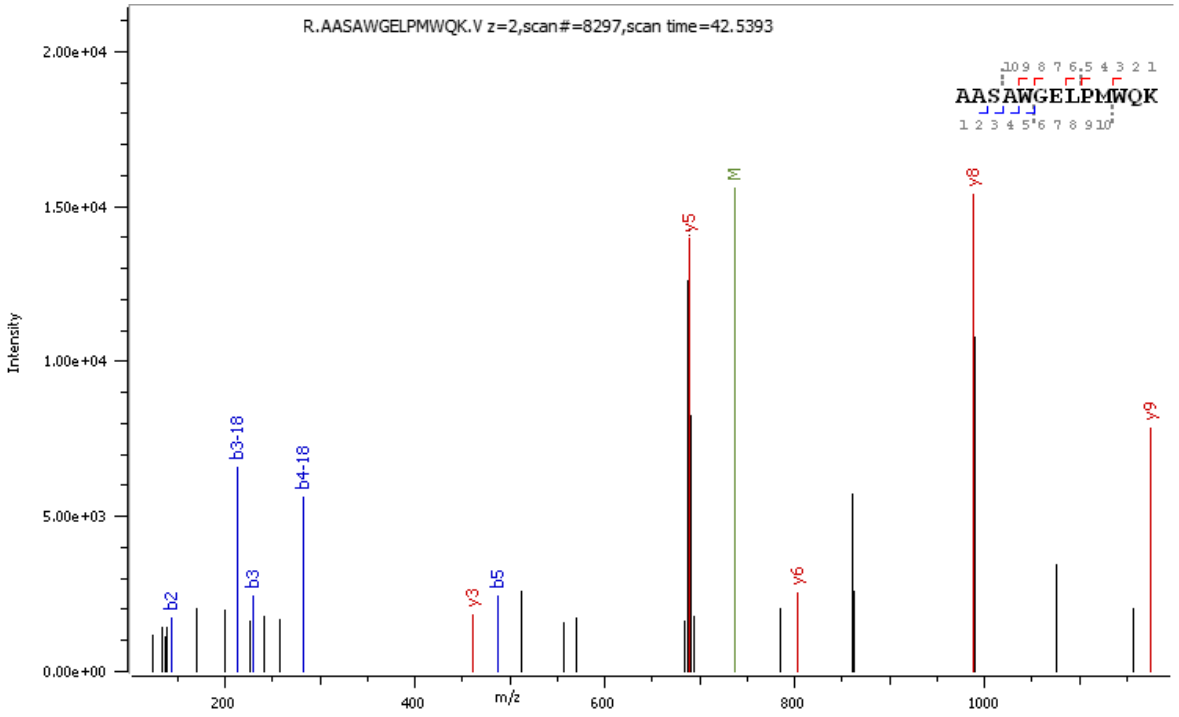
R.AASAWGELPMWQK.V z=2,scan#=8297,scan time=42.5393
AASAWGELPMWQK
Intensity
m/z
b2
b3
b3-18
b4-18
b5
y3
y5
M
y6
y8
y9

F

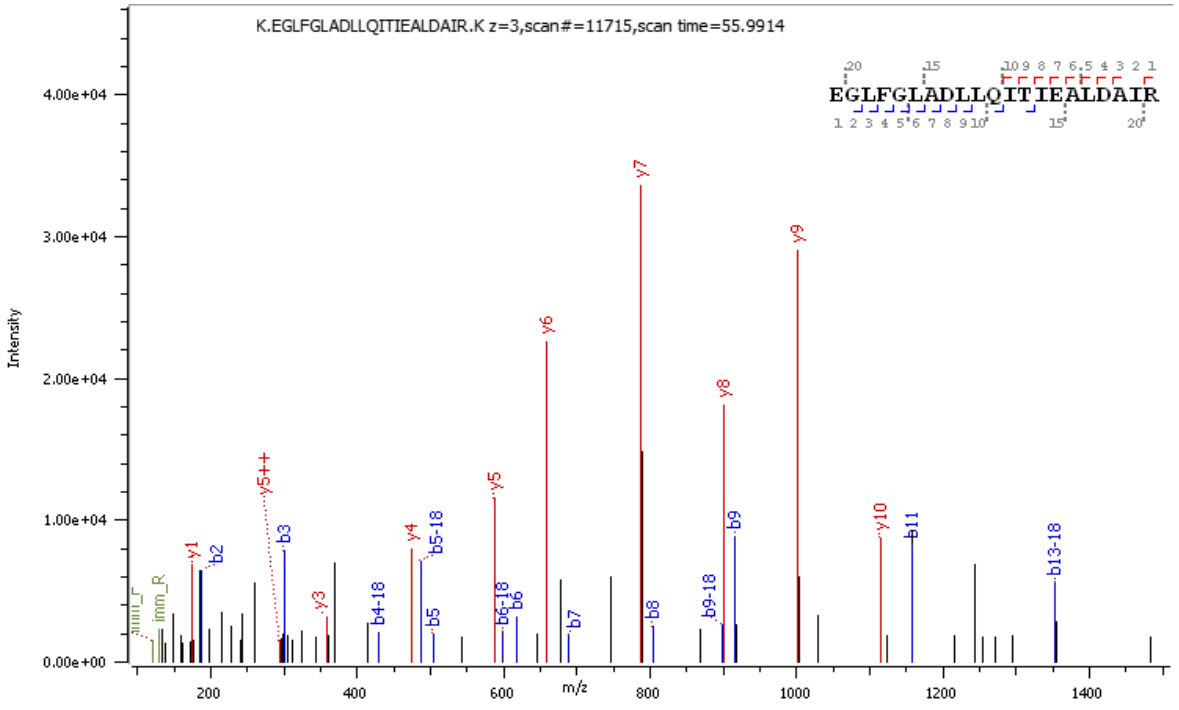
K.EGLFGLADLLQITTIEALDAIR.K z=3,scan#=11715,scan time=55.9914
EGLFGLADLLQITTIEALDAIR
Intensity
m/z
imm_F
imm_R
y1
b2
y5++
b3
y3
b4-18
y4
b5-18
b5
y5
b6-18
b6
y6
b7
y7
b8
y8
b9-18
b9
y9
y10
b11
b13-18

G

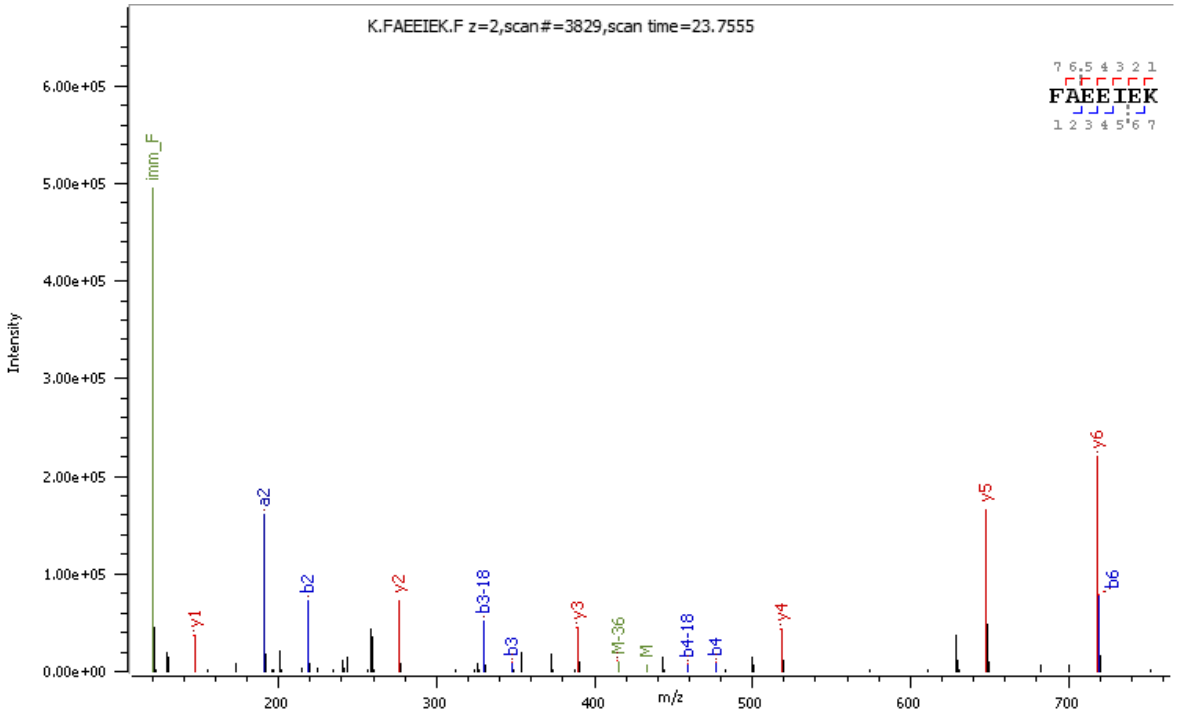
K.FAEEIEK.F z=2,scan#=3829,scan time=23.7555
FAEEIEK
Intensity
m/z
imm_F
y1
a2
b2
y2
b3-18
b3
y3
M-36
M
b4-18
b4
y4
y5
y6
b6

H

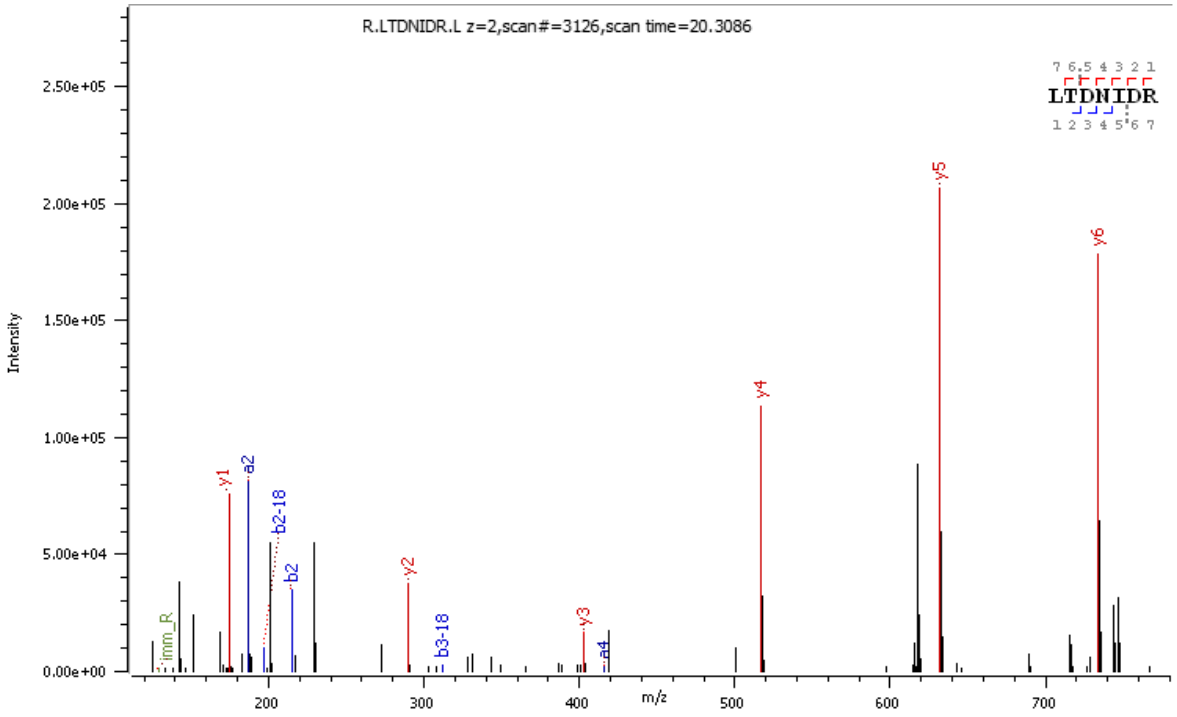
R.LTDNIDR.L z=2,scan#=3126,scan time=20.3086
LTDNIDR
Intensity
m/z
imm_R
y1
a2
b2-18
b2
y2
b3-18
y3
a4
y4
y5
y6

I

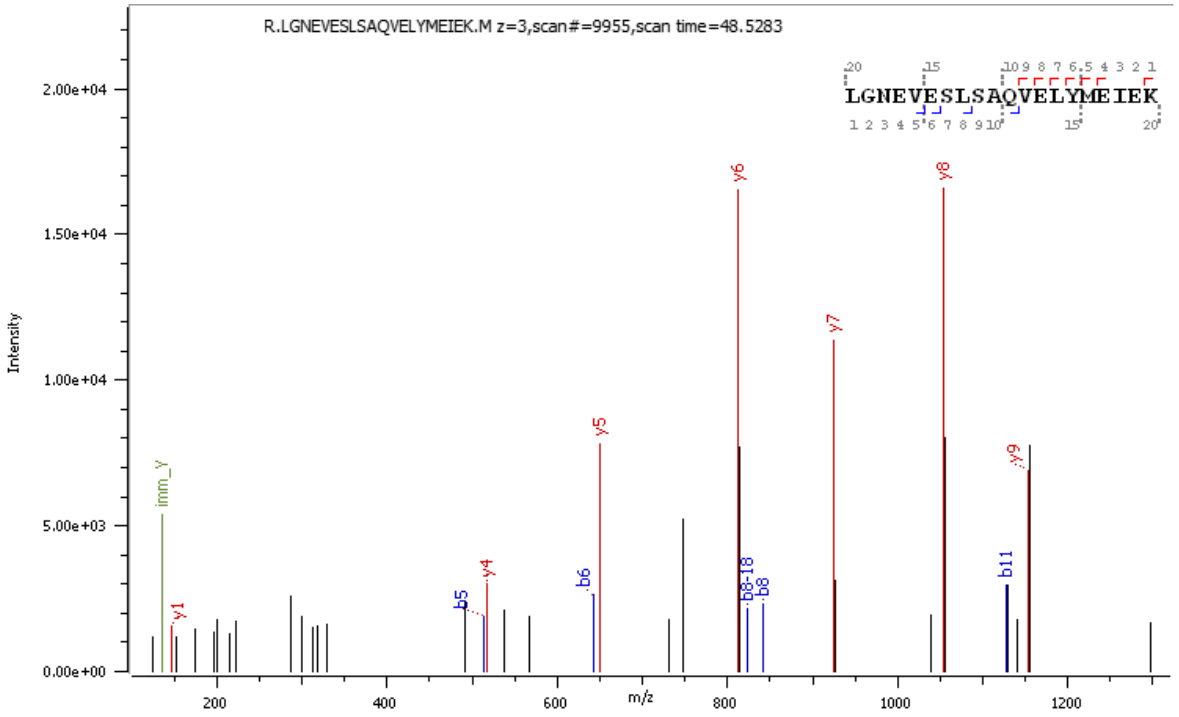
R.LGNEVESLSAQVELYMEIEK.M z=3,scan#=9955,scan time=48.5283
LGNEVESLSAQVELYMEIEK
Intensity
m/z
imm_y
y1
b5
y4
b6
y5
b8-18
b8
y6
y7
y8
y9
b11

J

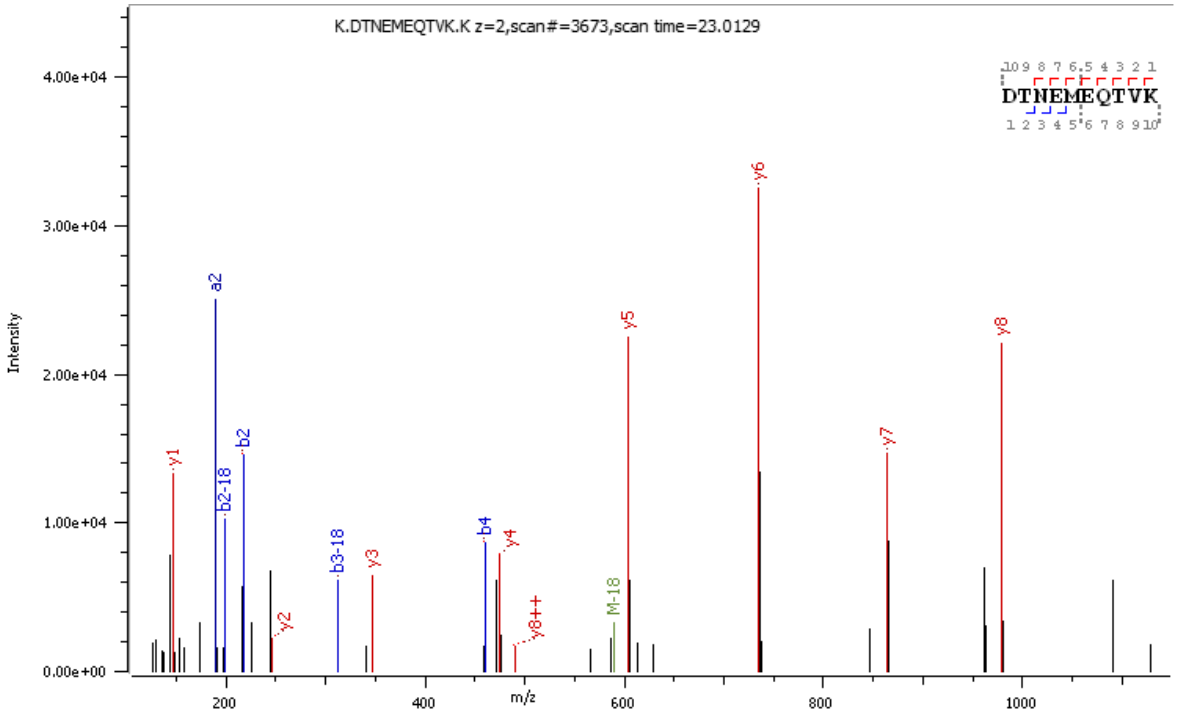
K.DTNEMEQTVK.K z=2,scan#=3673,scan time=23.0129
DTNEMEQTVK
Intensity
m/z
y1
a2
b2-18
b2
y2
b3-18
y3
b4
y4
y8++
M-18
y5
y6
y7
y8

K

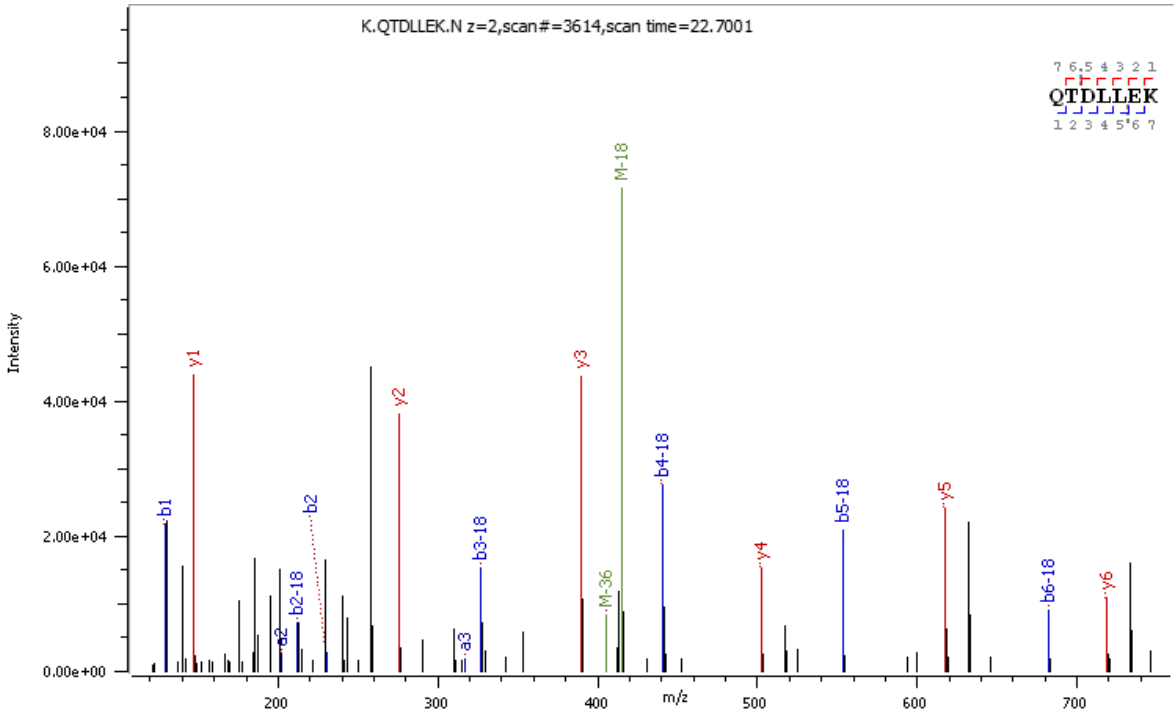
K.QTDLLEK.N z=2,scan#=3614,scan time=22.7001
QTDLLEK
Intensity
m/z
b1
y1
b2
y2
b2-18
a2
a3
b3-18
y3
M-36
M-18
b4-18
y4
b5-18
y5
b6-18
y6

L

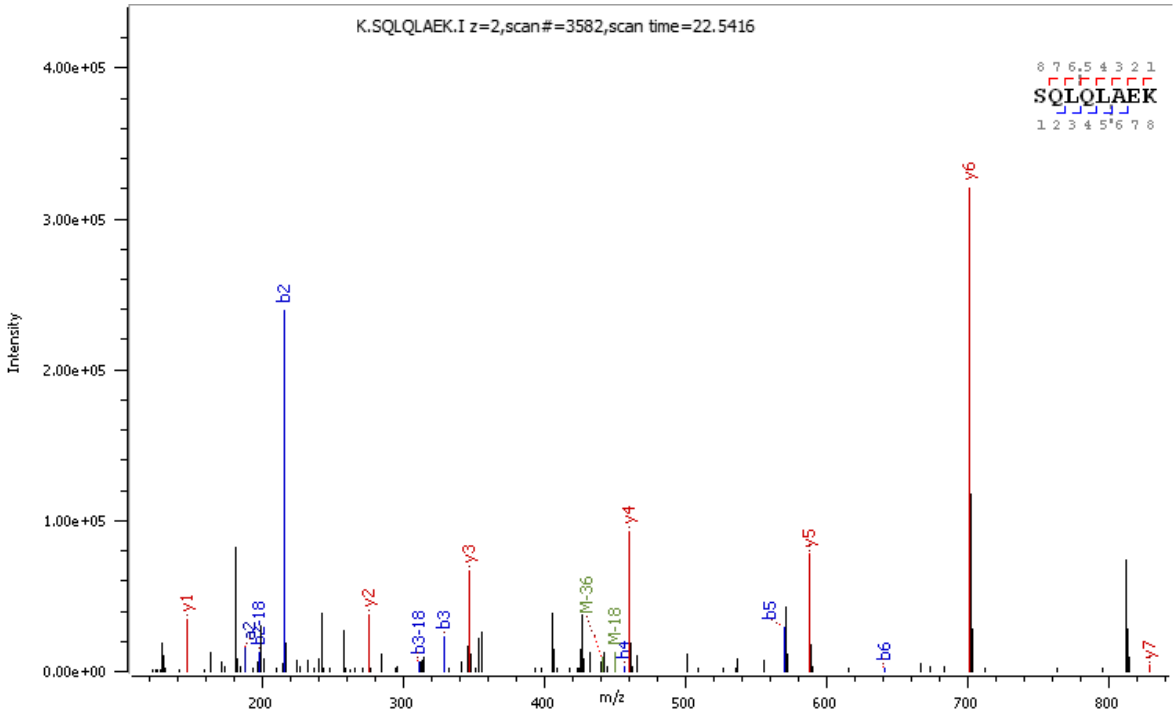
K.SQLQLAEK.I z=2,scan#=3582,scan time=22.5416
SQLQLAEK
Intensity
m/z
b2
y6
y1
a2
b2-18
y2
b3-18
b3
y3
M-36
M-18
b4
y4
b5
y5
b6
y7

M

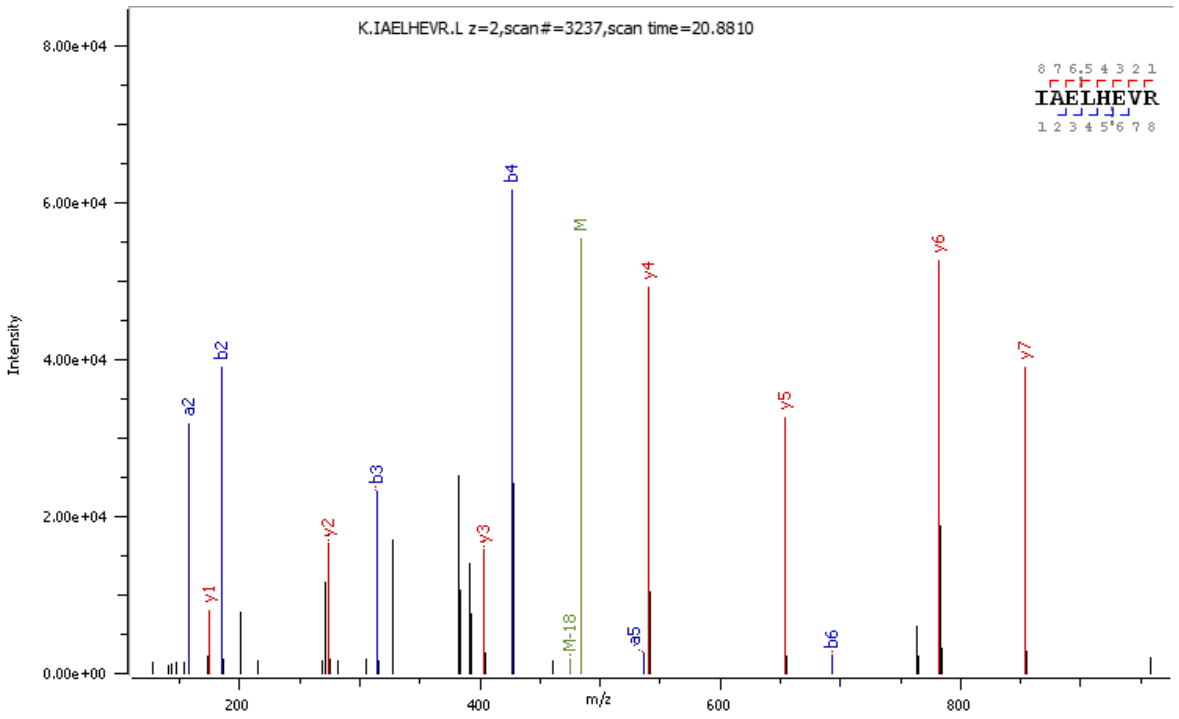
K.IAELHEVR.L z=2,scan#=3237,scan time=20.8810
IAELHEVR
Intensity
m/z
a2
b2
b3
b4
y1
y2
y3
M
M-18
a5
y4
y5
b6
y6
y7

N

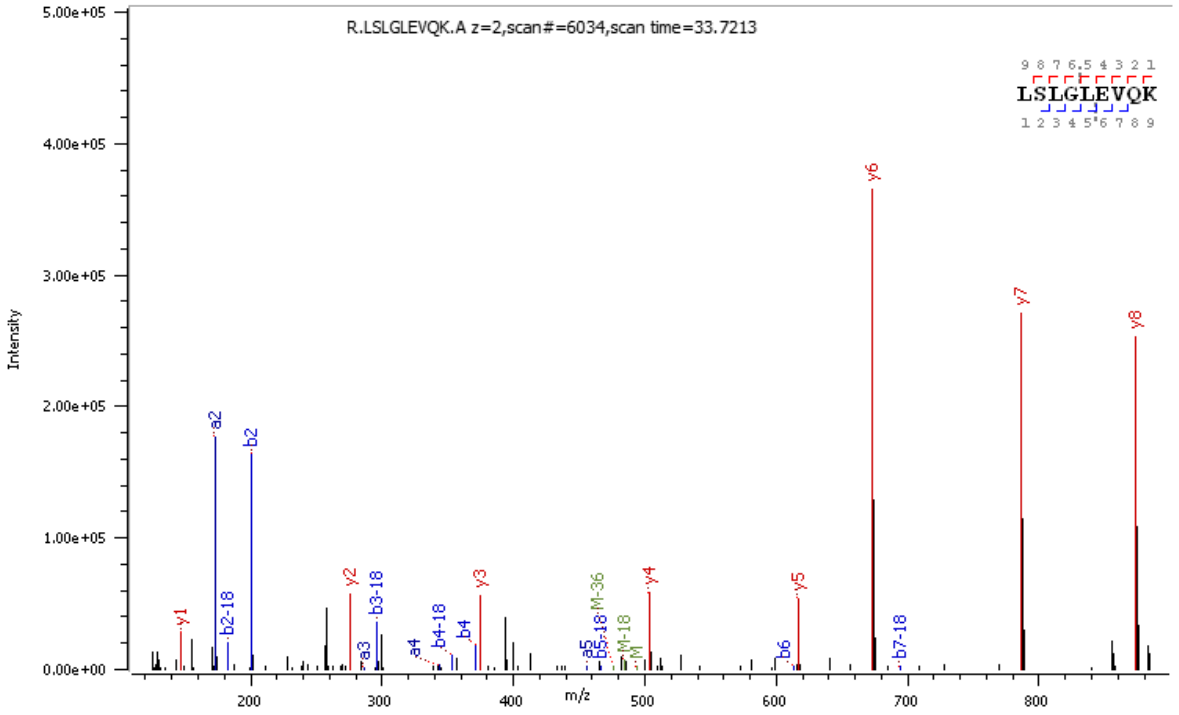
R.LSLGLEVQK.A z=2,scan#=6034,scan time=33.7213
LSLGLEVQK
Intensity
m/z
a2
b2
b2-18
y1
y2
b3-18
a3
a4
b4-18
b4
y3
a5
b5-18
M-36
M-18
M
y4
y5
b6
b7-18
y6
y7
y8

O

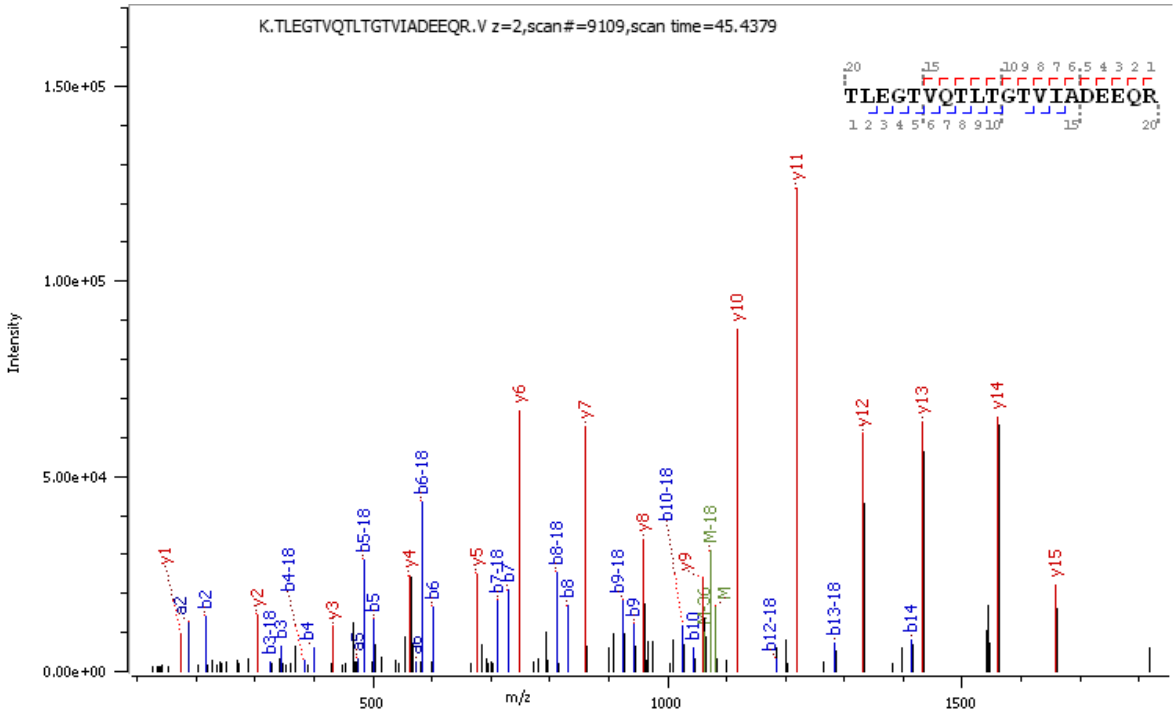
K.TLEGTVQTLTGTVIADEEQR.V z=2,scan#=9109,scan time=45.4379
TLEGTVQTLTGTVIADEEQR
Intensity
m/z
1.50e+05
1.00e+05
5.00e+04
0.00e+00
500
1000
1500

P

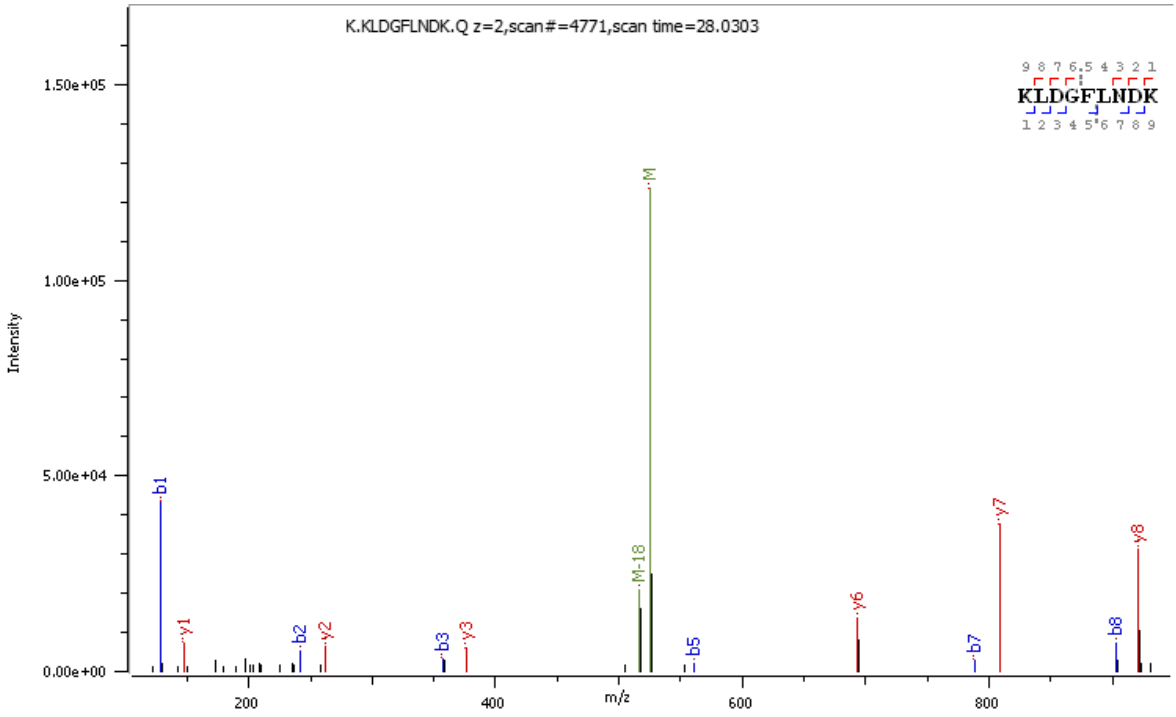
K.KLDGFLNDK.Q z=2,scan#=4771,scan time=28.0303
KLDGFLNDK
Intensity
m/z
1.50e+05
1.00e+05
5.00e+04
0.00e+00
200
400
600
800

Q

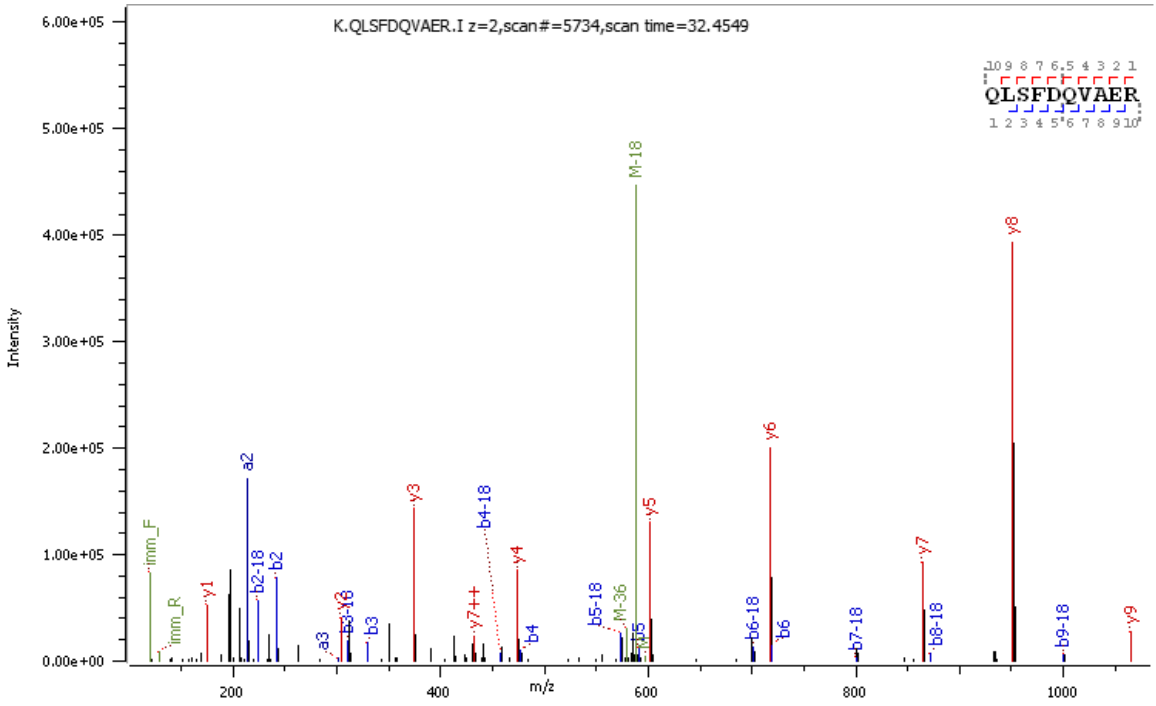

R

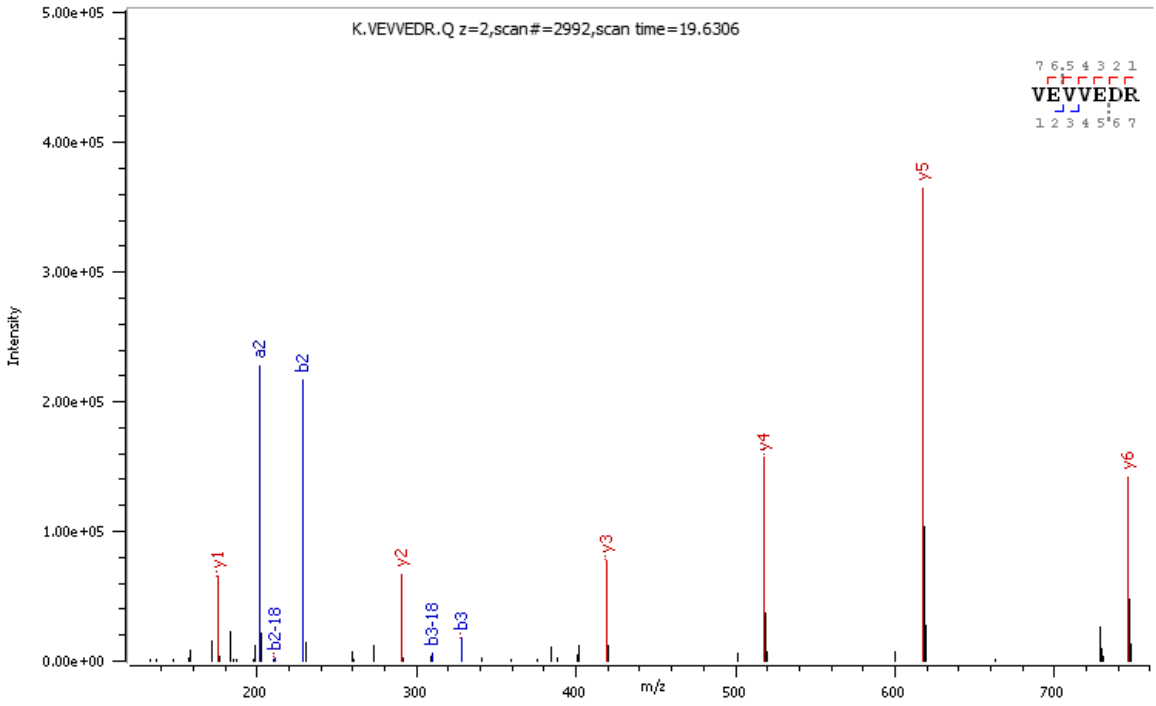

Figure 3.10. HCD MS2 spectra from tryptic digest of LegC7. Panel designation refers to peptides annotated in **Table 3.4** (green).

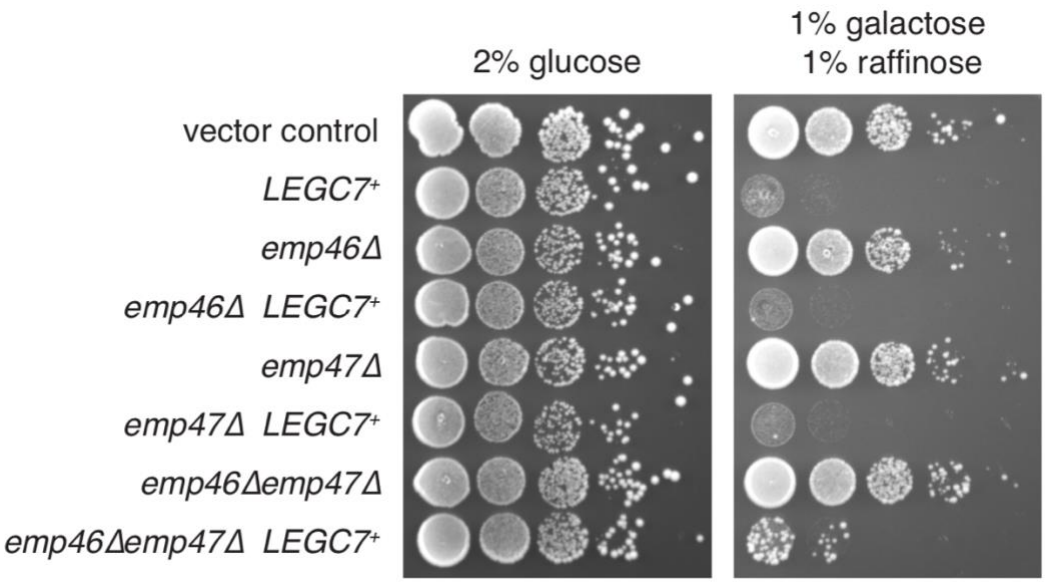

Figure 3.11. *EMP46/47* deletions do not significantly reduce LegC7-mediated growth inhibition. Yeast deletion mutants harboring either pYES2NT C or pYES2-*LEGC7*$^{+}$ were grown to saturation in CSM at 30°C. For each strain, 1 OD_{600} unit was harvested via centrifugation, resuspended in 1 mL of 0.9% NaCl, and serially diluted 1:10 four times. 5 µL of each dilution was plated onto CSM containing 2% glucose and CSM containing 1% galactose and 1% raffinose to induce LegC7 expression.

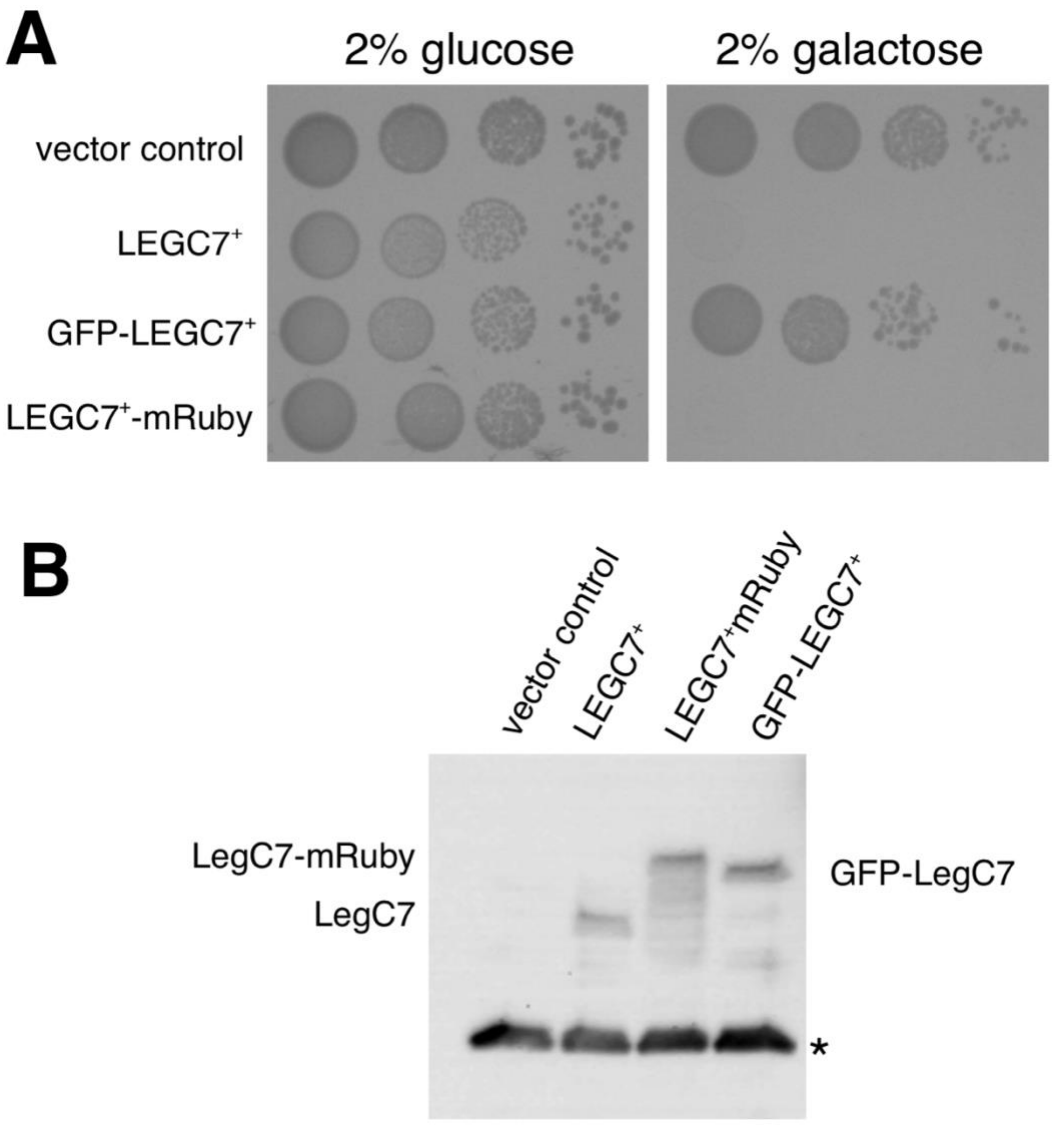

Figure 3.12. LegC7-mRuby2 inhibits yeast growth to a degree comparable to LegC7. (**A**) Yeast strains harboring LegC7 constructs in pYES2NT C were grown to saturation in CSM at 30°C. For each strain, 1 OD_{600} unit was harvested via centrifugation, resuspended in 1 mL of 0.9% NaCl, and serially diluted 1:10 four times. 5 µL of each dilution was plated onto CSM containing 2% glucose and CSM containing 2% galactose to induce LegC7 expression. (**B**) The same strains were grown to saturation in CSM medium at 30°C, harvested via centrifugation, resuspended in an equal volume of fresh CSM containing 2% galactose, and grown for an additional 18 h at 30°C. Equal amounts of each strain were harvested, protein was extracted, and equal volumes of each extract were separated via SDS-PAGE and immunoblotted for LegC7. Asterisk identifies an anti-LegC7 cross-reactive protein from yeast lysates that serves as a loading control.

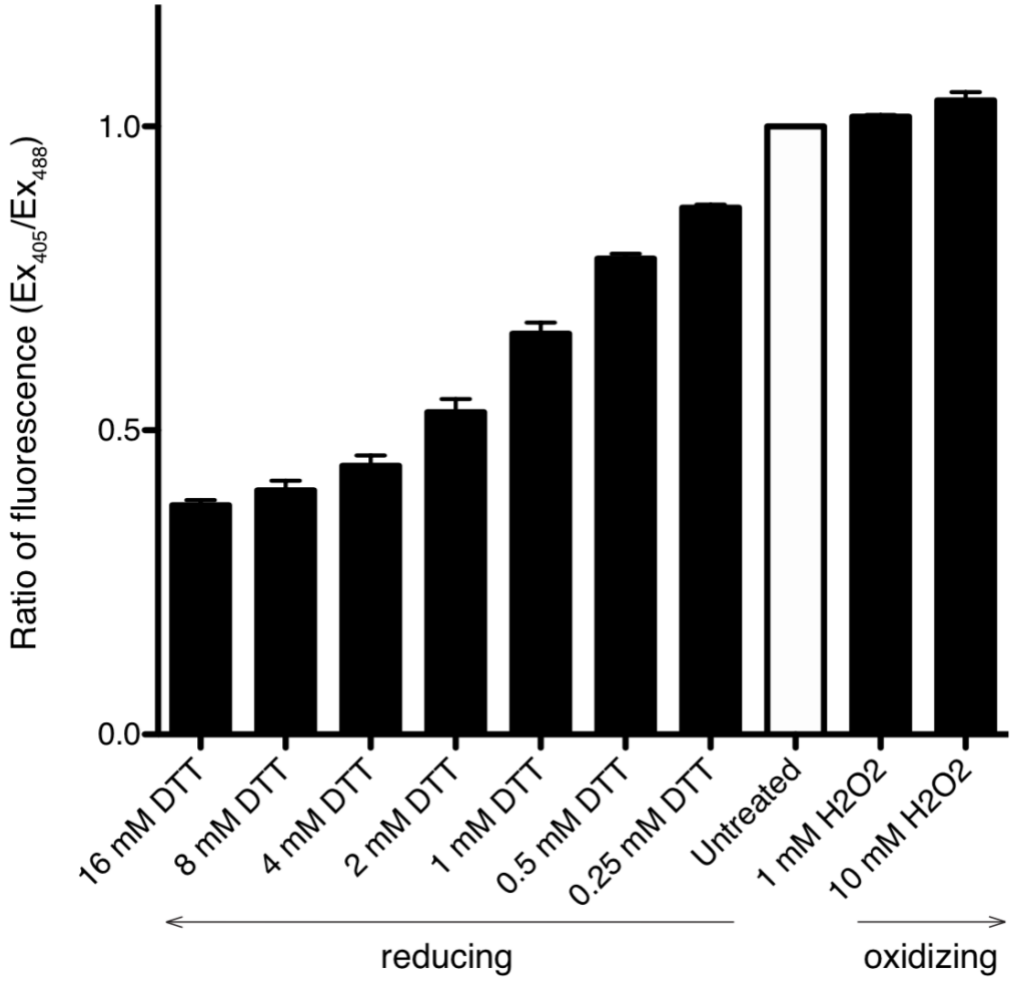

Figure 3.13. EroGFP can be utilized as a redox sensor of the ER lumen. Yeast strains containing ER-targeted, redox-sensitive eroGFP were grown to saturation, treated with varying concentrations of DTT or H_2O_2 and cells were analyzed via flow cytometry (n = 10^5). After low-fluorescence and dead cell populations were removed from the data sets (See **Fig. 3.7**), ratios of GFP fluorescence were calculated and normalized by the same factor such that the ratio for untreated cells = 1. Error bars represent ± the standard deviation across 3 independent experiments.

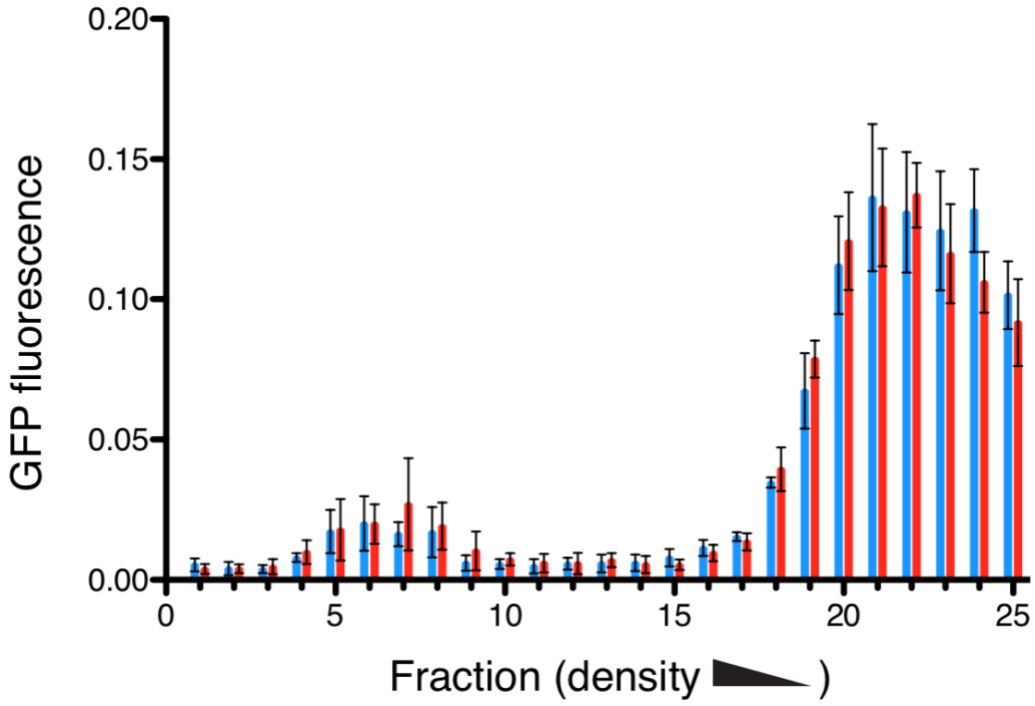

Figure 3.14. LegC7 expression in yeast strains containing endosome-directed CPYss-GFP$_{1-10}$ and CPYss-mRuby2-GFP$_{11}$ does not affect GFP fluorescence of subcellular fractions. Strains containing endosome-targeted CPYss-mRuby2-GFP$_{11}$ and endosome-targeted CPYss-GFP$_{1-10}$ and either pYES2NT C or pYES2-*LEGC7*$^{+}$ were grown to saturation in CSM medium at 30°C, harvested via centrifugation, resuspended in an equal volume of fresh CSM containing 1% raffinose and 1% galactose, and grown for an additional 18 h at 30°C. Equal amounts of each strain were dounced and fractionated into 25 fractions (**Materials and Methods**), and 20 µL volumes of each fraction were measured in triplicate for GFP fluorescence and averaged. Error bars represent ± the standard deviation across three independent experiments.

Discussion

To survive intracellularly, *L. pneumophila* translocates over 300 effector proteins into host cells via its Dot/Icm Type IVB secretion system, inducing dramatic changes to normal host ER and endolysosomal membrane trafficking pathways, such as forcing the aberrant activation of the host ER Rab1 GTPase [242, 243], inhibition of autophagy via RavZ[456], and inhibiting the function of the lysosomal V-type ATPase via the activity of SidK[475]. A critical component of LCV formation, however, is through the active recruitment of ER-derived membranes to the phagosomal membrane. While the precise mechanism by which *Legionella* induces ER:phagosome fusion is not completely known, the activities of *Legionella* LegC7/LegC2 have been shown to be important for optimal biogenesis of the LCV via ER membrane recruitment, although deletions of these genes do not result in overall intracellular proliferation defects[341, 459]. Accordingly, characterizing the in vivo activities of these proteins has proven difficult. Our previous discovery that LegC7 expression disrupts endosomal trafficking pathways in yeast[340], coupled with the discovery that LegC7 colocalizes with KDEL proteins[459] and forms a membrane fusion-competent, NSF/α-SNAP-resistant, SNARE-like complex with *Legionella* LegC2, LegC3, and host VAMP4 proteins[344], led us to explore the effects of LegC7 expression on potential ER and endosomal fusion events in vivo.

Supporting the previous discoveries that localize LegC7 to ER-containing structures in mammalian cells[339, 459], we describe drastic ER morphology changes upon expression of LegC7 in yeast (**Fig. 3.2**). Furthermore, we find that LegC7 immunoprecipitations enrich for Emp47p/Emp46/Ssp120p complex subunits, suggesting

an interaction between LegC7 and specific host cargo adapters for biosynthetic cargo leaving the ER. Interestingly, *emp46*Δ *emp47*Δ yeast strains appear to phenocopy the defective carboxypeptidase S vacuolar delivery phenotype of LegC7-expressing strains (**Fig. 3.1**)**,** indicating that LegC7 may inhibit Emp47p/Emp46p/Ssp120p complex function, either directly or indirectly. However, the fact that these *EMP46/47* deletions minimally suppress LegC7-mediated growth inhibition contradicts the notion that LegC7 simply functions to inhibit Emp47p/Emp46p, but rather indicates that defects in ER:Golgi cargo delivery appear to result in the same trafficking defects observed in LegC7-expressing strains. Perhaps host cargo adapters play a role in targeting LegC7 to ER exit sites and ER-derived compartments containing cargo beneficial to *L. pneumophila* during infection. Indeed, Emp46p and Emp47p are known to function in glycoprotein secretion[439], with a function similar to mammalian ERGIC-53/LMAN1[442], and glycoprotein acquisition has been shown to be important for nutrition and evasion of host immune defenses by bacterial pathogens, including *L. pneumophila*[476-478]. While there is no documented role for ERGIC-53 in intracellular bacterial infection, this possibility should be investigated in future studies. Although LegC7 was not determined to be glycosylated by yeast in these studies (**Fig. 3.10**), it may interact with these proteins via structural motifs, or be glycosylated in mammalian expression systems. Further experimentation to show direct interactions between LegC7 and Emp47p/Emp46p/Ssp120p complexes in vitro would be required to characterize these interactions.

Previous research has shown that, while LegC7 appears to localize to ER structures[339, 459], expression of LegC7 in yeast also induced the formation of large

punctate structures on the vacuole membrane and caused the mis-secretion of vacuole-bound CPY-invertase; these phenotypes were suggestive of defects in endosomal maturation or multivesicular body formation[339]. Our current findings that LegC7 expression induces the formation of Sec63-positive, Vps8p-positive compartments or structures (**Fig. 3.5A and B**) now help reconcile these discoveries and indicate that LegC7 activity – in the absence of other *Legionella* effectors – either recruits, or fuses, ER-derived vesicles to endosomes. This activity is also likely to disrupt ER:Golgi trafficking, as implied by defects in GFP-CPS trafficking in *emp46*Δ*emp47*Δ strains (**Fig. 1**). As mass disruptions in ER:Golgi traffic would be lethal to yeast cells[479], this is likely the reason for the toxic nature of LegC7/YlfA upon expression in yeast[459].

Strikingly, deletions of genes encoding for the core subunits of the conserved endolysosomal membrane tethering complexes CORVET and HOPS provide complete resistance to LegC7-mediated toxicity (**Fig. 3.3A**). We also find that deletion of the CORVET-specific *VPS8* gene provides more robust suppression of toxicity than the other complex-specific subunits. This suggests a more prominent role for the endosomal CORVET complex in LegC7 activity, further supported by our observation of colocalization of Vps8p and LegC7 in vivo (**Fig. 3.4A and F**). In addition to suppressing LegC7 toxicity, deletion of class C core complex subunit *VPS33* prevents LegC7-mediated alteration of ER morphology (**Fig. 3.2**) and the downstream effects such as Kar2p degradation (**Fig. 3.6**) and enhanced oxidation of the ER lumen (**Fig. 3.7**). This, coupled with the finding that LegC7-induced Kar2 degradation is also dependent upon the early endosomal t-SNARE, Pep12p, provides evidence that LegC7 induces aberrant SNARE-dependent fusion of ER-derived membrane and endosomes in vivo. While it is

well established that small GTPases are primarily responsible for recruiting tethering complexes, such as CORVET and HOPS, to their target membranes[256, 464, 480], it is worth noting recent evidence that SNAREs, to which LegC7 has been compared, also play a role in targeting tethering complexes to membranes[481]. The apparent genetic interaction between LegC7 and class C tethering complexes raises the possibility that these complexes, which are conserved in higher eukaryotes[480], are also utilized by *L. pneumophila* for optimal LCV biogenesis.

As stronger evidence of ER:endosome fusion observed in these studies, we found that Kar2p degradation is dependent upon active vacuolar proteases, showing authentic delivery of ER to degradative compartments; this degradation was not found to be due to ER-phagy or general autophagic pathways (**Fig. 3.6B**). Furthermore, endosomes and lysosomes are oxidative compartments[482] and the ER lumen is further oxidized with LegC7 expression, which cannot be attributed to ER stress induced by LegC7 expression, as the ER redox state remains the same when expressing LegC7 in a *vps33*Δ mutant. Lastly, the split-GFP assay developed for this study provides further evidence of LegC7-induced mixing of lumenal contents of ER-derived and endosomal compartments.

L. pneumophila regulates the activity of some Dot/Icm effectors with other Dot/Icm effectors, termed “metaeffectors”, by inactivation or marking target effectors for proteolytic degradation[286, 308, 317]. Multiple studies have shown that *L. pneumophila* accomplishes temporal regulation during infection by delayed secretion of metaeffectors[317] or continuous secretion into the host cytosol, titrating out the target effector over time[286]. A recent study showed that LegC7-mediated growth inhibition in

yeast is suppressed by co-expression of the Dot/Icm substrate MavE[308]. Perhaps the suppression of growth inhibition is an indication that MavE regulates LegC7 during infection through inactivation or degradation. It is known that LegC7 is part of the subset of Dot/Icm effectors first secreted into the host, many of which affect vesicular traffic[157, 483], and MavE likely functions to provide the proper spatiotemporal regulation for LegC7 activity during *Legionella* pathogenesis, although whether or not MavE expression suppresses the LegC7-dependent ER:endosome fusion events observed in yeast has not yet been explored. This work provides evidence that LegC7 is capable of redirecting host biosynthetic traffic in a manner that is independent of other Dot/Icm substrates, but reliant on conserved host endolysosomal fusion machinery. Our findings are consistent with the notion that this redirected cargo is directed to the LCV, as the LCV lipid and protein composition has been compared to that of trans-Golgi and early endosomes[199].

Despite the strong link of LegC7 to the activities of CORVET and endosomal SNARE proteins, we were surprised to note that we never detected any co-precipitating yeast SNARE proteins or multisubunit tethering factors in our multiple LegC7 immunoprecipitations. While these interactions may be sufficiently transient so that they would be undetectable in these pulldowns, it is important to note that it has been suggested that LegC2/3/7 proteins engage host R-SNARE proteins in an NSF/a-SNAP-resistant complex[344]. Therefore, these interacting proteins may only be observed when all three LegC proteins are co-expressed. Nevertheless, LegC7 has an in vivo activity distinct from either LegC2 or LegC3, suggesting differences in localization and protein:protein interactions, at least in yeast but also possibly in higher organisms.

Importantly, SNARE proteins generally do not form fusion-competent complexes promiscuously in vivo, only forming complexes with specific combinations of other SNARE proteins, and the absence of any one SNARE protein prevents complex formation[348]. Therefore, if LegC2/3/7 form a specific and cognate 3Q-SNARE complex, we might expect limited functionality of these LegC proteins in the absence of other complex members. As such, the presence of observable phenotypes, let alone distinct phenotypes, produced by individual LegC proteins in yeast is generally uncharacteristic of SNARE proteins that form a 3Q-SNARE complex. Similarly, the fact that proteins that specifically antagonize LegC3 (LupA) and LegC7 (MavE) have been evolutionarily maintained in *Legionella* suggests that LegC3 and LegC7 probably function independent of each other during infection[308]. Furthermore, LegC2 and LegC7 form homooligomeric complexes through interaction between cytosolic domains[341], which is also distinct from SNARE proteins. These findings suggest potential multifunctionality and/or promiscuity of LegC proteins, which could be cost-effective for *Legionella* during infection. As such, future studies utilizing heterologous co-expression of combinations of LegC proteins or comparing phenotypes of *legC* single, double, and triple knockout mutants, as well as host CORVET/HOPS disruptions, could better our understanding of LegC protein functionality during *Legionella* pathogenesis.

Materials and Methods

Yeast strains and plasmid constructions

All yeast strains used in this study were derivatives of *Saccharomyces cerevisiae* strain BY4742 (MATα *his3Δ1 leu2Δ0 lys2Δ0*). Where denoted, expression of *GAL1*-

based promoters was initiated with the addition of 1% raffinose and 1% galactose as the carbon source, in place of 2% glucose.

To create HaloTag® LegC7 lacking the transmembrane domain, we amplified LegC7 using the primers LegC7HaloF and LegC7HaloF (**Table 3.2**) utilizing pVJS52 [458] as a template. The resulting PCR product and pHis6-Halo (Promega Corporation) were digested with PvuI and NotI and ligated to create pVJS77 that was confirmed via sequencing (Georgia Genomics Facility, University of Georgia).

To construct the vectors for expressing the components of the split-GFP bimolecular fluorescence complementation assay, a combination of overlap PCR and homologous recombination techniques were used (**Table 3.2**). To generate plasmid pRS415-*KAR2*$_{pr}$-mRuby2-G$_3$AS-*SCS2*TM-PWG$_3$SM-GFP$_{11}$ for directing the GFP$_{11}$ helix to the ER lumen, four separate PCR fragments were amplified: Fragment A was amplified from BY4742 genomic DNA with the primer pair RSG F1 and RSG R1, Fragment B was amplified from pFA6a-link-yomRuby2-SpHis5 [484] with primer pair RSG F2 and RSG R2, Fragment C was amplified from BY4742 genomic DNA with primer pair RSG F3 and RSG R3, and Fragment D was amplified from pSJ1321 [473] with primer pair RSG F4 and RSG R4; resultant amplicons were then used as templates for overlap PCR. Fragments A and B were allowed to self-prime, then amplified with primer pair RSG F1 and RSG R2 to create Fragment E. Fragments C and D were allowed to self-prime, then amplified with primer pair RSG F3 and RSG R4 to generate Fragment F. Finally, Fragments E and F were allowed to self-prime, then amplified with primer pair RSG F1 and RSG R4 to create the final amplicon. This final amplicon was co-transformed into BY4742 with pRS415 (*CEN/ARS, LEU2*$^+$) which had been

previously linearized with XhoI and SpeI, using standard lithium acetate techniques[485].

To generate plasmid pRS425-CPY$_{pr+1-50}$-mRuby2-[G$_3$S]$_2$LE-GFP$_{11}$ for directing the GFP$_{11}$ helix to endosomes/lysosomes, three separate amplicons were generated: Fragment G was amplified from BY4742 genomic DNA with primer pair CRG F1 and CRG R1, Fragment H was amplified from pFA6a-link-yomRuby2-SpHis5 with primer pair CRG F2 and CRG R2, and Fragment I was amplified from pSJ1321 with primer pair CRG F3 and RSG R4. Resultant amplicons were all mixed, allowed to self-prime, and the final amplicon was amplified with primer pair CRG F1 and RSG R4. This final amplicon was co-transformed into BY4742 with pRS425 (2µ*, LEU2*$^+$) which had been previously linearized with XhoI and SpeI.

To generate plasmid pRS423-CPY$_{pr+1-50}$-GFP$_{1-10}$ for directing the non-fluorescent GFP$_{1-10}$ protein to endosomes/lysosomes, two separate amplicons were generated: Fragment J was amplified from BY4742 genomic DNA with primer pair CRG F1 and CG R1, and Fragment K was amplified from pSJ1726 [473] with primer pair CG F2 and CG R2. Resultant amplicons were mixed, allowed to self-prime, and the final amplicon was amplified with primer pair CRG F1 and CG R2. This final amplicon was co-transformed into BY4742 with pRS423 (2µ*, HIS3*$^+$) which had been previously linearized with XhoI and SpeI. All plasmid constructs were confirmed by sequencing (Eton Bioscience, Inc.).

Reagent preparation

To prepare the α-LegC7 resin used for immunoprecipitation**,** Rosetta 2 (DE3) pLysS cells (Novagen®) containing pVJS77 were grown in Terrific Broth (TB) to an OD of 1.5-2. Expression of LegC7ΔTM-Halo was induced by addition of 1mM IPTG, and

cells were grown at 18° for 18 hours. Cells were harvested by centrifugation and cell pellets were disrupted by a single pass through a One Shot Cell Disruptor (OS Model, Pressure BioSciences Inc.) at 20,000 psi. Lysates were cleared (20 min, 20,000 x *g*, 4°C) after the addition of 1mM PMSF and DNase. The resulting supernatant was applied to 500 µL Halo resin and incubated for 1 hour at 4°C. The resin was washed with 30 mL of Halo buffer (50mM HEPES pH 6.5, 300 mM NaCl, and 0.5 mM EDTA) before a 30 min incubation at 22°C with Halo buffer containing 1mM ATP and 10 mM $MgCl_2$. The column was then washed with 30 mL of Halo buffer containing 1% Triton before a final wash of 30 mL Halo buffer. Polyclonal antiserum raised against LegC7[340] was then passed over the column and washed with 10 mL of IgG binding buffer (100mM Sodium Phosphate, 150mM NaCl). Bound antibodies were then eluted using 1 mL of elution buffer (0.2 M Glycine pH 2.0), and then conjugated to IgG resin using the Pierce Protein A IgG Plus Orientation Kit (Thermo Fisher), according to manufacturer's instructions. Bound antibodies were cross-linked using disuccinimidyl suberate (DSS) and any additional DSS sites were blocked with 0.1M ethanolamine.

Cell lysis, subcellular fractionation, and split-GFP fluorescence assay

Strains harboring the *GAL*-inducible pYES2-NT C control vector or pYES2-*LEGC7*$^{+}$ plasmid[458] were grown to saturation at 30°C in CSM-uracil medium. Cells were then harvested via centrifugation, resuspended in an equal volume of fresh CSM-uracil medium containing 1% raffinose and 1% galactose, and grown for an additional 18 h at 30°C. 50 OD_{600} units were harvested from each condition via centrifugation, then washed with 10 mL of azide buffer (50 mM Tris-HCl pH 7.5, 10 mM NaN_3) to halt energy-dependent processes. Cells were resuspended in 5 mL of disulfide reduction

buffer (100 mM Tris-HCl pH 9.4, 10 mM NaN_3, 50 mM β-mercaptoethanol) and incubated at room temperature for 10 minutes. Cells were then washed with 3 mL spheroplasting buffer (1 M sorbitol, 40 mM HEPES-NaOH pH 7.5, 10 mM NaN_3), harvested, then suspended again in 3 mL of spheroplasting buffer containing 100 µg oxalyticase (Zymolyase®-20T, AMSBIO). Mixtures were incubated at 37°C for 1 hr with gentle shaking, then harvested via centrifugation. Spheroplasts were then gently suspended in 3 mL of lysis buffer (200 mM sorbitol, 50 mM KOAc, 2 mM EDTA, 20 mM HEPES-NaOH pH 6.8) containing a protease inhibitor cocktail (Pierce™ Protease Inhibitor Tablet, EDTA-free, Thermo Fisher Scientific), and transferred to a Dounce homogenizer on ice. Spheroplasts were homogenized with a tightly-fitting pestle (15 strokes), and lysates were cleared by centrifugation (2 times, 5 min, 500 x *g* at 4°C) and collected.

2 mL of each lysate prepared above was applied to the top of a discontinuous Histodenz density gradient, prepared in lysis buffer (1 mL 43%, 1 mL 37%, 1 mL 31%, 1.5 mL 27%, 1.5 mL 23%, 1.5 mL 20%, 1 mL 17%, 1 mL 13%, 1 mL 8%). Samples were centrifuged in polyallomer tubes (175000 x *g*, 18 h, 4°C), then secured to a ring stand. The bottom of each tube was pierced with an 18 g needle, and the samples were removed with a peristaltic pump set to 1.5 ml min^{-1}. Flow was directed to a fraction collector set to collect 500 µl fractions (Retriever® 500, Teledyne ISCO), which were then saved on ice.

In order to detect GFP fluorescence resulting from the reconstitution of GFP from the non-fluorescent GFP_{1-10} and GFP_{11} fragments, 20 µl of each fraction collected above was loaded, in triplicate, to a black 384-well plate (Corning®) and fluorescence

was measured (λ_{ex} = 479; λ_{em} = 520) on a plate-reading fluorimeter (SynergyMX, BioTek, Gen5 v. 2.09). Relative fluorescence values for each fraction are reported as the average across the three samples for each fraction measured.

Western blotting

Total protein from cell lysates and subcellular fractions from indicated strains were precipitated with the addition of trichloroacetic acid (final 2% w/v) and placed on ice for 10 min. Protein was collected via centrifugation (10 min, 17000 x *g*, 4°C), washed twice with 300 µL ice-cold acetone, and allowed to dry at room temperature for 10 minutes. Dry pellets were solubilized in 2x SDS Dye (100 mM Tris-HCl pH 6.8, 200 mM DTT, 4% SDS, 0.2% bromophenol blue, 20% glycerol) and incubated at 98°C for 10 min. Equal volumes of samples were separated on 13% SDS-PAGE gels and immunoblotted for indicated proteins using polyclonal or monoclonal antibodies (1:1000) in blocking buffer (0.1% Tween-20 and 5% dry non-fat milk). Goat anti-rabbit (1:20000, Thermo Fisher Scientific) and anti-mouse (1:20000, Thermo Fisher Scientific) IgGs conjugated to HRP were used as secondary antibodies. Blots were developed with SuperSignal™ West Pico PLUS chemiluminescent substrate (Thermo Scientific).

Microscopy

Strains were grown to saturation at 30°C in selective media. Cells were harvested and resuspended in fresh media with or without inducer (1% raffinose and 1% galactose, where indicated) and grown for an additional 18 hr at 30°C. Strains were harvested via centrifugation, washed, then mounted to glass slides which had been pretreated with a 1:1 mixture of concanavalin A (2 mg ml^{-1}):polylysine (10% w/v). Slides

were imaged with a Nikon Ti-U fluorescence microscope, equipped with appropriate filter sets. Images were processed with the Fiji software package[486, 487].

Flow Cytometry

To measure the redox environment of the ER-localized eroGFP protein, indicated yeast strains were transformed with pPM28[471], and resultant strains were grown to saturation at 30°C in selective media. Cells were harvested, resuspended in fresh media with inducer (1% raffinose and 1% galactose), and grown for an additional 6 hrs at 30°C. 100,000 cells per strain were analyzed with a BD Biosciences LSR II flow cytometer (UGA Flow Cytometry Core), exciting with 405 nm and 488 nm lasers, and collecting fluorescence between 500-550 nm. Cells treated with DTT were analyzed 20 minutes after addition of DTT to the media, and cells treated with hydrogen peroxide were analyzed 5 minutes after addition of hydrogen peroxide to the media. Data analysis was performed within FlowJo 10.6. Gates defining populations of low fluorescence cells and dead cells were created with the Autogating tool, adjusted to maximum size (>98% of cells).

Statistical Analysis

Statistical analysis was performed within the Prism software package (GraphPad Software, version 5.0f). Column statistics were performed via one-tailed, unpaired t-tests with Welch's correction.

Protease digestion and LC-MS/MS analysis of LegC7 sample

Precipitation of protein from SDS buffer and reduction/carbamidomethylation

Cold acetone was added to the protein mixture in SDS buffer and incubated overnight at -20 °C. The precipitate obtained was recovered by centrifugation and

washed with cold acetone. Protein precipitate was redissolved in digestion buffer (50 mM aq. NH_4CO_3), reduced by DTT (25 mM for 45 min), carbamidomethylated by Iodoacetamide (90 mM for 45 min) and dialyzed against ddH_2O.

Trypsin digestion

25 µL of digestion buffer (50 mM aq. NH_4CO_3) was added to 20 µL of Sample (~ 20.0 µg) protein solution. The protein sample was digested by adding 5 µL sequencing-grade trypsin (Promega, 0.5 µg/µL) and incubated at 37 ºC for 24 h. The digests were desalted by C18 centrifuge cartridges. The digests in elution buffer (80 % acetonitrile and 0.1 % formic acid) were dried under speed vac. The peptides and glycopeptides were subsequently re-dissolved in solvent A (0.1% formic acid in water) and stored at -30 ºC until analysis by nano-LC-MS/MS.

Data acquisition of protein digest samples using nano-LC-MS/MS

Desalted peptides were analyzed on an Orbitrap Fusion instrument (Thermo Scientific) equipped with a nanospray ion source with CID, HCD and ETD fragmentation options and connected to a Dionex binary solvent system. Pre-packed nano-LC columns of 15 cm length with 75 µm internal diameter (id), filled with 2 µm C18 material (reverse phase) were used for chromatographic separation of samples. After the precursor ion scan at 120000 resolution in Orbitrap analyzer, precursors at a time frame of 3 sec were selected for subsequent fragmentation using HCD at normalized collision energy of 28. Another acquisition with a program HCD product triggered ETD, where ETD fragmentation occurs based on the presence of glycan oxonium ions in the HCD fragmentation of the same peptide, was also employed. The threshold for triggering an MS/MS event on ion-trap was set to 500 counts. Charge state screening was enabled,

and precursors with unknown charge state or a charge state of +1 were excluded (positive ion mode). Dynamic exclusion was enabled (exclusion duration of 60 s). The fragment ions were analyzed on orbitrap for HCD at 30000 resolution.

Peptides and glycopeptide analysis

The .raw files of the LC-MS/MS acquisition were analyzed through Byonic v2.6 and Proteome Discoverer 1.4 software against the .fasta sequence of LegC7 sample. Search was conducted with modifications such as oxidation of methionine, carbamidomethylation of cysteine and possible *N*-glycans from the corresponding expression species. A precursor ion tolerance of 10 ppm and fragment ion tolerance of 0.1 Da was set for the search with up to two missed cleavage for the target enzyme trypsin. Based on the identifications of the software and manual validation of spectra, sequences of amino acids on the peptides were validated. The HCD MS^2 spectra of glycopeptides were evaluated for the glycan neutral loss pattern, oxonium ions and the glycopeptide fragmentations to assign the sequence and the presence of glycans in the glycopeptides.

Acknowledgments

The authors would like to thank Dr. Alexey Merz for providing essential reagents and Drs. Greg Odorizzi and Youngsoo Jun for providing essential insight and suggestions. pFA6a-link-yomRuby2-SpHis5 was a gift from Wendell Lim and Kurt Thorn (Addgene plasmid # 44858). pSJ1321 (pRS315-NOP1pr-GFP11-mCherry-PUS1) and pSJ1726 (pFA6-NATMX-CDC42pr-KAR2SS-GFP1-10) were gifts from Sue Jaspersen (Addgene plasmids # 86413 and # 86421). YCPlac33-sGFP-VRG4 was a gift from Benjamin Glick (Addgene plasmid # 25447). V.J.S. was supported by a grant from the

National Institute of Allergy and Infectious Diseases (R01-AI100913). This research was supported in part by the National Institutes of Health grants 1S10OD018530 and P41GM10349010 to the Complex Carbohydrate Research Center. The Authors have no conflicts of interest to declare.

CONCLUSIONS

Since its discovery as the causal agent of Legionnaires' disease, *Legionella pneumophila* has been subject to extensive scientific study to understand its capacity to infect diverse hosts. Over evolutionary time, *L. pneumophila* has carved out an ecological niche in natural freshwater environments by living intracellularly in a wide variety of protozoan hosts. Due to the diversity among its hosts, *L. pneumophila* necessarily developed a breadth of tools for intracellular survival, including the largest arsenal of secreted effector proteins of any known bacterial pathogen, and those tools allow this pathogen to also survive and replicate in human alveolar macrophages. Once phagocytosed by a macrophage, *L. pneumophila* acquires nutrients and avoids degradation largely through modulation of its host's membrane trafficking by secreted effectors. Thus, these secreted effectors have garnered much attention from researchers who want to better understand *L. pneumophila* pathogenesis.

LegC7, one of the aforementioned secreted effectors, is the focus of this work. Previous studies have shown that LegC7 affects host cell membrane trafficking such that ER is recruited to the Legionella-containing vacuole (LCV), potentially by driving membrane fusion through interaction with other "SNARE-like" secreted effectors LegC2 and LegC3 to form a canonical Qabc-SNARE complex[341, 344, 488]. However, this work shows that LegC7 is capable of driving membrane fusion independent of other secreted effectors in a yeast model system. In yeast, LegC7 alters perinuclear ER morphology, pulling it away from the nucleus to form large patches uncharacteristic of

typical ER (**Fig. 3.2A**). This altered morphology is organelle-specific, as there is no apparent change to other intracellular structures like Golgi (**Fig. 3.2B**) or the yeast vacuole (**Fig. 3.4E**). LegC7 also causes the mixing of ER and endosomal lumenal contents, a defining feature of membrane fusion. Yeast vacuolar proteases trafficked to the vacuole via endosomes are synthesized as inactive precursors at the ER and only activated after leaving the Golgi. Thus, the vacuolar protease-dependent degradation of ER resident ATPase Kar2p upon expression of LegC7 strongly suggests ER:endosome fusion (**Figs. 3.6A, B, and 3.8B**). Subsequent experiments following the observation of Kar2p degradation found LegC7-induced oxidation of the ER lumen (**Figs. 3.7G, H, and K**) and reconstitution of ER- and endosome-directed split-GFP constructs (**Fig. 3.8**), providing further evidence of ER:endosome fusion. Importantly, the intracellular compartments that fuse during LegC7 expression—ER and endosomes—are analogous to the ER and the nascent LCV following phagocytosis of *L. pneumophila*, providing further evidence that LegC7 plays an active role in recruiting ER to the LCV during infection.

The mechanism by which LegC7-induced membrane fusion occurs remains to be elucidated, but class C tethering complexes are undoubtedly involved. This is interesting considering that the class C tethering complexes do not participate in membrane trafficking between the ER and the Golgi[415, 418]. Nevertheless, fluorescence microscopy indicates colocalization of CORVET and the ER (**Fig. 5A and B**) with LegC7 expression, and all observed phenotypes indicating ER:endosome fusion are reversed in class C deficient mutants (**Figs. 5C, 6B, and 7K**). While class C complexes have been shown to interact with SNAREs (See *VPS Class C Tethering*

Complexes, page 49), to which LegC7 has been compared, recruitment of the complexes by Rab GTPases is thought to be a prerequisite for those interactions[415, 418]. However, there has been recent evidence of SNAREs targeting vesicles to specific destinations through interaction with multisubunit tethering complexes in a manner that is independent of trans-SNARE pairing[481]. During *L. pneumophila* infection, recruitment of class C tethering complexes to ER and ER-derived vesicles could provide a dual benefit by simultaneously promoting fusion of secretory vesicles with the LCV and preventing endosomal maturation of the LCV via sequestration of the tethering complexes.

In considering the possibility that LegC7 acts as a SNARE in yeast, there are notable caveats. First, no yeast SNAREs were detected in LegC7 immunoprecipitations (**Table 3.1**), making it unlikely that LegC7 forms canonical SNARE assemblies with yeast SNAREs. It is known, however, that LegC7 forms homooligomers[341], but if homooligomerization of LegC7 on apposed membranes drives membrane fusion, it would be unprecedented in SNARE biology. While SNARE homodimerization has been reported, it occurs among proteins within the same membrane via an interaction between transmembrane domains and doesn't appear to play a role in membrane fusion events[489-491]. Lastly, LegC7 is unique among LegC proteins in its ability to inhibit yeast growth, which implies that, if it forms Qabc-SNARE assemblies with LegC2 and LegC3, it has an additional function to induce such toxicity.

The interaction between LegC7 and the Emp46p/Emp47p complex (**Table 3.1**) raises the possibility that LegC7 is targeted to ER exit sites or ER-derived vesicles in a cargo adapter-specific manner. This would be an effective way of targeting LegC7 to

compartments containing desirable cargo. Indeed, Emp46p/Emp47p complexes package glycosylated proteins into ER-derived COPII vesicles, and glycoproteins have been shown to be important for nutrition and evasion of host immune defenses by bacteria. Importantly, LegC7 is not itself glycosylated, meaning its interaction with the Emp46p/Emp47p complex is separate from the carbohydrate-binding function of the complex. This interaction between the Emp46p/Emp47p complex and LegC7 could also result in the alteration or inhibition of cargo adapter function. Analysis of Carboxypeptidase S (CPS) trafficking in *emp46*Δ*emp47*Δ and LegC7-expressing cells (**Fig. 3.1**) revealed that CPS is ineffectively trafficked to the yeast vacuole in both strains. Furthermore, the Emp46p/Emp47p complex requires interaction with COPII machinery to initiate COPII vesicle budding from the ER[439-441], and while there was a strong enrichment of Emp46p/Emp47p complex subunits in LegC7 immunoprecipitations, no COPII coatamer subunits were detected (**Table 3.1**). This means that either (i) Emp46p/Emp47p complex-directed cargo is not trafficked to the Golgi with LegC7 expression, or (ii) the interaction between the Emp46p/Emp47p complex and COPII machinery is generally transient such that it dissociates during immunoprecipitation of LegC7.

A possibility worth addressing is that the LegC7-induced ER phenotypes are the result of ER stress upon LegC7 expression. ER stress generally occurs when the ER protein folding capacity becomes saturated, which coincides with increased levels of misfolded proteins and oxidative stress. The cell's response to ER stress, the unfolded protein response (UPR), triggers various pathways to decrease protein synthesis, increase protein folding capacity, and remove terminally misfolded proteins via ER-

associated degradation (ERAD)[492-494]. While it is imaginable that LegC7 misfolding or inhibition of ER-to-Golgi traffic by LegC7 would result in the induction of UPR, the notion that the data in this work is a reflection of that reality is untenable. First, there is no evidence that LegC7 is misfolded, causing the cell to mark it for subsequent ERAD. We detect no degradation of LegC7 via immunoblot (data not shown), no modifications of LegC7 indicative of ERAD such as N-terminal glycosylation (**Fig. 3.10**), and no ERAD machinery in LegC7 immunoprecipitations (**Table 3.1**). Furthermore, if LegC7-induced oxidation of the ER (**Figs. 3.7G, H, and K**) were an indication of oxidative stress typical of ER stress, it would not be alleviated by the deletion of class C complex core subunit *VPS33* (**Figs. 3.7I, J, and K)**. Similarly, if Kar2p degradation (**Figs. 3.6A and 8B**) were the result of ERAD, it would not be dependent on vacuolar proteases and endosomal fusion machinery (**Fig. 3.6B**), as ERAD occurs independent of lysosomal degradation[493, 494]. For these reasons, it seems highly unlikely that the observations in this body of work are attributable to fundamental ER stress induced by LegC7 expression.

Through heterologous expression of LegC7 in *S. cerevisiae*, this work has shown that LegC7 facilitates membrane fusion in a compartment-specific manner that is both independent of other Dot/Icm-secreted effectors and dependent on endosomal fusion machinery. Additionally, this work supports the possibility that this effector is targeted to ER and/or ER-derived membranes in a cargo-specific manner through interaction with host cargo adapters. These findings provide further insight into the involvement of LegC7 in the recruitment of host ER to the LCV during *L. pneumophila* infection. Future studies concerning LegC7 should aim to determine the mechanism by which LegC7

induces the phenotypes observed in yeast not only to better understand *L. pneumophila* pathogenesis, but potentially to add to our current understanding of membrane fusion. Comparison of mass spectroscopy analysis of subcellular fractions (See **Cell lysis, subcellular fractionation, and split-GFP fluorescence assay** in **Materials and Methods**, page 116) from cells with and without LegC7 expression could provide a more granular view of the altered membrane traffic caused by LegC7 by highlighting what cargo is affected and indicating how global or cargo-specific the alteration is. Additionally, mass spectroscopy analysis of purifications of endosomal fusion machinery from yeast cells expressing LegC7 may provide insight into the nature of the genetic interactions between said fusion machinery and LegC7. Future studies may also aim to determine how the findings in this work translate to other model systems. For example, it would be useful to determine if siRNA knockdowns of specific host cargo receptors like Emp47p homolog ERGIC-53 limit recruitment of ER to the LCV in macrophage infection models. Testing for host ER on the LCV can be accomplished via α-calnexin immunoblotting of protein extracts from isolated LCVs[341]. Similarly, studies may aim to determine whether LegC proteins interact with host tethering complexes to facilitate membrane fusion during infection by testing siRNA knockdowns of HOPS and/or CORVET for efficient ER recruitment to the LCV. Collectively, the work in this study and future efforts focusing on modulation of host cell biology by *L. pneumophila* Dot/Icm effectors can better our understanding of both *L. pneumophila* as a human pathogen and eukaryotic membrane trafficking.

REFERENCES

1. Fraser, D.W., et al., *Legionnaires' disease: description of an epidemic of pneumonia.* N Engl J Med, 1977. **297**(22): p. 1189-97.

2. Brenner, D.J., A.G. Steigerwalt, and J.E. McDade, *Classification of the Legionnaires' disease bacterium: Legionella pneumophila, genus novum, species nova, of the family Legionellaceae, familia nova.* Ann Intern Med, 1979. **90**(4): p. 656-8.

3. Fields, B.S., R.F. Benson, and R.E. Besser, *Legionella and Legionnaires' disease: 25 years of investigation.* Clin Microbiol Rev, 2002. **15**(3): p. 506-26.

4. Parte, A.C., *LPSN - List of Prokaryotic names with Standing in Nomenclature (bacterio.net), 20 years on.* 2018, International Journal of Systemic and Evolutionary Microbiology p. 1825-1829.

5. Adeleke, A.A., et al., *Legionella drozanskii sp. nov., Legionella rowbothamii sp. nov. and Legionella fallonii sp. nov.: three unusual new Legionella species.* Int J Syst Evol Microbiol, 2001. **51**(Pt 3): p. 1151-1160.

6. BENSON, R.F., et al., *Legionella waltersii sp. nov. and an Unnamed Legionella Genomospecies Isolated from Water in Australia.* International Journal of Systematic and Evolutionary Microbiology, 1996. **46**(3): p. 631-634.

7. Campbell, J., et al., *Legionella sainthelensi: a new species of Legionella isolated from water near Mt. St. Helens.* Appl Environ Microbiol, 1984. **47**(2): p. 369-73.

8. Campocasso, A., et al., *Legionella tunisiensis sp. nov. and Legionella massiliensis sp. nov., isolated from environmental water samples.* Int J Syst Evol Microbiol, 2012. **62**(Pt 12): p. 3003-3006.

9. Carvalho, F.R., et al., *Occurrence and diversity of Legionellaceae in polar lakes of the Antarctic peninsula.* Curr Microbiol, 2008. **57**(4): p. 294-300.

10. Kuroki, H., et al., *Legionella impletisoli sp. nov. and Legionella yabuuchiae sp. nov., isolated from soils contaminated with industrial wastes in Japan.* Syst Appl Microbiol, 2007. **30**(4): p. 273-9.

11. Lösch, L.S. and L.A. Merino, *Presencia de Legionella spp. en depósitos domiciliarios de agua potable en Resistencia, Chaco, Argentina. Informe preliminar.* Revista Argentina de Microbiología, 2016. **48**(4): p. 329-332.

12. Fliermans, C.B., *Ecology of Legionella: From data to knowledge with a little wisdom.* Microbial Ecology, 1996. **32**(2): p. 203-228.

13. van Heijnsbergen, E., et al., *Confirmed and Potential Sources of Legionella Reviewed.* Environmental Science & Technology, 2015. **49**(8): p. 4797-4815.

14. Steele, T.W., J. Lanser, and N. Sangster, *Isolation of Legionella longbeachae serogroup 1 from potting mixes.* Applied and Environmental Microbiology, 1990. **56**(1): p. 49-53.

15. Steele, T.W., C.V. Moore, and N. Sangster, *Distribution of Legionella longbeachae serogroup 1 and other legionellae in potting soils in Australia.* Applied and Environmental Microbiology, 1990. **56**(10): p. 2984-2988.

16. Anand, C.M., et al., *Interaction of L. pneumophila and a free living amoeba (Acanthamoeba palestinensis).* 1983. **91**(02): p. 167.

17. Barker, J., et al., *Relationship between Legionella pneumophila and Acanthamoeba polyphaga: physiological status and susceptibility to chemical inactivation.* Appl Environ Microbiol, 1992. **58**(8): p. 2420-5.

18. Cirillo, J.D., S. Falkow, and L.S. Tompkins, *Growth of Legionella pneumophila in Acanthamoeba castellanii enhances invasion.* Infect Immun, 1994. **62**(8): p. 3254-61.

19. King, C.H., et al., *Survival of coliforms and bacterial pathogens within protozoa during chlorination.* Appl Environ Microbiol, 1988. **54**(12): p. 3023-33.

20. Cirillo, J.D., et al., *Intracellular growth in Acanthamoeba castellanii affects monocyte entry mechanisms and enhances virulence of Legionella pneumophila.* Infect Immun, 1999. **67**(9): p. 4427-34.

21. Rogers, J., et al., *Influence of temperature and plumbing material selection on biofilm formation and growth of Legionella pneumophila in a model potable water system containing complex microbial flora.* Appl Environ Microbiol, 1994. **60**(5): p. 1585-92.

22. Declerck, P., *Biofilms: the environmental playground ofLegionella pneumophila.* Environmental Microbiology, 2010. **12**(3): p. 557-566.

23. Rowbotham, T.J., *Preliminary report on the pathogenicity of Legionella pneumophila for freshwater and soil amoebae.* Journal of Clinical Pathology, 1980. **33**(12): p. 1179-1183.

24. Glick, T.H., et al., *Pontiac fever. An epidemic of unknown etiology in a health department: I. Clinical and epidemiologic aspects.* Am J Epidemiol, 1978. **107**(2): p. 149-60.

25. Bartley, P.B., et al., *Hospital-wide Eradication of a Nosocomial Legionella pneumophila Serogroup 1 Outbreak.* Clin Infect Dis, 2016. **62**(3): p. 273-279.

26. Dooling, K.L., et al., *Active Bacterial Core Surveillance for Legionellosis - United States, 2011-2013.* MMWR Morb Mortal Wkly Rep, 2015. **64**(42): p. 1190-3.

27. Marston, B.J., H.B. Lipman, and R.F. Breiman, *Surveillance for Legionnaires' disease. Risk factors for morbidity and mortality.* Arch Intern Med, 1994. **154**(21): p. 2417-22.

28. Beer, K.D., et al., *Surveillance for Waterborne Disease Outbreaks Associated with Drinking Water - United States, 2011-2012.* MMWR Morb Mortal Wkly Rep, 2015. **64**(31): p. 842-8.

29. Benedict, K.M., et al., *Surveillance for Waterborne Disease Outbreaks Associated with Drinking Water - United States, 2013-2014.* MMWR Morb Mortal Wkly Rep, 2017. **66**(44): p. 1216-1221.

30. Demirjian, A., et al., *The Importance of Clinical Surveillance in Detecting Legionnaires' Disease Outbreaks: A Large Outbreak in a Hospital With a Legionella Disinfection System--Pennsylvania, 2011-2012.* 2015. **60**(11): p. 1596-1602.

31. Granseth, G., et al., *Notes from the Field: Two Cases of Legionnaires' Disease in Newborns After Water Births - Arizona, 2016.* MMWR Morb Mortal Wkly Rep, 2017. **66**(22): p. 590-591.

32. Schwake, D.O., et al., *Legionella DNA Markers in Tap Water Coincident with a Spike in Legionnaires' Disease in Flint, MI.* Environmental Science & Technology Letters, 2016. **3**(9): p. 311-315.

33. Weiss, D., et al., *A Large Community Outbreak of Legionnaires' Disease Associated With a Cooling Tower in New York City, 2015.* Public Health Rep, 2017. **132**(2): p. 241-250.

34. Garrison, L.E., et al., *Vital Signs: Deficiencies in Environmental Control Identified in Outbreaks of Legionnaires' Disease - North America, 2000-2014.* MMWR Morb Mortal Wkly Rep, 2016. **65**(22): p. 576-84.

35. Walser, S.M., et al., *Assessing the environmental health relevance of cooling towers--a systematic review of legionellosis outbreaks.* Int J Hyg Environ Health, 2014. **217**(2-3): p. 145-54.

36. O'Connor, B.A., et al., *Does using potting mix make you sick? Results from a Legionella longbeachae case-control study in South Australia.* Epidemiology and Infection, 2007. **135**(1): p. 34-39.

37. Pravinkumar, S.J., et al., *A cluster of Legionnaires' disease caused by Legionella longbeachae linked to potting compost in Scotland, 2008-2009.* Eurosurveillance, 2010. **15**(8): p. 19496.

38. Correia, A.M., et al., *Probable Person-to-Person Transmission of Legionnaires' Disease.* New England Journal of Medicine, 2016. **374**(5): p. 497-498.

39. Fields, B.S., R.F. Benson, and R.E. Besser, *Legionella and Legionnaires' Disease: 25 Years of Investigation.* Clinical Microbiology Reviews, 2002. **15**(3): p. 506-526.

40. Plouffe, J.F., L.R. Webster, and B. Hackman, *Relationship between colonization of hospital building with Legionella pneumophila and hot water temperatures.* Appl Environ Microbiol, 1983. **46**(3): p. 769-70.

41. Bohach, G.A. and I.S. Snyder, *Characterization of surfaces involved in adherence of Legionella pneumophila to Fischerella species.* Infection and Immunity, 1983. **42**(1): p. 318-325.

42. Koide, M., et al., *Role of Brevundimonas vesicularis in supporting the growth of Legionella in nutrient-poor environments.* The new microbiologica, 2014. **37**(1): p. 33-39.

43. Lau, H.Y. and N.J. Ashbolt, *The role of biofilms and protozoa in Legionella pathogenesis: implications for drinking water.* 2009. **107**(2): p. 368-378.

44. Mampel, J., et al., *Planktonic Replication Is Essential for Biofilm Formation by Legionella pneumophila in a Complex Medium under Static and Dynamic Flow Conditions.* Applied and Environmental Microbiology, 2006. **72**(4): p. 2885-2895.

45. Plouffe, J.F., L.R. Webster, and B. Hackman, *Relationship between colonization of hospital building with Legionella pneumophila and hot water temperatures.* Applied and Environmental Microbiology, 1983. **46**(3): p. 769-770.

46. Pope, D.H., et al., *Growth ofLegionella pneumophila in two-membered cultures with green algae and cyanobacteria.* Current Microbiology, 1982. **7**(5): p. 319-321.

47. Stewart, C.R., V. Muthye, and N.P. Cianciotto, *Legionella pneumophila Persists within Biofilms Formed by Klebsiella pneumoniae, Flavobacterium sp., and Pseudomonas fluorescens under Dynamic Flow Conditions.* PLoS ONE, 2012. **7**(11): p. e50560.

48. Stout, J.E., et al., *A note on symbiosis of Legionella pneumophila and Tatlockia micdadei with human respiratory flora.* 1986. **60**(4): p. 297-299.

49. Tison, D.L., et al., *Growth of Legionella pneumophila in association with blue-green algae (cyanobacteria).* Applied and Environmental Microbiology, 1980. **39**(2): p. 456-459.

50. Wadowsky, R.M. and R.B. Yee, *Satellite growth of Legionella pneumophila with an environmental isolate of Flavobacterium breve.* Applied and Environmental Microbiology, 1983. **46**(6): p. 1447-1449.

51. Temmerman, R., et al., *Necrotrophic Growth of Legionella pneumophila.* Applied and Environmental Microbiology, 2006. **72**(6): p. 4323-4328.

52. Berk, S.G., et al., *Production of Respirable Vesicles Containing Live Legionella pneumophila Cells by Two Acanthamoeba spp.* Applied and Environmental Microbiology, 1998. **64**(1): p. 279-286.

53. Biurrun, A., et al., *Treatment of a Legionella pneumophila -Colonized Water Distribution System Using Copper-Silver Ionization and Continuous Chlorination •.* 1999. **20**(6): p. 426-428.

54. Bouyer, S., et al., *Long-term survival of Legionella pneumophila associated with Acanthamoeba castellanii vesicles.* Environmental Microbiology, 2007. **9**(5): p. 1341-1344.

55. Buse, H.Y. and N.J. Ashbolt, *Differential growth of Legionella pneumophila strains within a range of amoebae at various temperatures associated with in-premise plumbing.* Letters in Applied Microbiology, 2011. **53**(2): p. 217-224.

56. Cervero-Arago, S., et al., *Effect of Common Drinking Water Disinfectants, Chlorine and Heat, on Free Legionella and Amoebae-Associated Legionella.* PLoS One, 2015. **10**(8): p. e0134726.

57. Cervero-Arago, S., R. Sommer, and R.M. Araujo, *Effect of UV irradiation (253.7 nm) on free Legionella and Legionella associated with its amoebae hosts.* Water Res, 2014. **67**: p. 299-309.

58. García, M.T., et al., *Persistence of chlorine-sensitiveLegionella pneumophilain hyperchlorinated installations.* Journal of Applied Microbiology, 2008. **105**(3): p. 837-847.

59. Kikuhara, H., et al., *Intracellular multiplication of Legionella pneumophila in Tetrahymena thermophila.* J UOEH, 1994. **16**(4): p. 263-75.

60. Kilvington, S. and J. Price, *Survival ofLegionella pneumophilawithin cysts ofAcanthamoeba polyphagafollowing chlorine exposure.* 1990. **68**(5): p. 519-525.

61. Rasch, J., et al., *Legionella-protozoa-nematode interactions in aquatic biofilms and influence of Mip on Caenorhabditis elegans colonization.* International Journal of Medical Microbiology, 2016. **306**(6): p. 443-451.

62. Smith-Somerville, H.E., et al., *Survival of Legionella pneumophila in the cold-water ciliate Tetrahymena vorax.* Applied and Environmental Microbiology, 1991. **57**(9): p. 2742-2749.

63. Storey, M.V., et al., *The Efficacy of Heat and Chlorine Treatment against Thermotolerant Acanthamoebae and Legionellae.* Scandinavian Journal of Infectious Diseases, 2004. **36**(9): p. 656-662.

64. Boamah, D.K., et al., *From Many Hosts, One Accidental Pathogen: The Diverse Protozoan Hosts of Legionella.* Frontiers in Cellular and Infection Microbiology, 2017. **7**(477).

65. Abu Kwaik, Y., *The phagosome containing Legionella pneumophila within the protozoan Hartmannella vermiformis is surrounded by the rough endoplasmic reticulum.* Applied and Environmental Microbiology, 1996. **62**(6): p. 2022-2028.

66. Amaro, F., et al., *Diverse protist grazers select for virulence-related traits in Legionella.* 2015. **9**(7): p. 1607-1618.

67. Barbaree, J.M., et al., *Isolation of protozoa from water associated with a legionellosis outbreak and demonstration of intracellular multiplication of Legionella pneumophila.* Applied and Environmental Microbiology, 1986. **51**(2): p. 422-424.

68. Berk, S.G., et al., *Packaging of live Legionella pneumophila into pellets expelled by Tetrahymena spp. does not require bacterial replication and depends on a Dot/Icm-mediated survival mechanism.* Appl Environ Microbiol, 2008. **74**(7): p. 2187-99.

69. Cianciotto, N.P. and B.S. Fields, *Legionella pneumophila mip gene potentiates intracellular infection of protozoa and human macrophages.* 1992. **89**(11): p. 5188-5191.

70. Declerck, P., et al., *Impact of Non-Legionella Bacteria on the Uptake and Intracellular Replication of Legionella pneumophila in Acanthamoeba castellanii and Naegleria lovaniensis.* 2005. **50**(4): p. 536-549.

71. Dupuy, M., et al., *Permissiveness of freshly isolated environmental strains of amoebae for growth of Legionella pneumophila.* 2016. **363**(5): p. fnw022.

72. Fields, B.S., et al., *Comparison of guinea pig and protozoan models for determining virulence of Legionella species.* Infection and Immunity, 1986. **53**(3): p. 553-559.

73. Fields, B.S., et al., *Intracellular multiplication ofLegionella pneumophila in amoebae isolated from hospital hot water tanks.* Current Microbiology, 1989. **18**(2): p. 131-137.

74. Fields, B.S., et al., *Proliferation of Legionella pneumophila as an intracellular parasite of the ciliated protozoan Tetrahymena pyriformis.* Applied and Environmental Microbiology, 1984. **47**(3): p. 467-471.

75. Gao, L.Y., O.S. Harb, and Y. Abu Kwaik, *Utilization of similar mechanisms by Legionella pneumophila to parasitize two evolutionarily distant host cells, mammalian macrophages and protozoa.* Infection and Immunity, 1997. **65**(11): p. 4738-4746.

76. Hagele, S., et al., *Dictyostelium discoideum: a new host model system for intracellular pathogens of the genus Legionella.* 2000. **2**(2): p. 165-171.

77. Harf, C., et al., *Flow cytometric determination of endocytosis of viable labelled Legionella pneumophila by Acanthamoeba palestinensis.* Cytometry, 1997. **27**(3): p. 269-74.

78. Hilbi, H., G. Segal, and H.A. Shuman, *Icm/Dot-dependent upregulation of phagocytosis by Legionella pneumophila.* Molecular Microbiology, 2008. **42**(3): p. 603-617.

79. Hojo, F., et al., *Ciliates Expel Environmental Legionella-Laden Pellets To Stockpile Food.* Applied and Environmental Microbiology, 2012. **78**(15): p. 5247-5257.

80. Kao, P.-M., et al., *Differential Legionella spp. survival between intracellular and extracellular forms in thermal spring environments.* Environmental Science and Pollution Research, 2013. **20**(5): p. 3098-3106.

81. King, C.H., et al., *Effects of cytochalasin D and methylamine on intracellular growth of Legionella pneumophila in amoebae and human monocyte-like cells.* Infection and Immunity, 1991. **59**(3): p. 758-763.

82. Koubar, M., et al., *Passage through Tetrahymena tropicalis enhances the resistance to stress and the infectivity of Legionella pneumophila.* 2011. **325**(1): p. 10-15.

83. Marciano-Cabral, F. and G. Cabral, *Acanthamoeba spp. as Agents of Disease in Humans.* Clinical Microbiology Reviews, 2003. **16**(2): p. 273-307.

84. Mengue, L., et al., *Legionella pneumophila prevents proliferation of its natural host Acanthamoeba castellanii.* 2016. **6**: p. 36448.

85. Moffat, J.F. and L.S. Tompkins, *A quantitative model of intracellular growth of Legionella pneumophila in Acanthamoeba castellanii.* Infection and Immunity, 1992. **60**(1): p. 296-301.

86. Molmeret, M., et al., *Amoebae as Training Grounds for Intracellular Bacterial Pathogens.* Applied and Environmental Microbiology, 2005. **71**(1): p. 20-28.

87. Newsome, A.L., et al., *Interactions between Naegleria fowleri and Legionella pneumophila.* Infection and Immunity, 1985. **50**(2): p. 449-452.

88. Rowbotham, T.J., *Current views on the relationships between amoebae, legionellae and man.* Israel journal of medical sciences, 1986. **22**(9): p. 678-689.

89. Shadrach, W.S., et al., *Balamuthia mandrillaris, Free-Living Ameba and Opportunistic Agent of Encephalitis, Is a Potential Host for Legionella pneumophila Bacteria.* Applied and Environmental Microbiology, 2005. **71**(5): p. 2244-2249.

90. Solomon, J.M., et al., *Intracellular Growth of Legionella pneumophila in Dictyostelium discoideum, a System for Genetic Analysis of Host-Pathogen Interactions.* Infection and Immunity, 2000. **68**(5): p. 2939-2947.

91. Tyndall, R.L. and E.L. Domingue, *Cocultivation of Legionella pneumophila and free-living amoebae.* Applied and Environmental Microbiology, 1982. **44**(4): p. 954-959.

92. Tyson, J.Y., et al., *Multiple Legionella pneumophila Type II Secretion Substrates, Including a Novel Protein, Contribute to Differential Infection of the Amoebae Acanthamoeba castellanii, Hartmannella vermiformis, and Naegleria lovaniensis.* Infection and Immunity, 2013. **81**(5): p. 1399-1410.

93. Tyson, J.Y., P. Vargas, and N.P. Cianciotto, *The novel Legionella pneumophila type II secretion substrate NttC contributes to infection of amoebae Hartmannella vermiformis and Willaertia magna.* Microbiology (Reading, England), 2014. **160**(Pt 12): p. 2732-2744.

94. Watanabe, K., et al., *Ciliate Paramecium is a natural reservoir of Legionella pneumophila.* 2016. **6**: p. 24322.

95. Wadowsky, R.M., et al., *Gentamicin-Containing Peptone-Yeast Extract Medium for Cocultivation of Hartmannella vermiformis ATCC 50256 and Virulent Strains of Legionella pneumophila.* Applied and Environmental Microbiology, 1995. **61**(12): p. 4464-4467.

96. Breiman, R.F., et al., *Association of shower use with Legionnaires' disease. Possible role of amoebae.* JAMA, 1990. **263**(21): p. 2924-6.

97. Conza, L., S. Casati Pagani, and V. Gaia, *Influence of climate and geography on the occurrence of Legionella and amoebae in composting facilities.* BMC Research Notes, 2014. **7**(1): p. 831.

98. Conza, L., S.C. Pagani, and V. Gaia, *Presence of Legionella and free-living Amoebae in composts and bioaerosols from composting facilities.* PloS one, 2013. **8**(7): p. e68244-e68244.

99. Declerck, P., et al., *Detection of Legionella spp. and some of their amoeba hosts in floating biofilms from anthropogenic and natural aquatic environments.* Water Research, 2007. **41**(14): p. 3159-3167.

100. Hsu, B.M., et al., *Comparison of potentially pathogenic free-living amoeba hosts by Legionella spp. in substrate-associated biofilms and floating biofilms from spring environments.* Water Res, 2011. **45**(16): p. 5171-83.

101. Hsu, B.M., C.L. Lin, and F.C. Shih, *Survey of pathogenic free-living amoebae and Legionella spp. in mud spring recreation area.* Water Res, 2009. **43**(11): p. 2817-28.

102. Hsu, T.K., et al., *Surveillance of parasitic Legionella in surface waters by using immunomagnetic separation and amoebae enrichment.* Pathog Glob Health, 2015. **109**(7): p. 328-35.

103. Huang, S.W. and B.M. Hsu, *Survey of Naegleria and its resisting bacteria-Legionella in hot spring water of Taiwan using molecular method.* Parasitol Res, 2010. **106**(6): p. 1395-402.

104. Ji, W.T., et al., *Surveillance and evaluation of the infection risk of free-living amoebae and Legionella in different aquatic environments.* Sci Total Environ, 2014. **499**: p. 212-9.

105. Kurtz, J.B., et al., *Legionella pneumophila in cooling water systems. Report of a survey of cooling towers in London and a pilot trial of selected biocides.* J Hyg (Lond), 1982. **88**(3): p. 369-81.

106. Marciano-Cabral, F., M. Jamerson, and E.S. Kaneshiro, *Free-living amoebae, Legionella and Mycobacterium in tap water supplied by a municipal drinking water utility in the USA.* J Water Health, 2010. **8**(1): p. 71-82.

107. Nahapetian, K., et al., *The intracellular multiplication of Legionella pneumophila in protozoa from hospital plumbing systems.* Res Microbiol, 1991. **142**(6): p. 677-85.

108. Rohr, U., et al., *Comparison of free-living amoebae in hot water systems of hospitals with isolates from moist sanitary areas by identifying genera and determining temperature tolerance.* Appl Environ Microbiol, 1998. **64**(5): p. 1822-4.

109. Scheikl, U., et al., *Free-living amoebae (FLA) co-occurring with legionellae in industrial waters.* Eur J Protistol, 2014. **50**(4): p. 422-9.

110. Steinert, M., et al., *Regrowth of Legionella pneumophila in a heat-disinfected plumbing system.* Zentralbl Bakteriol, 1998. **288**(3): p. 331-42.

111. Thomas, V., et al., *Biodiversity of amoebae and amoeba-resisting bacteria in a hospital water network.* Appl Environ Microbiol, 2006. **72**(4): p. 2428-38.

112. Valster, R.M., et al., *Relationships between free-living protozoa, cultivable Legionella spp., and water quality characteristics in three drinking water supplies in the Caribbean.* Appl Environ Microbiol, 2011. **77**(20): p. 7321-8.

113. Valster, R.M., B.A. Wullings, and D. Van Der Kooij, *Detection of Protozoan Hosts for Legionella pneumophila in Engineered Water Systems by Using a Biofilm Batch Test.* Applied and Environmental Microbiology, 2010. **76**(21): p. 7144-7153.

114. Yamamoto, H., et al., *Factors Stimulating Propagation of Legionellae in Cooling Tower Water.* Applied and Environmental Microbiology, 1992. **58**(4): p. 1394-1397.

115. Zbikowska, E., et al., *Coexistence of Legionella pneumophila Bacteria and Free-Living Amoebae in Lakes Serving as a Cooling System of a Power Plant.* Water Air Soil Pollut, 2014. **225**: p. 2066.

116. Zbikowska, E., M. Walczak, and A. Krawiec, *Distribution of Legionella pneumophila bacteria and Naegleria and Hartmannella amoebae in thermal saline baths used in balneotherapy.* Parasitol Res, 2013. **112**(1): p. 77-83.

117. O'Connor, T.J., et al., *Minimization of the Legionella pneumophila genome reveals chromosomal regions involved in host range expansion.* Proceedings of the National Academy of Sciences, 2011. **108**(36): p. 14733-14740.

118. Robertson, P., H. Abdelhady, and R.A. Garduã±O, *The many forms of a pleomorphic bacterial pathogenâ€"the developmental network of Legionella pneumophila.* 2014. **5**.

119. Abdelhady, H. and R.A. Garduno, *The progeny of Legionella pneumophila in human macrophages shows unique developmental traits.* FEMS Microbiol Lett, 2013. **349**(2): p. 99-107.

120. Cazalet, C., et al., *Evidence in the Legionella pneumophila genome for exploitation of host cell functions and high genome plasticity.* Nat Genet, 2004. **36**(11): p. 1165-73.

121. Chien, M., et al., *The genomic sequence of the accidental pathogen Legionella pneumophila.* Science, 2004. **305**(5692): p. 1966-8.

122. Faucher, S.P., C.A. Mueller, and H.A. Shuman, *Legionella Pneumophila Transcriptome during Intracellular Multiplication in Human Macrophages.* Front Microbiol, 2011. **2**: p. 60.

123. Bruggemann, H., et al., *Virulence strategies for infecting phagocytes deduced from the in vivo transcriptional program of Legionella pneumophila.* Cell Microbiol, 2006. **8**(8): p. 1228-40.

124. Hovel-Miner, G., et al., *SigmaS controls multiple pathways associated with intracellular multiplication of Legionella pneumophila.* J Bacteriol, 2009. **191**(8): p. 2461-73.

125. McDade, J.E., et al., *Legionnaires' disease: isolation of a bacterium and demonstration of its role in other respiratory disease.* N Engl J Med, 1977. **297**(22): p. 1197-203.

126. Rodgers, F.G., A.D. Macrae, and M.J. Lewis, *Electron microscopy of the organism of Legionnaires' disease.* Nature, 1978. **272**(5656): p. 825-6.

127. Al-Bana, B.H., M.T. Haddad, and R.A. Garduno, *Stationary phase and mature infectious forms of Legionella pneumophila produce distinct viable but non-culturable cells.* Environ Microbiol, 2014. **16**(2): p. 382-95.

128. Byrne, B. and M.S. Swanson, *Expression of Legionella pneumophila Virulence Traits in Response to Growth Conditions.* Infection and Immunity, 1998. **66**(7): p. 3029-3034.

129. Garduno, R.A., et al., *Intracellular Growth of Legionella pneumophila Gives Rise to a Differentiated Form Dissimilar to Stationary-Phase Forms.* 2002. **70**(11): p. 6273-6283.

130. Ohno, A., et al., *Factors influencing survival of Legionella pneumophila serotype 1 in hot spring water and tap water.* Appl Environ Microbiol, 2003. **69**(5): p. 2540-7.

131. Piao, Z., et al., *Temperature-regulated formation of mycelial mat-like biofilms by Legionella pneumophila.* Appl Environ Microbiol, 2006. **72**(2): p. 1613-22.

132. Sauer, J.D., M.A. Bachman, and M.S. Swanson, *The phagosomal transporter A couples threonine acquisition to differentiation and replication of Legionella pneumophila in macrophages.* Proc Natl Acad Sci U S A, 2005. **102**(28): p. 9924-9.

133. Steinert, M., et al., *Resuscitation of viable but nonculturable Legionella pneumophila Philadelphia JR32 by Acanthamoeba castellanii.* Appl Environ Microbiol, 1997. **63**(5): p. 2047-53.

134. Hammerschlag, M.R., *The intracellular life of chlamydiae.* Semin Pediatr Infect Dis, 2002. **13**(4): p. 239-48.

135. Molofsky, A.B. and M.S. Swanson, *Differentiate to thrive: lessons from the Legionella pneumophila life cycle.* Molecular Microbiology, 2004. **53**(1): p. 29-40.

136. Samuel, J.E., K. Kiss, and S. Varghees, *Molecular pathogenesis of Coxiella burnetii in a genomics era.* Ann N Y Acad Sci, 2003. **990**: p. 653-63.

137. Hammer, B.K. and M.S. Swanson, *Co-ordination of legionella pneumophila virulence with entry into stationary phase by ppGpp.* Mol Microbiol, 1999. **33**(4): p. 721-31.

138. Zusman, T., O. Gal-Mor, and G. Segal, *Characterization of a Legionella pneumophila relA insertion mutant and toles of RelA and RpoS in virulence gene expression.* J Bacteriol, 2002. **184**(1): p. 67-75.

139. Potrykus, K. and M. Cashel, *(p)ppGpp: still magical?* Annu Rev Microbiol, 2008. **62**: p. 35-51.

140. Dalebroux, Z.D., R.L. Edwards, and M.S. Swanson, *SpoT governs Legionella pneumophila differentiation in host macrophages.* Mol Microbiol, 2009. **71**(3): p. 640-58.

141. Haugen, S.P., W. Ross, and R.L. Gourse, *Advances in bacterial promoter recognition and its control by factors that do not bind DNA.* Nat Rev Microbiol, 2008. **6**(7): p. 507-19.

142. Jishage, M., et al., *Regulation of sigma factor competition by the alarmone ppGpp.* Genes Dev, 2002. **16**(10): p. 1260-70.

143. Dalebroux, Z.D. and M.S. Swanson, *ppGpp: magic beyond RNA polymerase.* Nat Rev Microbiol, 2012. **10**(3): p. 203-12.

144. Osterberg, S., T. del Peso-Santos, and V. Shingler, *Regulation of alternative sigma factor use.* Annu Rev Microbiol, 2011. **65**: p. 37-55.

145. Bougdour, A., S. Wickner, and S. Gottesman, *Modulating RssB activity: IraP, a novel regulator of sigma(S) stability in Escherichia coli.* Genes Dev, 2006. **20**(7): p. 884-97.

146. Costanzo, A., et al., *ppGpp and DksA likely regulate the activity of the extracytoplasmic stress factor sigmaE in Escherichia coli by both direct and indirect mechanisms.* Mol Microbiol, 2008. **67**(3): p. 619-32.

147. Bachman, M.A. and M.S. Swanson, *RpoS co-operates with other factors to induce Legionella pneumophila virulence in the stationary phase.* Mol Microbiol, 2001. **40**(5): p. 1201-14.

148. Hales, L.M. and H.A. Shuman, *The Legionella pneumophila rpoS gene is required for growth within Acanthamoeba castellanii.* J Bacteriol, 1999. **181**(16): p. 4879-89.

149. Hammer, B.K., E.S. Tateda, and M.S. Swanson, *A two-component regulator induces the transmission phenotype of stationary-phase Legionella pneumophila.* Mol Microbiol, 2002. **44**(1): p. 107-18.

150. Heuner, K. and M. Steinert, *The flagellum of Legionella pneumophila and its link to the expression of the virulent phenotype.* Int J Med Microbiol, 2003. **293**(2-3): p. 133-43.

151. Jacobi, S., R. Schade, and K. Heuner, *Characterization of the Alternative Sigma Factor 54 and the Transcriptional Regulator FleQ of Legionella pneumophila, Which Are Both Involved in the Regulation Cascade of Flagellar Gene Expression.* 2004. **186**(9): p. 2540-2547.

152. Heuner, K., et al., *Influence of the alternative sigma(28) factor on virulence and flagellum expression of Legionella pneumophila.* Infect Immun, 2002. **70**(3): p. 1604-8.

153. Schulz, T., et al., *FliA expression analysis and influence of the regulatory proteins RpoN, FleQ and FliA on virulence and in vivo fitness in Legionella pneumophila.* 2012. **194**(12): p. 977-989.

154. Molofsky, A.B., L.M. Shetron-Rama, and M.S. Swanson, *Components of the Legionella pneumophila flagellar regulon contribute to multiple virulence traits, including lysosome avoidance and macrophage death.* Infect Immun, 2005. **73**(9): p. 5720-34.

155. Gal-Mor, O. and G. Segal, *The Legionella pneumophila GacA homolog (LetA) is involved in the regulation of icm virulence genes and is required for intracellular multiplication in Acanthamoeba castellanii.* Microb Pathog, 2003. **34**(4): p. 187-94.

156. Lynch, D., et al., *The response regulator LetA regulates the stationary-phase stress response in Legionella pneumophila and is required for efficient infection of Acanthamoeba castellanii.* FEMS Microbiol Lett, 2003. **219**(2): p. 241-8.

157. Rasis, M. and G. Segal, *The LetA-RsmYZ-CsrA regulatory cascade, together with RpoS and PmrA, post-transcriptionally regulates stationary phase activation of Legionella pneumophila Icm/Dot effectors.* Mol Microbiol, 2009. **72**(4): p. 995-1010.

158. Sahr, T., et al., *Two small ncRNAs jointly govern virulence and transmission in Legionella pneumophila.* Mol Microbiol, 2009. **72**(3): p. 741-62.

159. Molofsky, A.B. and M.S. Swanson, *Legionella pneumophila CsrA is a pivotal repressor of transmission traits and activator of replication.* Mol Microbiol, 2003. **50**(2): p. 445-61.

160. Nevo, O., et al., *Identification of Legionella pneumophila Effectors Regulated by the LetAS-RsmYZ-CsrA Regulatory Cascade, Many of Which Modulate Vesicular Trafficking.* 2014. **196**(3): p. 681-692.

161. Al-Khodor, S., et al., *The PmrA/PmrB two-component system of Legionella pneumophila is a global regulator required for intracellular replication within macrophages and protozoa.* Infect Immun, 2009. **77**(1): p. 374-86.

162. Altman, E. and G. Segal, *The response regulator CpxR directly regulates expression of several Legionella pneumophila icm/dot components as well as new translocated substrates.* J Bacteriol, 2008. **190**(6): p. 1985-96.

163. Gal-Mor, O. and G. Segal, *Identification of CpxR as a positive regulator of icm and dot virulence genes of Legionella pneumophila.* J Bacteriol, 2003. **185**(16): p. 4908-19.

164. Zusman, T., et al., *The response regulator PmrA is a major regulator of the icm/dot type IV secretion system in Legionella pneumophila and Coxiella burnetii.* Mol Microbiol, 2007. **63**(5): p. 1508-23.

165. Tiaden, A., et al., *The Legionella pneumophila response regulator LqsR promotes host cell interactions as an element of the virulence regulatory network controlled by RpoS and LetA.* Cell Microbiol, 2007. **9**(12): p. 2903-20.

166. Sahr, T., et al., *The Legionella pneumophila genome evolved to accommodate multiple regulatory mechanisms controlled by the CsrA-system.* PLoS Genet, 2017. **13**(2): p. e1006629.

167. Hochstrasser, R. and H. Hilbi, *Intra-Species and Inter-Kingdom Signaling of Legionella pneumophila.* Front Microbiol, 2017. **8**: p. 79.

168. Schell, U., et al., *The alpha-hydroxyketone LAI-1 regulates motility, Lqs-dependent phosphorylation signalling and gene expression of Legionella pneumophila.* Mol Microbiol, 2016. **99**(4): p. 778-93.

169. Jameson-Lee, M., R.A. Garduno, and P.S. Hoffman, *DsbA2 (27 kDa Com1-like protein) of Legionella pneumophila catalyses extracytoplasmic disulphide-bond formation in proteins including the Dot/Icm type IV secretion system.* Mol Microbiol, 2011. **80**(3): p. 835-52.

170. Kpadeh, Z.Z., et al., *Disulfide bond oxidoreductase DsbA2 of Legionella pneumophila exhibits protein disulfide isomerase activity.* J Bacteriol, 2013. **195**(8): p. 1825-33.

171. Morash, M.G., et al., *Reciprocal expression of integration host factor and HU in the developmental cycle and infectivity of Legionella pneumophila.* Appl Environ Microbiol, 2009. **75**(7): p. 1826-37.

172. Pitre, C.A.J., et al., *Regulatory control of temporally expressed integration host factor (IHF) in Legionella pneumophila.* Microbiology, 2013. **159**(Pt 3): p. 475-492.

173. Prashar, A., et al., *Mechanism of invasion of lung epithelial cells by filamentousLegionella pneumophila.* Cellular Microbiology, 2012. **14**(10): p. 1632-1655.

174. Charpentier, X., et al., *Antibiotics and UV radiation induce competence for natural transformation in Legionella pneumophila.* J Bacteriol, 2011. **193**(5): p. 1114-21.

175. Elliott, T.S. and F.G. Rodgers, *Morphological response and growth characteristics of Legionella pneumophila exposed to ampicillin and erythromycin.* J Med Microbiol, 1985. **19**(3): p. 383-90.

176. Smalley, D.L., et al., *Antibiotic-induced filament formation of Legionella pneumophila.* Am J Clin Pathol, 1980. **74**(6): p. 852.

177. Warren, W.J. and R.D. Miller, *Growth of Legionnaires disease bacterium (Legionella pneumophila) in chemically defined medium.* J Clin Microbiol, 1979. **10**(1): p. 50-5.

178. Fettes, P.S., et al., *Overexpresssion of a Legionella pneumophila homologue of the E. coli regulator csrA affects cell size, flagellation, and pigmentation.* Int J Med Microbiol, 2001. **291**(5): p. 353-60.

179. Garduno R.A., C.A., *The Legionella pneumophila Chaperonin 60 and the Art of Keeping Several Moonlighting Jobs*, in *Moonlighting Cell Stress Proteins in Microbial Infections*. 2013, Springer, Dordrecht.

180. Nasrallah, G.K., et al., *Deletion of potD, encoding a putative spermidine-binding protein, results in a complex phenotype in Legionella pneumophila.* Int J Med Microbiol, 2014. **304**(5-6): p. 703-16.

181. Prashar, A., et al., *Filamentous morphology of bacteria delays the timing of phagosome morphogenesis in macrophages.* J Cell Biol, 2013. **203**(6): p. 1081-97.

182. Aderem, A. and D.M. Underhill, *Mechanisms of phagocytosis in macrophages.* Annu Rev Immunol, 1999. **17**: p. 593-623.

183. Conner, S.D. and S.L. Schmid, *Regulated portals of entry into the cell.* Nature, 2003. **422**(6927): p. 37-44.

184. Horwitz, M.A., *Phagocytosis of the legionnaires' disease bacterium (legionella pneumophila) occurs by a novel mechanism: Engulfment within a Pseudopod coil.* 1984. **36**(1): p. 27-33.

185. Bozue, J.A. and W. Johnson, *Interaction of Legionella pneumophila with Acanthamoeba castellanii: uptake by coiling phagocytosis and inhibition of phagosome-lysosome fusion.* Infection and immunity, 1996. **64**(2): p. 668-673.

186. Rechnitzer, C. and J. Blom, *Engulfment of the Philadelphia strain of Legionella pneumophila within pseudopod coils in human phagocytes.* 1989. **97**(1-6): p. 105-114.

187. Watarai, M., et al., *Legionella pneumophila Is Internalized by a Macropinocytotic Uptake Pathway Controlled by the Dot/Icm System and the Mouse Lgn1 Locus✪.* Journal of Experimental Medicine, 2001. **194**(8): p. 1081-1096.

188. Weber, S., M. Wagner, and H. Hilbi, *Live-cell imaging of phosphoinositide dynamics and membrane architecture during Legionella infection.* mBio, 2014. **5**(1): p. e00839-13.

189. Dreyfus, L.A., *Virulence associated ingestion of Legionella pneumophila by HeLa cells.* Microb Pathog, 1987. **3**(1): p. 45-52.

190. McCusker, K.T., et al., *Legionella pneumophila inhibits protein synthesis in Chinese hamster ovary cells.* Infection and Immunity, 1991. **59**(1): p. 240-246.

191. Newton, H.J., et al., *Significant Role for ladC in Initiation of Legionella pneumophila Infection.* 2008. **76**(7): p. 3075-3085.

192. Gibson III, F.C., A.O. Tzianabos, and F.G. Rodgers, *Adherence of Legionella pneumophila to U-937 cells, guinea-pig alveolar macrophages, and MRC-5 cells by a novel, complement-independent binding mechanism.* Canadian Journal of Microbiology, 1994. **40**(10): p. 865-872.

193. Rodgers, F.G. and F.C. Gibson III, *Opsonin-independent adherence and intracellular development of Legionella pneumophila within U-937 cells.* Canadian Journal of Microbiology, 1993. **39**(7): p. 718-722.

194. Weissgerber, P., et al., *Investigation of mechanisms involved in phagocytosis of Legionella pneumophila by human cells.* FEMS Microbiology Letters, 2003. **219**(2): p. 173-179.

195. Reynolds, H.Y. and H.H. Newball, *Analysis of proteins and respiratory cells obtained from human lungs by bronchial lavage.* Journal of Laboratory and Clinical Medicine, 1974. **84**(4): p. 559-573.

196. Khelef, N., H.A. Shuman, and F.R. Maxfield, *Phagocytosis of Wild-Type Legionella pneumophila Occurs through a Wortmannin-Insensitive Pathway.* Infection and Immunity, 2001. **69**(8): p. 5157-5161.

197. Weber, S.S., et al., *Legionella pneumophila Exploits PI(4)P to Anchor Secreted Effector Proteins to the Replicative Vacuole.* PLoS Pathogens, 2006. **2**(5): p. e46.

198. Tachado, S.D., M.M. Samrakandi, and J.D. Cirillo, *Non-Opsonic Phagocytosis of Legionella pneumophila by Macrophages Is Mediated by Phosphatidylinositol 3-Kinase.* PLoS ONE, 2008. **3**(10): p. e3324.

199. Steiner, B., S. Weber, and H. Hilbi, *Formation of the Legionella-containing vacuole: phosphoinositide conversion, GTPase modulation and ER dynamics.* Int J Med Microbiol, 2018. **308**(1): p. 49-57.

200. Tilney, L.G., et al., *How the parasitic bacterium Legionella pneumophila modifies its phagosome and transforms it into rough ER: implications for conversion of plasma membrane to the ER membrane.* J Cell Sci, 2001. **114**(Pt 24): p. 4637-50.

201. Isberg, R.R., T.J. O'Connor, and M. Heidtman, *The Legionella pneumophila replication vacuole: making a cosy niche inside host cells.* Nat Rev Microbiol, 2009. **7**(1): p. 13-24.

202. Hubber, A. and C.R. Roy, *Modulation of Host Cell Function byLegionella pneumophilaType IV Effectors.* Annual Review of Cell and Developmental Biology, 2010. **26**(1): p. 261-283.

203. Charpentier, X., et al., *Chemical Genetics Reveals Bacterial and Host Cell Functions Critical for Type IV Effector Translocation by Legionella pneumophila.* 2009. **5**(7): p. e1000501.

204. Horwitz, M.A., *Characterization of avirulent mutant Legionella pneumophila that survive but do not multiply within human monocytes.* J Exp Med, 1987. **166**(5): p. 1310-28.

205. Marra, A., et al., *Identification of a Legionella pneumophila locus required for intracellular multiplication in human macrophages.* Proc Natl Acad Sci U S A, 1992. **89**(20): p. 9607-11.

206. Berger, K.H. and R.R. Isberg, *Two distinct defects in intracellular growth complemented by a single genetic locus in Legionella pneumophila.* 1993. **7**(1): p. 7-19.

207. Berger, K.H., J.J. Merriam, and R.R. Isberg, *Altered intracellular targeting properties associated with mutations in the Legionella pneumophila dotA gene.* Mol Microbiol, 1994. **14**(4): p. 809-22.

208. Segal, G., M. Purcell, and H.A. Shuman, *Host cell killing and bacterial conjugation require overlapping sets of genes within a 22-kb region of the*

Legionella pneumophila genome. Proc Natl Acad Sci U S A, 1998. **95**(4): p. 1669-74.

209. Sadosky, A.B., L.A. Wiater, and H.A. Shuman, *Identification of Legionella pneumophila genes required for growth within and killing of human macrophages.* Infect Immun, 1993. **61**(12): p. 5361-73.

210. Segal, G. and H.A. Shuman, *Characterization of a new region required for macrophage killing by Legionella pneumophila.* Infect Immun, 1997. **65**(12): p. 5057-66.

211. Andrews, H.L., J.P. Vogel, and R.R. Isberg, *Identification of linked Legionella pneumophila genes essential for intracellular growth and evasion of the endocytic pathway.* Infect Immun, 1998. **66**(3): p. 950-8.

212. Sexton, J.A. and J.P. Vogel, *Type IVB secretion by intracellular pathogens.* Traffic, 2002. **3**(3): p. 178-85.

213. Yerushalmi, G., T. Zusman, and G. Segal, *Additive effect on intracellular growth by Legionella pneumophila Icm/Dot proteins containing a lipobox motif.* Infect Immun, 2005. **73**(11): p. 7578-87.

214. Vincent, C.D., et al., *Identification of the core transmembrane complex of the Legionella Dot/Icm type IV secretion system.* Molecular Microbiology, 2006. **62**(5): p. 1278-1291.

215. Komano, T., et al., *The transfer region of IncI1 plasmid R64: similarities between R64 tra and legionella icm/dot genes.* Mol Microbiol, 2000. **35**(6): p. 1348-59.

216. Vogel, J.P., et al., *Conjugative transfer by the virulence system of Legionella pneumophila.* Science, 1998. **279**(5352): p. 873-6.

217. Ghosal, D., et al., *Molecular architecture, polar targeting and biogenesis of the Legionella Dot/Icm T4SS.* Nature Microbiology, 2019. **4**(7): p. 1173-1182.

218. Jeong, K.C., et al., *Polar delivery of Legionella type IV secretion system substrates is essential for virulence.* Proc Natl Acad Sci U S A, 2017. **114**(30): p. 8077-8082.

219. Dumenil, G., et al., *IcmR-regulated membrane insertion and efflux by the Legionella pneumophila IcmQ protein.* J Biol Chem, 2004. **279**(6): p. 4686-95.

220. Ninio, S., et al., *The Legionella IcmS-IcmW protein complex is important for Dot/Icm-mediated protein translocation.* Mol Microbiol, 2005. **55**(3): p. 912-26.

221. Raychaudhury, S., et al., *Structure and function of interacting IcmR-IcmQ domains from a type IVb secretion system in Legionella pneumophila.* Structure, 2009. **17**(4): p. 590-601.

222. Hsu, F., et al., *Structural basis for substrate recognition by a unique Legionella phosphoinositide phosphatase.* Proc Natl Acad Sci U S A, 2012. **109**(34): p. 13567-72.

223. Newton, H.J., et al., *Molecular pathogenesis of infections caused by Legionella pneumophila.* Clin Microbiol Rev, 2010. **23**(2): p. 274-98.

224. Balla, T., *Phosphoinositides: tiny lipids with giant impact on cell regulation.* Physiol Rev, 2013. **93**(3): p. 1019-137.

225. Nasuhoglu, C., et al., *Nonradioactive analysis of phosphatidylinositides and other anionic phospholipids by anion-exchange high-performance liquid chromatography with suppressed conductivity detection.* Anal Biochem, 2002. **301**(2): p. 243-54.

226. Wenk, M.R., et al., *Phosphoinositide profiling in complex lipid mixtures using electrospray ionization mass spectrometry.* Nat Biotechnol, 2003. **21**(7): p. 813-7.

227. Herman, P.K., et al., *A novel protein kinase homolog essential for protein sorting to the yeast lysosome-like vacuole.* Cell, 1991. **64**(2): p. 425-37.

228. Schu, P.V., et al., *Phosphatidylinositol 3-kinase encoded by yeast VPS34 gene essential for protein sorting.* Science, 1993. **260**(5104): p. 88-91.

229. Simonsen, A., et al., *EEA1 links PI(3)K function to Rab5 regulation of endosome fusion.* Nature, 1998. **394**(6692): p. 494-8.

230. Stenmark, H. and R. Aasland, *FYVE-finger proteins--effectors of an inositol lipid.* J Cell Sci, 1999. **112 (Pt 23)**: p. 4175-83.

231. Katzmann, D.J., et al., *Vps27 recruits ESCRT machinery to endosomes during MVB sorting.* J Cell Biol, 2003. **162**(3): p. 413-23.

232. Mizushima, N. and M. Komatsu, *Autophagy: renovation of cells and tissues.* Cell, 2011. **147**(4): p. 728-41.

233. Blumental-Perry, A., et al., *Phosphatidylinositol 4-phosphate formation at ER exit sites regulates ER export.* Dev Cell, 2006. **11**(5): p. 671-82.

234. De Matteis, M.A., A. Di Campli, and A. Godi, *The role of the phosphoinositides at the Golgi complex.* Biochim Biophys Acta, 2005. **1744**(3): p. 396-405.

235. Toulabi, L., et al., *Identification and structural characterization of a Legionella phosphoinositide phosphatase.* J Biol Chem, 2013. **288**(34): p. 24518-27.

236. Dong, N., et al., *Modulation of membrane phosphoinositide dynamics by the phosphatidylinositide 4-kinase activity of the Legionella LepB effector.* Nat Microbiol, 2016. **2**: p. 16236.

237. Norris, F.A., et al., *SopB, a protein required for virulence of Salmonella dublin, is an inositol phosphate phosphatase.* Proc Natl Acad Sci U S A, 1998. **95**(24): p. 14057-9.

238. Zhu, W., et al., *Comprehensive identification of protein substrates of the Dot/Icm type IV transporter of Legionella pneumophila.* PLoS One, 2011. **6**(3): p. e17638.

239. Luo, Z.Q. and R.R. Isberg, *Multiple substrates of the Legionella pneumophila Dot/Icm system identified by interbacterial protein transfer.* Proc Natl Acad Sci U S A, 2004. **101**(3): p. 841-6.

240. Ragaz, C., et al., *The Legionella pneumophila phosphatidylinositol-4 phosphate-binding type IV substrate SidC recruits endoplasmic reticulum vesicles to a replication-permissive vacuole.* Cell Microbiol, 2008. **10**(12): p. 2416-33.

241. Ingmundson, A., et al., *Legionella pneumophila proteins that regulate Rab1 membrane cycling.* Nature, 2007. **450**(7168): p. 365-9.

242. Machner, M.P. and R.R. Isberg, *A bifunctional bacterial protein links GDI displacement to Rab1 activation.* Science, 2007. **318**(5852): p. 974-7.

243. Murata, T., et al., *The Legionella pneumophila effector protein DrrA is a Rab1 guanine nucleotide-exchange factor.* Nat Cell Biol, 2006. **8**(9): p. 971-7.

244. Schoebel, S., et al., *High-affinity binding of phosphatidylinositol 4-phosphate by Legionella pneumophila DrrA.* EMBO Rep, 2010. **11**(8): p. 598-604.

245. Brombacher, E., et al., *Rab1 guanine nucleotide exchange factor SidM is a major phosphatidylinositol 4-phosphate-binding effector protein of Legionella pneumophila.* J Biol Chem, 2009. **284**(8): p. 4846-56.

246. Neunuebel, M.R., et al., *Legionella pneumophila LidA affects nucleotide binding and activity of the host GTPase Rab1.* J Bacteriol, 2012. **194**(6): p. 1389-400.

247. Schoebel, S., et al., *Protein LidA from Legionella is a Rab GTPase supereffector.* Proc Natl Acad Sci U S A, 2011. **108**(44): p. 17945-50.

248. Finsel, I., et al., *The Legionella effector RidL inhibits retrograde trafficking to promote intracellular replication.* Cell Host Microbe, 2013. **14**(1): p. 38-50.

249. Harding, C.R., et al., *LtpD is a novel Legionella pneumophila effector that binds phosphatidylinositol 3-phosphate and inositol monophosphatase IMPA1.* Infect Immun, 2013. **81**(11): p. 4261-70.

250. Hubber, A., et al., *The machinery at endoplasmic reticulum-plasma membrane contact sites contributes to spatial regulation of multiple Legionella effector proteins.* PLoS Pathog, 2014. **10**(7): p. e1004222.

251. Jank, T., et al., *Domain organization of Legionella effector SetA.* Cell Microbiol, 2012. **14**(6): p. 852-68.

252. Wennerberg, K., K.L. Rossman, and C.J. Der, *The Ras superfamily at a glance.* J Cell Sci, 2005. **118**(Pt 5): p. 843-6.

253. Etienne-Manneville, S. and A. Hall, *Rho GTPases in cell biology.* Nature, 2002. **420**(6916): p. 629-35.

254. Memon, A.R., *The role of ADP-ribosylation factor and SAR1 in vesicular trafficking in plants.* Biochim Biophys Acta, 2004. **1664**(1): p. 9-30.

255. Repasky, G.A., E.J. Chenette, and C.J. Der, *Renewing the conspiracy theory debate: does Raf function alone to mediate Ras oncogenesis?* Trends Cell Biol, 2004. **14**(11): p. 639-47.

256. Zerial, M. and H. McBride, *Rab proteins as membrane organizers.* Nat Rev Mol Cell Biol, 2001. **2**(2): p. 107-17.

257. Vetter, I.R. and A. Wittinghofer, *The guanine nucleotide-binding switch in three dimensions.* Science, 2001. **294**(5545): p. 1299-304.

258. Cherfils, J. and M. Zeghouf, *Regulation of small GTPases by GEFs, GAPs, and GDIs.* Physiol Rev, 2013. **93**(1): p. 269-309.

259. Aktories, K., *Bacterial protein toxins that modify host regulatory GTPases.* Nat Rev Microbiol, 2011. **9**(7): p. 487-98.

260. Hutagalung, A.H. and P.J. Novick, *Role of Rab GTPases in membrane traffic and cell physiology.* Physiol Rev, 2011. **91**(1): p. 119-49.

261. Weis, K., *Regulating access to the genome: nucleocytoplasmic transport throughout the cell cycle.* Cell, 2003. **112**(4): p. 441-51.

262. Nagai, H., et al., *A bacterial guanine nucleotide exchange factor activates ARF on Legionella phagosomes.* Science, 2002. **295**(5555): p. 679-82.

263. Cherfils, J., *Arf GTPases and their effectors: assembling multivalent membrane-binding platforms.* Curr Opin Struct Biol, 2014. **29**: p. 67-76.

264. Kagan, J.C. and C.R. Roy, *Legionella phagosomes intercept vesicular traffic from endoplasmic reticulum exit sites.* Nat Cell Biol, 2002. **4**(12): p. 945-54.

265. Robinson, C.G. and C.R. Roy, *Attachment and fusion of endoplasmic reticulum with vacuoles containing Legionella pneumophila.* Cell Microbiol, 2006. **8**(5): p. 793-805.

266. Del Campo, C.M., et al., *Structural basis for PI(4)P-specific membrane recruitment of the Legionella pneumophila effector DrrA/SidM.* Structure, 2014. **22**(3): p. 397-408.

267. Machner, M.P. and R.R. Isberg, *Targeting of host Rab GTPase function by the intravacuolar pathogen Legionella pneumophila.* Dev Cell, 2006. **11**(1): p. 47-56.

268. Schoebel, S., et al., *RabGDI displacement by DrrA from Legionella is a consequence of its guanine nucleotide exchange activity.* Mol Cell, 2009. **36**(6): p. 1060-72.

269. Hardiman, C.A. and C.R. Roy, *AMPylation is critical for Rab1 localization to vacuoles containing Legionella pneumophila.* mBio, 2014. **5**(1): p. e01035-13.

270. Muller, M.P., et al., *The Legionella effector protein DrrA AMPylates the membrane traffic regulator Rab1b.* Science, 2010. **329**(5994): p. 946-9.

271. Neunuebel, M.R., et al., *De-AMPylation of the small GTPase Rab1 by the pathogen Legionella pneumophila.* Science, 2011. **333**(6041): p. 453-6.

272. Rigden, D.J., *Identification and modelling of a PPM protein phosphatase fold in the Legionella pneumophila deAMPylase SidD.* FEBS Lett, 2011. **585**(17): p. 2749-54.

273. Tan, Y. and Z.Q. Luo, *Legionella pneumophila SidD is a deAMPylase that modifies Rab1.* Nature, 2011. **475**(7357): p. 506-9.

274. Mihai Gazdag, E., et al., *Mechanism of Rab1b deactivation by the Legionella pneumophila GAP LepB.* EMBO Rep, 2013. **14**(2): p. 199-205.

275. Mishra, A.K., et al., *The Legionella pneumophila GTPase activating protein LepB accelerates Rab1 deactivation by a non-canonical hydrolytic mechanism.* J Biol Chem, 2013. **288**(33): p. 24000-11.

276. Campanacci, V., et al., *Structure of the Legionella effector AnkX reveals the mechanism of phosphocholine transfer by the FIC domain.* EMBO J, 2013. **32**(10): p. 1469-77.

277. Goody, P.R., et al., *Reversible phosphocholination of Rab proteins by Legionella pneumophila effector proteins.* EMBO J, 2012. **31**(7): p. 1774-84.

278. Mukherjee, S., et al., *Modulation of Rab GTPase function by a protein phosphocholine transferase.* Nature, 2011. **477**(7362): p. 103-6.

279. Tan, Y., R.J. Arnold, and Z.Q. Luo, *Legionella pneumophila regulates the small GTPase Rab1 activity by reversible phosphorylcholination.* Proc Natl Acad Sci U S A, 2011. **108**(52): p. 21212-7.

280. Gazdag, E.M., et al., *The structure of the N-terminal domain of the Legionella protein SidC.* J Struct Biol, 2014. **186**(1): p. 188-94.

281. Horenkamp, F.A., et al., *Legionella pneumophila subversion of host vesicular transport by SidC effector proteins.* Traffic, 2014. **15**(5): p. 488-99.

282. Hsu, F., et al., *The Legionella effector SidC defines a unique family of ubiquitin ligases important for bacterial phagosomal remodeling.* Proc Natl Acad Sci U S A, 2014. **111**(29): p. 10538-43.

283. Hoffmann, C., et al., *Functional analysis of novel Rab GTPases identified in the proteome of purified Legionella-containing vacuoles from macrophages.* Cell Microbiol, 2014. **16**(7): p. 1034-52.

284. Urwyler, S., et al., *Proteome analysis of Legionella vacuoles purified by magnetic immunoseparation reveals secretory and endosomal GTPases.* Traffic, 2009. **10**(1): p. 76-87.

285. Qiu, J., et al., *Ubiquitination independent of E1 and E2 enzymes by bacterial effectors.* Nature, 2016. **533**(7601): p. 120-4.

286. Qiu, J., et al., *A unique deubiquitinase that deconjugates phosphoribosyl-linked protein ubiquitination.* Cell Res, 2017. **27**(7): p. 865-881.

287. Ku, B., et al., *VipD of Legionella pneumophila targets activated Rab5 and Rab22 to interfere with endosomal trafficking in macrophages.* PLoS Pathog, 2012. **8**(12): p. e1003082.

288. Rothmeier, E., et al., *Activation of Ran GTPase by a Legionella effector promotes microtubule polymerization, pathogen vacuole motility and infection.* PLoS Pathog, 2013. **9**(9): p. e1003598.

289. Hilbi, H., et al., *Beyond Rab GTPases Legionella activates the small GTPase Ran to promote microtubule polymerization, pathogen vacuole motility, and infection.* Small GTPases, 2014. **5**(3): p. 1-6.

290. Hershko, A. and A. Ciechanover, *The ubiquitin system.* Annu Rev Biochem, 1998. **67**: p. 425-79.

291. Komander, D. and M. Rape, *The Ubiquitin Code.* Annual Review of Biochemistry, 2012. **81**(1): p. 203-229.

292. Rytkonen, A. and D.W. Holden, *Bacterial interference of ubiquitination and deubiquitination.* Cell Host Microbe, 2007. **1**(1): p. 13-22.

293. Ye, Y. and M. Rape, *Building ubiquitin chains: E2 enzymes at work.* Nat Rev Mol Cell Biol, 2009. **10**(11): p. 755-64.

294. Wilkinson, K.D., *DUBs at a glance.* J Cell Sci, 2009. **122**(Pt 14): p. 2325-9.

295. Ashida, H., M. Kim, and C. Sasakawa, *Exploitation of the host ubiquitin system by human bacterial pathogens.* Nat Rev Microbiol, 2014. **12**(6): p. 399-413.

296. Lin, Y.H. and M.P. Machner, *Exploitation of the host cell ubiquitin machinery by microbial effector proteins.* J Cell Sci, 2017. **130**(12): p. 1985-1996.

297. Zhou, Y. and Y. Zhu, *Diversity of bacterial manipulation of the host ubiquitin pathways.* Cell Microbiol, 2015. **17**(1): p. 26-34.

298. Dorer, M.S., et al., *RNA interference analysis of Legionella in Drosophila cells: exploitation of early secretory apparatus dynamics.* PLoS Pathog, 2006. **2**(4): p. e34.

299. Bhogaraju, S., et al., *Phosphoribosylation of Ubiquitin Promotes Serine Ubiquitination and Impairs Conventional Ubiquitination.* Cell, 2016. **167**(6): p. 1636-1649 e13.

300. Ensminger, A.W. and R.R. Isberg, *E3 ubiquitin ligase activity and targeting of BAT3 by multiple Legionella pneumophila translocated substrates.* Infect Immun, 2010. **78**(9): p. 3905-19.

301. Gan, N., et al., *Legionella pneumophila inhibits immune signalling via MavC-mediated transglutaminase-induced ubiquitination of UBE2N.* Nat Microbiol, 2019. **4**(1): p. 134-143.

302. Kubori, T., A. Hyakutake, and H. Nagai, *Legionella translocates an E3 ubiquitin ligase that has multiple U-boxes with distinct functions.* Mol Microbiol, 2008. **67**(6): p. 1307-19.

303. Lin, Y.H., et al., *Host Cell-catalyzed S-Palmitoylation Mediates Golgi Targeting of the Legionella Ubiquitin Ligase GobX.* J Biol Chem, 2015. **290**(42): p. 25766-81.

304. Lin, Y.H., et al., *RavN is a member of a previously unrecognized group of Legionella pneumophila E3 ubiquitin ligases.* PLoS Pathog, 2018. **14**(2): p. e1006897.

305. Lomma, M., et al., *The Legionella pneumophila F-box protein Lpp2082 (AnkB) modulates ubiquitination of the host protein parvin B and promotes intracellular replication.* Cellular Microbiology, 2010. **12**(9): p. 1272-1291.

306. Price, C.T., et al., *Molecular mimicry by an F-box effector of Legionella pneumophila hijacks a conserved polyubiquitination machinery within macrophages and protozoa.* PLoS Pathog, 2009. **5**(12): p. e1000704.

307. Sheedlo, M.J., et al., *Structural basis of substrate recognition by a bacterial deubiquitinase important for dynamics of phagosome ubiquitination.* Proc Natl Acad Sci U S A, 2015. **112**(49): p. 15090-5.

308. Urbanus, M.L., et al., *Diverse mechanisms of metaeffector activity in an intracellular bacterial pathogen, Legionella pneumophila.* Mol Syst Biol, 2016. **12**(12): p. 893.

309. Metzger, M.B., et al., *RING-type E3 ligases: master manipulators of E2 ubiquitin-conjugating enzymes and ubiquitination.* Biochim Biophys Acta, 2014. **1843**(1): p. 47-60.

310. Schulman, B.A., et al., *Insights into SCF ubiquitin ligases from the structure of the Skp1–Skp2 complex.* Nature, 2000. **408**(6810): p. 381-386.

311. Hubber, A., T. Kubori, and H. Nagai, *Modulation of the ubiquitination machinery by Legionella.* Curr Top Microbiol Immunol, 2013. **376**: p. 227-47.

312. Desmots, F., et al., *The reaper-binding protein scythe modulates apoptosis and proliferation during mammalian development.* Mol Cell Biol, 2005. **25**(23): p. 10329-37.

313. Desmots, F., et al., *Scythe regulates apoptosis-inducing factor stability during endoplasmic reticulum stress-induced apoptosis.* J Biol Chem, 2008. **283**(6): p. 3264-71.

314. Sasaki, T., et al., *HLA-B-associated transcript 3 (Bat3)/Scythe is essential for p300-mediated acetylation of p53.* Genes Dev, 2007. **21**(7): p. 848-61.

315. Tsukahara, T., et al., *Scythe/BAT3 regulates apoptotic cell death induced by papillomavirus binding factor in human osteosarcoma.* Cancer Sci, 2009. **100**(1): p. 47-53.

316. Zhang, Y., et al., *Distinct roles of two structurally closely related focal adhesion proteins, alpha-parvins and beta-parvins, in regulation of cell morphology and survival.* J Biol Chem, 2004. **279**(40): p. 41695-705.

317. Kubori, T., et al., *Legionella metaeffector exploits host proteasome to temporally regulate cognate effector.* PLoS Pathog, 2010. **6**(12): p. e1001216.

318. Quaile, A.T., et al., *Molecular Characterization of LubX: Functional Divergence of the U-Box Fold by Legionella pneumophila.* Structure, 2015. **23**(8): p. 1459-1469.

319. Luo, X., et al., *Structure of the Legionella Virulence Factor, SidC Reveals a Unique PI(4)P-Specific Binding Domain Essential for Its Targeting to the Bacterial Phagosome.* PLoS Pathog, 2015. **11**(6): p. e1004965.

320. Simon, N.C., K. Aktories, and J.T. Barbieri, *Novel bacterial ADP-ribosylating toxins: structure and function.* Nat Rev Microbiol, 2014. **12**(9): p. 599-611.

321. Kotewicz, K.M., et al., *A Single Legionella Effector Catalyzes a Multistep Ubiquitination Pathway to Rearrange Tubular Endoplasmic Reticulum for Replication.* Cell Host Microbe, 2017. **21**(2): p. 169-181.

322. Puvar, K., et al., *Legionella effector MavC targets the Ube2N~Ub conjugate for noncanonical ubiquitination.* Nat Commun, 2020. **11**(1): p. 2365.

323. Siepmann, T.J., et al., *Protein interactions within the N-end rule ubiquitin ligation pathway.* J Biol Chem, 2003. **278**(11): p. 9448-57.

324. Qiu, J. and Z.Q. Luo, *Hijacking of the Host Ubiquitin Network by Legionella pneumophila.* Front Cell Infect Microbiol, 2017. **7**: p. 487.

325. Liu, Y. and Z.Q. Luo, *The Legionella pneumophila effector SidJ is required for efficient recruitment of endoplasmic reticulum proteins to the bacterial phagosome.* Infect Immun, 2007. **75**(2): p. 592-603.

326. Gao, L.Y. and Y. Abu Kwaik, *Activation of caspase 3 during Legionella pneumophila-induced apoptosis.* Infect Immun, 1999. **67**(9): p. 4886-94.

327. Neumeister, B., et al., *Legionella pneumophila induces apoptosis via the mitochondrial death pathway.* Microbiology, 2002. **148**(Pt 11): p. 3639-3650.

328. Abu-Zant, A., et al., *Anti-apoptotic signalling by the Dot/Icm secretion system of L. pneumophila.* Cell Microbiol, 2007. **9**(1): p. 246-64.

329. Losick, V.P. and R.R. Isberg, *NF-κB translocation prevents host cell death after low-dose challenge byLegionella pneumophila.* The Journal of Experimental Medicine, 2006. **203**(9): p. 2177-2189.

330. Ge, J., et al., *A Legionella type IV effector activates the NF-kappaB pathway by phosphorylating the IkappaB family of inhibitors.* Proc Natl Acad Sci U S A, 2009. **106**(33): p. 13725-30.

331. Bartfeld, S., et al., *Temporal resolution of two-tracked NF-kappaB activation by Legionella pneumophila.* Cell Microbiol, 2009. **11**(11): p. 1638-51.

332. Banga, S., et al., *Legionella pneumophila inhibits macrophage apoptosis by targeting pro-death members of the Bcl2 protein family.* Proc Natl Acad Sci U S A, 2007. **104**(12): p. 5121-6.

333. Laguna, R.K., et al., *A Legionella pneumophila-translocated substrate that is required for growth within macrophages and protection from host cell death.* Proc Natl Acad Sci U S A, 2006. **103**(49): p. 18745-50.

334. Aurell, H., et al., *Legionella pneumophila serogroup 1 strain Paris: endemic distribution throughout France.* J Clin Microbiol, 2003. **41**(7): p. 3320-2.

335. D'Auria, G., et al., *Legionella pneumophila pangenome reveals strain-specific virulence factors.* BMC Genomics, 2010. **11**: p. 181.

336. Glockner, G., et al., *Identification and characterization of a new conjugation/type IVA secretion system (trb/tra) of Legionella pneumophila Corby localized on two mobile genomic islands.* Int J Med Microbiol, 2008. **298**(5-6): p. 411-28.

337. Schroeder, G.N., et al., *Legionella pneumophila strain 130b possesses a unique combination of type IV secretion systems and novel Dot/Icm secretion system effector proteins.* J Bacteriol, 2010. **192**(22): p. 6001-16.

338. Campodonico, E.M., L. Chesnel, and C.R. Roy, *A yeast genetic system for the identification and characterization of substrate proteins transferred into host cells by the Legionella pneumophila Dot/Icm system.* Molecular Microbiology, 2005. **56**(4): p. 918-933.

339. de Felipe, K.S., et al., *Legionella eukaryotic-like type IV substrates interfere with organelle trafficking.* PLoS Pathog, 2008. **4**(8): p. e1000117.

340. O'Brien, K.M., E.L. Lindsay, and V.J. Starai, *The Legionella pneumophila effector protein, LegC7, alters yeast endosomal trafficking.* PLoS One, 2015. **10**(2): p. e0116824.

341. Campodonico, E.M., C.R. Roy, and S. Ninio, *Legionella pneumophila Type IV Effectors YlfA and YlfB Are SNARE-Like Proteins that Form Homo- and Heteromeric Complexes and Enhance the Efficiency of Vacuole Remodeling.* PLoS One, 2016. **11**(7): p. e0159698.

342. Gomez-Valero, L., C. Rusniok, and C. Buchrieser, *Legionella pneumophila: population genetics, phylogeny and genomics.* Infect Genet Evol, 2009. **9**(5): p. 727-39.

343. Lomma, M., et al., *Legionella pneumophila - Host Interactions: Insights Gained from Comparative Genomics and Cell Biology.* Genome Dyn, 2009. **6**: p. 170-186.

344. Shi, X., et al., *Direct targeting of membrane fusion by SNARE mimicry: Convergent evolution of Legionella effectors.* Proc Natl Acad Sci U S A, 2016. **113**(31): p. 8807-12.

345. Delevoye, C., et al., *SNARE protein mimicry by an intracellular bacterium.* PLoS Pathog, 2008. **4**(3): p. e1000022.

346. Ronzone, E. and F. Paumet, *Two coiled-coil domains of Chlamydia trachomatis IncA affect membrane fusion events during infection.* PLoS One, 2013. **8**(7): p. e69769.

347. Fasshauer, D., et al., *Conserved structural features of the synaptic fusion complex: SNARE proteins reclassified as Q- and R-SNAREs.* 1998. **95**(26): p. 15781-15786.

348. Sudhof, T.C. and J.E. Rothman, *Membrane Fusion: Grappling with SNARE and SM Proteins.* Science, 2009. **323**(5913): p. 474-477.

349. Ensminger, A.W., *Legionella pneumophila, armed to the hilt: justifying the largest arsenal of effectors in the bacterial world.* Curr Opin Microbiol, 2016. **29**: p. 74-80.

350. Siggers, K.A. and C.F. Lesser, *The Yeast Saccharomyces cerevisiae: A Versatile Model System for the Identification and Characterization of Bacterial Virulence Proteins.* Cell Host & Microbe, 2008. **4**(1): p. 8-15.

351. Sisko, J.L., et al., *Multifunctional analysis of Chlamydia-specific genes in a yeast expression system.* Mol Microbiol, 2006. **60**(1): p. 51-66.

352. Lesser, C.F. and S.I. Miller, *Expression of microbial virulence proteins in Saccharomyces cerevisiae models mammalian infection.* EMBO J, 2001. **20**(8): p. 1840-9.

353. Slagowski, N.L., et al., *A functional genomic yeast screen to identify pathogenic bacterial proteins.* PLoS Pathog, 2008. **4**(1): p. e9.

354. Matsuda, S., et al., *A cytotoxic type III secretion effector of Vibrio parahaemolyticus targets vacuolar H+-ATPase subunit c and ruptures host cell lysosomes.* PLoS Pathog, 2012. **8**(7): p. e1002803.

355. Arnoldo, A., et al., *Identification of small molecule inhibitors of Pseudomonas aeruginosa exoenzyme S using a yeast phenotypic screen.* PLoS Genet, 2008. **4**(2): p. e1000005.

356. Feyder, S., et al., *Membrane Trafficking in the Yeast Saccharomyces cerevisiae Model.* International Journal of Molecular Sciences, 2015. **16**(1): p. 1509-1525.

357. Barlowe, C.K. and E.A. Miller, *Secretory protein biogenesis and traffic in the early secretory pathway.* Genetics, 2013. **193**(2): p. 383-410.

358. Dancourt, J. and C. Barlowe, *Protein sorting receptors in the early secretory pathway.* Annu Rev Biochem, 2010. **79**: p. 777-802.

359. Belden, W.J. and C. Barlowe, *Distinct roles for the cytoplasmic tail sequences of Emp24p and Erv25p in transport between the endoplasmic reticulum and Golgi complex.* J Biol Chem, 2001. **276**(46): p. 43040-8.

360. Belden, W.J. and C. Barlowe, *Role of Erv29p in collecting soluble secretory proteins into ER-derived transport vesicles.* Science, 2001. **294**(5546): p. 1528-31.

361. Bue, C.A., C.M. Bentivoglio, and C. Barlowe, *Erv26p directs pro-alkaline phosphatase into endoplasmic reticulum-derived coat protein complex II transport vesicles.* Mol Biol Cell, 2006. **17**(11): p. 4780-9.

362. Castillon, A., H. Shen, and E. Huq, *Blue light induces degradation of the negative regulator phytochrome interacting factor 1 to promote photomorphogenic development of Arabidopsis seedlings.* Genetics, 2009. **182**(1): p. 161-71.

363. Miller, E.A., et al., *Multiple cargo binding sites on the COPII subunit Sec24p ensure capture of diverse membrane proteins into transport vesicles.* Cell, 2003. **114**(4): p. 497-509.

364. Powers, J. and C. Barlowe, *Transport of axl2p depends on erv14p, an ER-vesicle protein related to the Drosophila cornichon gene product.* J Cell Biol, 1998. **142**(5): p. 1209-22.

365. Gomez-Navarro, N. and E. Miller, *Protein sorting at the ER–Golgi interface.* Journal of Cell Biology, 2016. **215**(6): p. 769-778.

366. Phan, H.L., et al., *The Saccharomyces cerevisiae APS1 gene encodes a homolog of the small subunit of the mammalian clathrin AP-1 complex: evidence for functional interaction with clathrin at the Golgi complex.* EMBO J, 1994. **13**(7): p. 1706-17.

367. Black, M.W. and H.R. Pelham, *A selective transport route from Golgi to late endosomes that requires the yeast GGA proteins.* J Cell Biol, 2000. **151**(3): p. 587-600.

368. Boman, A.L., et al., *A family of ADP-ribosylation factor effectors that can alter membrane transport through the trans-Golgi.* Mol Biol Cell, 2000. **11**(4): p. 1241-55.

369. Hirst, J., et al., *A family of proteins with gamma-adaptin and VHS domains that facilitate trafficking between the trans-Golgi network and the vacuole/lysosome.* J Cell Biol, 2000. **149**(1): p. 67-80.

370. Duncan, M.C., G. Costaguta, and G.S. Payne, *Yeast epsin-related proteins required for Golgi-endosome traffic define a gamma-adaptin ear-binding motif.* Nat Cell Biol, 2003. **5**(1): p. 77-81.

371. Friant, S., et al., *Ent3p Is a PtdIns(3,5)P2 effector required for protein sorting to the multivesicular body.* Dev Cell, 2003. **5**(3): p. 499-511.

372. Bowers, K. and T.H. Stevens, *Protein transport from the late Golgi to the vacuole in the yeast Saccharomyces cerevisiae.* Biochim Biophys Acta, 2005. **1744**(3): p. 438-54.

373. Lauwers, E., et al., *The ubiquitin code of yeast permease trafficking.* Trends Cell Biol, 2010. **20**(4): p. 196-204.

374. Henne, W.M., N.J. Buchkovich, and S.D. Emr, *The ESCRT pathway.* Dev Cell, 2011. **21**(1): p. 77-91.

375. Cowles, C.R., et al., *Novel Golgi to vacuole delivery pathway in yeast: identification of a sorting determinant and required transport component.* EMBO J, 1997. **16**(10): p. 2769-82.

376. Cowles, C.R., et al., *The AP-3 adaptor complex is essential for cargo-selective transport to the yeast vacuole.* Cell, 1997. **91**(1): p. 109-18.

377. Odorizzi, G., C.R. Cowles, and S.D. Emr, *The AP-3 complex: a coat of many colours.* Trends Cell Biol, 1998. **8**(7): p. 282-8.

378. Guo, W., et al., *The exocyst is an effector for Sec4p, targeting secretory vesicles to sites of exocytosis.* EMBO J, 1999. **18**(4): p. 1071-80.

379. TerBush, D.R., et al., *The Exocyst is a multiprotein complex required for exocytosis in Saccharomyces cerevisiae.* EMBO J, 1996. **15**(23): p. 6483-94.

380. Conibear, E., *Converging views of endocytosis in yeast and mammals.* Curr Opin Cell Biol, 2010. **22**(4): p. 513-8.

381. Madania, A., et al., *The Saccharomyces cerevisiae homologue of human Wiskott-Aldrich syndrome protein Las17p interacts with the Arp2/3 complex.* Mol Biol Cell, 1999. **10**(10): p. 3521-38.

382. Moreau, V., et al., *The Saccharomyces cerevisiae actin-related protein Arp2 is involved in the actin cytoskeleton.* J Cell Biol, 1996. **134**(1): p. 117-32.

383. Munn, A.L., et al., *end5, end6, and end7: mutations that cause actin delocalization and block the internalization step of endocytosis in Saccharomyces cerevisiae.* Mol Biol Cell, 1995. **6**(12): p. 1721-42.

384. Reggiori, F. and D.J. Klionsky, *Autophagic processes in yeast: mechanism, machinery and regulation.* Genetics, 2013. **194**(2): p. 341-61.

385. Titorenko, V.I., et al., *Isolation and characterization of mutants impaired in the selective degradation of peroxisomes in the yeast Hansenula polymorpha.* J Bacteriol, 1995. **177**(2): p. 357-63.

386. Tuttle, D.L., A.S. Lewin, and W.A. Dunn, Jr., *Selective autophagy of peroxisomes in methylotrophic yeasts.* Eur J Cell Biol, 1993. **60**(2): p. 283-90.

387. Muller, O., et al., *Autophagic tubes: vacuolar invaginations involved in lateral membrane sorting and inverse vesicle budding.* J Cell Biol, 2000. **151**(3): p. 519-28.

388. Sattler, T. and A. Mayer, *Cell-free reconstitution of microautophagic vacuole invagination and vesicle formation.* J Cell Biol, 2000. **151**(3): p. 529-38.

389. Reggiori, F., et al., *Early stages of the secretory pathway, but not endosomes, are required for Cvt vesicle and autophagosome assembly in Saccharomyces cerevisiae.* Mol Biol Cell, 2004. **15**(5): p. 2189-204.

390. Oku, M., et al., *Role of Vac8 in formation of the vacuolar sequestering membrane during micropexophagy.* Autophagy, 2006. **2**(4): p. 272-9.

391. Oku, M., et al., *Peroxisome degradation requires catalytically active sterol glucosyltransferase with a GRAM domain.* EMBO J, 2003. **22**(13): p. 3231-41.

392. Sakai, Y., et al., *Peroxisome degradation by microautophagy in Pichia pastoris: identification of specific steps and morphological intermediates.* J Cell Biol, 1998. **141**(3): p. 625-36.

393. Noda, T., K. Suzuki, and Y. Ohsumi, *Yeast autophagosomes: de novo formation of a membrane structure.* Trends Cell Biol, 2002. **12**(5): p. 231-5.

394. Kim, J., et al., *Convergence of multiple autophagy and cytoplasm to vacuole targeting components to a perivacuolar membrane compartment prior to de novo vesicle formation.* J Biol Chem, 2002. **277**(1): p. 763-73.

395. Suzuki, K., et al., *The pre-autophagosomal structure organized by concerted functions of APG genes is essential for autophagosome formation.* EMBO J, 2001. **20**(21): p. 5971-81.

396. Suzuki, K., et al., *Hierarchy of Atg proteins in pre-autophagosomal structure organization.* Genes Cells, 2007. **12**(2): p. 209-18.

397. Geng, J., et al., *Post-Golgi Sec proteins are required for autophagy in Saccharomyces cerevisiae.* Mol Biol Cell, 2010. **21**(13): p. 2257-69.

398. Lynch-Day, M.A., et al., *Trs85 directs a Ypt1 GEF, TRAPPIII, to the phagophore to promote autophagy.* Proc Natl Acad Sci U S A, 2010. **107**(17): p. 7811-6.

399. Mari, M., et al., *An Atg9-containing compartment that functions in the early steps of autophagosome biogenesis.* J Cell Biol, 2010. **190**(6): p. 1005-22.

400. Taylor, R., Jr., et al., *KCS1 deletion in Saccharomyces cerevisiae leads to a defect in translocation of autophagic proteins and reduces autophagosome formation.* Autophagy, 2012. **8**(9): p. 1300-11.

401. van der Vaart, A., J. Griffith, and F. Reggiori, *Exit from the Golgi is required for the expansion of the autophagosomal phagophore in yeast Saccharomyces cerevisiae.* Mol Biol Cell, 2010. **21**(13): p. 2270-84.

402. Wang, K., et al., *Phosphatidylinositol 4-kinases are required for autophagic membrane trafficking.* J Biol Chem, 2012. **287**(45): p. 37964-72.

403. Yen, W.L., et al., *The conserved oligomeric Golgi complex is involved in double-membrane vesicle formation during autophagy.* J Cell Biol, 2010. **188**(1): p. 101-14.

404. Nair, U., et al., *A role for Atg8-PE deconjugation in autophagosome biogenesis.* Autophagy, 2012. **8**(5): p. 780-93.

405. Nakatogawa, H., et al., *Atg4 recycles inappropriately lipidated Atg8 to promote autophagosome biogenesis.* Autophagy, 2012. **8**(2): p. 177-86.

406. Lynch-Day, M.A. and D.J. Klionsky, *The Cvt pathway as a model for selective autophagy.* FEBS Lett, 2010. **584**(7): p. 1359-66.

407. Oda, M.N., et al., *Identification of a cytoplasm to vacuole targeting determinant in aminopeptidase I.* J Cell Biol, 1996. **132**(6): p. 999-1010.

408. Segui-Real, B., M. Martinez, and I.V. Sandoval, *Yeast aminopeptidase I is post-translationally sorted from the cytosol to the vacuole by a mechanism mediated by its bipartite N-terminal extension.* EMBO J, 1995. **14**(22): p. 5476-84.

409. Shintani, T., et al., *Mechanism of cargo selection in the cytoplasm to vacuole targeting pathway.* Dev Cell, 2002. **3**(6): p. 825-37.

410. Stenmark, H., *Rab GTPases as coordinators of vesicle traffic.* Nat Rev Mol Cell Biol, 2009. **10**(8): p. 513-25.

411. Chia, P.Z. and P.A. Gleeson, *Membrane tethering.* F1000Prime Rep, 2014. **6**: p. 74.

412. Wideman, J.G., et al., *The Cell Biology of the Endocytic System from an Evolutionary Perspective.* Cold Spring Harbor Perspectives in Biology, 2014. **6**(4): p. a016998-a016998.

413. Gillingham, A.K. and S. Munro, *Long coiled-coil proteins and membrane traffic.* 2003. **1641**(2-3): p. 71-85.

414. Bröcker, C., S. Engelbrecht-Vandré, and C. Ungermann, *Multisubunit Tethering Complexes and Their Role in Membrane Fusion.* Current Biology, 2010. **20**(21): p. R943-R952.

415. Balderhaar, H.J. and C. Ungermann, *CORVET and HOPS tethering complexes - coordinators of endosome and lysosome fusion.* J Cell Sci, 2013. **126**(Pt 6): p. 1307-16.

416. Peplowska, K., et al., *The CORVET Tethering Complex Interacts with the Yeast Rab5 Homolog Vps21 and Is Involved in Endo-Lysosomal Biogenesis.* 2007. **12**(5): p. 739-750.

417. Seals, D.F., et al., *A Ypt/Rab effector complex containing the Sec1 homolog Vps33p is required for homotypic vacuole fusion.* 2000. **97**(17): p. 9402-9407.

418. Huotari, J. and A. Helenius, *Endosome maturation.* EMBO J, 2011. **30**(17): p. 3481-500.

419. Rieder, S.E. and S.D. Emr, *A Novel RING Finger Protein Complex Essential for a Late Step in Protein Transport to the Yeast Vacuole.* 1997. **8**(11): p. 2307-2327.

420. Yogosawa, S., et al., *Monoubiquitylation of GGA3 by hVPS18 regulates its ubiquitin-binding ability.* 2006. **350**(1): p. 82-90.

421. Sato, T.K., et al., *Class C Vps protein complex regulates vacuolar SNARE pairing and is required for vesicle docking/fusion.* Mol Cell, 2000. **6**(3): p. 661-71.

422. Lurick, A., et al., *The Habc domain of the SNARE Vam3 interacts with the HOPS tethering complex to facilitate vacuole fusion.* J Biol Chem, 2015. **290**(9): p. 5405-13.

423. Baker, R.W., et al., *A direct role for the Sec1/Munc18-family protein Vps33 as a template for SNARE assembly.* Science, 2015. **349**(6252): p. 1111-4.

424. Kramer, L. and C. Ungermann, *HOPS drives vacuole fusion by binding the vacuolar SNARE complex and the Vam7 PX domain via two distinct sites.* Mol Biol Cell, 2011. **22**(14): p. 2601-11.

425. Lobingier, B.T. and A.J. Merz, *Sec1/Munc18 protein Vps33 binds to SNARE domains and the quaternary SNARE complex.* Mol Biol Cell, 2012. **23**(23): p. 4611-22.

426. Stroupe, C., et al., *Purification of active HOPS complex reveals its affinities for phosphoinositides and the SNARE Vam7p.* EMBO J, 2006. **25**(8): p. 1579-89.

427. Zick, M. and W. Wickner, *The tethering complex HOPS catalyzes assembly of the soluble SNARE Vam7 into fusogenic trans-SNARE complexes.* Mol Biol Cell, 2013. **24**(23): p. 3746-53.

428. Starai, V.J., C.M. Hickey, and W. Wickner, *HOPS proofreads the trans-SNARE complex for yeast vacuole fusion.* Mol Biol Cell, 2008. **19**(6): p. 2500-8.

429. Hong, W., *SNAREs and traffic.* Biochim Biophys Acta, 2005. **1744**(2): p. 120-44.

430. Hanson, P.I., et al., *Structure and conformational changes in NSF and its membrane receptor complexes visualized by quick-freeze/deep-etch electron microscopy.* Cell, 1997. **90**(3): p. 523-35.

431. Weber, T., et al., *SNAREpins: Minimal Machinery for Membrane Fusion.* Cell, 1998. **92**(6): p. 759-772.

432. Dulubova, I., et al., *Convergence and divergence in the mechanism of SNARE binding by Sec1/Munc18-like proteins.* Proc Natl Acad Sci U S A, 2003. **100**(1): p. 32-7.

433. Misura, K.M., R.H. Scheller, and W.I. Weis, *Three-dimensional structure of the neuronal-Sec1-syntaxin 1a complex.* Nature, 2000. **404**(6776): p. 355-62.

434. Dulubova, I., et al., *How Tlg2p/syntaxin 16 'snares' Vps45.* EMBO J, 2002. **21**(14): p. 3620-31.

435. Yamaguchi, T., et al., *Sly1 binds to Golgi and ER syntaxins via a conserved N-terminal peptide motif.* Dev Cell, 2002. **2**(3): p. 295-305.

436. Mayer, A., W. Wickner, and A. Haas, *Sec18p (NSF)-driven release of Sec17p (alpha-SNAP) can precede docking and fusion of yeast vacuoles.* Cell, 1996. **85**(1): p. 83-94.

437. Sollner, T., et al., *A protein assembly-disassembly pathway in vitro that may correspond to sequential steps of synaptic vesicle docking, activation, and fusion.* Cell, 1993. **75**(3): p. 409-18.

438. Burri, L. and T. Lithgow, *A complete set of SNAREs in yeast.* Traffic, 2004. **5**(1): p. 45-52.

439. Sato, K. and A. Nakano, *Emp47p and Its Close Homolog Emp46p Have a Tyrosine-containing Endoplasmic Reticulum Exit Signal and Function in Glycoprotein Secretion in Saccharomyces cerevisiae.* Molecular Biology of the Cell, 2002. **13**(7): p. 2518-2532.

440. Margulis, N.G., et al., *Analysis of COPII Vesicles Indicates a Role for the Emp47-Ssp120 Complex in Transport of Cell Surface Glycoproteins.* Traffic, 2016. **17**(3): p. 191-210.

441. Sato, K., *Oligomerization of a Cargo Receptor Directs Protein Sorting into COPII-coated Transport Vesicles.* 2003. **14**(7): p. 3055-3063.

442. Babu, M., et al., *Interaction landscape of membrane-protein complexes in Saccharomyces cerevisiae.* Nature, 2012. **489**(7417): p. 585-9.

443. Sidhu, R.S., S. Mathewes, and A.P. Bollon, *Selection of secretory protein-encoding genes by fusion with PHO5 in Saccharomyces cerevisiae.* Gene, 1991. **107**(1): p. 111-8.

444. Zhang, B., et al., *Bleeding due to disruption of a cargo-specific ER-to-Golgi transport complex.* Nat Genet, 2003. **34**(2): p. 220-5.

445. Zhang, B., *Recent developments in the understanding of the combined deficiency of FV and FVIII.* Br J Haematol, 2009. **145**(1): p. 15-23.

446. Nyfeler, B., et al., *Cargo selectivity of the ERGIC-53/MCFD2 transport receptor complex.* Traffic, 2006. **7**(11): p. 1473-81.

447. Kamiya, Y., et al., *Molecular basis of sugar recognition by the human L-type lectins ERGIC-53, VIPL, and VIP36.* J Biol Chem, 2008. **283**(4): p. 1857-61.

448. Nishio, M., et al., *Structural basis for the cooperative interplay between the two causative gene products of combined factor V and factor VIII deficiency.* Proc Natl Acad Sci U S A, 2010. **107**(9): p. 4034-9.

449. Satoh, T., et al., *Structural basis for disparate sugar-binding specificities in the homologous cargo receptors ERGIC-53 and VIP36.* PLoS One, 2014. **9**(2): p. e87963.

450. Fields, B.S., et al., *Comparison of guinea pig and protozoan models for determining virulence of Legionella species.* Infect Immun, 1986. **53**(3): p. 553-9.

451. Fliermans, C.B., et al., *Ecological distribution of Legionella pneumophila.* Appl Environ Microbiol, 1981. **41**(1): p. 9-16.

452. Bozue, J.A. and W. Johnson, *Interaction of Legionella pneumophila with Acanthamoeba castellanii: uptake by coiling phagocytosis and inhibition of phagosome-lysosome fusion.* Infect Immun, 1996. **64**(2): p. 668-73.

453. Centers for Disease Control and Prevention, *National Notifiable Diseases Surveillance System, 2017 Annual Tables of Infectious Disease Data*. 2018, CDC Division of Health Informatics and Surveillance, 2018: Atlanta, GA.

454. Hubber, A. and C.R. Roy, *Modulation of host cell function by Legionella pneumophila type IV effectors.* Annu Rev Cell Dev Biol, 2010. **26**: p. 261-83.

455. Shohdy, N., et al., *Pathogen effector protein screening in yeast identifies Legionella factors that interfere with membrane trafficking.* Proc Natl Acad Sci U S A, 2005. **102**(13): p. 4866-71.

456. Choy, A., et al., *The Legionella effector RavZ inhibits host autophagy through irreversible Atg8 deconjugation.* Science, 2012. **338**(6110): p. 1072-6.

457. Franco, I.S., N. Shohdy, and H.A. Shuman, *The Legionella pneumophila effector VipA is an actin nucleator that alters host cell organelle trafficking.* PLoS pathogens, 2012. **8**(2): p. e1002546-e1002546.

458. Bennett, T.L., et al., *LegC3, an effector protein from Legionella pneumophila, inhibits homotypic yeast vacuole fusion in vivo and in vitro.* PLoS One, 2013. **8**(2): p. e56798.

459. Campodonico, E.M., L. Chesnel, and C.R. Roy, *A yeast genetic system for the identification and characterization of substrate proteins transferred into host cells by the Legionella pneumophila Dot/Icm system.* Mol Microbiol, 2005. **56**(4): p. 918-33.

460. Jahn, R. and R.H. Scheller, *SNAREs--engines for membrane fusion.* Nat Rev Mol Cell Biol, 2006. **7**(9): p. 631-43.

461. Prinz, W.A., et al., *Mutants affecting the structure of the cortical endoplasmic reticulum in Saccharomyces cerevisiae.* J Cell Biol, 2000. **150**(3): p. 461-74.

462. Losev, E., et al., *Golgi maturation visualized in living yeast.* Nature, 2006. **441**(7096): p. 1002-6.

463. Markgraf, D.F., et al., *The CORVET subunit Vps8 cooperates with the Rab5 homolog Vps21 to induce clustering of late endosomal compartments.* Mol Biol Cell, 2009. **20**(24): p. 5276-89.

464. Peplowska, K., et al., *The CORVET tethering complex interacts with the yeast Rab5 homolog Vps21 and is involved in endo-lysosomal biogenesis.* Dev Cell, 2007. **12**(5): p. 739-50.

465. Price, A., et al., *The docking stage of yeast vacuole fusion requires the transfer of proteins from a cis-SNARE complex to a Rab/Ypt protein.* J Cell Biol, 2000. **148**(6): p. 1231-8.

466. Seals, D.F., et al., *A Ypt/Rab effector complex containing the Sec1 homolog Vps33p is required for homotypic vacuole fusion.* Proc Natl Acad Sci U S A, 2000. **97**(17): p. 9402-7.

467. Wurmser, A.E., T.K. Sato, and S.D. Emr, *New component of the vacuolar class C-Vps complex couples nucleotide exchange on the Ypt7 GTPase to SNARE-dependent docking and fusion.* J Cell Biol, 2000. **151**(3): p. 551-62.

468. Arlt, H., et al., *Spatiotemporal dynamics of membrane remodeling and fusion proteins during endocytic transport.* Mol Biol Cell, 2015. **26**(7): p. 1357-70.

469. Matsuura, A., et al., *Apg1p, a novel protein kinase required for the autophagic process in Saccharomyces cerevisiae.* Gene, 1997. **192**(2): p. 245-50.

470. Straub, M., M. Bredschneider, and M. Thumm, *AUT3, a serine/threonine kinase gene, is essential for autophagocytosis in Saccharomyces cerevisiae.* J Bacteriol, 1997. **179**(12): p. 3875-83.

471. Merksamer, P.I., A. Trusina, and F.R. Papa, *Real-time redox measurements during endoplasmic reticulum stress reveal interlinked protein folding functions.* Cell, 2008. **135**(5): p. 933-47.

472. Bulleid, N.J., *Disulfide bond formation in the mammalian endoplasmic reticulum.* Cold Spring Harb Perspect Biol, 2012. **4**(11).

473. Smoyer, C.J., et al., *Analysis of membrane proteins localizing to the inner nuclear envelope in living cells.* J Cell Biol, 2016. **215**(4): p. 575-590.

474. Johnson, L.M., V.A. Bankaitis, and S.D. Emr, *Distinct sequence determinants direct intracellular sorting and modification of a yeast vacuolar protease.* Cell, 1987. **48**(5): p. 875-85.

475. Xu, L., et al., *Inhibition of Host Vacuolar H+-ATPase Activity by a Legionella pneumophila Effector.* PLOS Pathogens, 2010. **6**(3): p. e1000822.

476. Garbe, J. and M. Collin, *Bacterial Hydrolysis of Host Glycoproteins – Powerful Protein Modification and Efficient Nutrient Acquisition.* Journal of Innate Immunity, 2012. **4**(2): p. 121-131.

477. Rehman, S., et al., *Structure and functional analysis of the Legionella pneumophila chitinase ChiA reveals a novel mechanism of metal-dependent mucin degradation.* PLOS Pathogens, 2020. **16**(5): p. e1008342.

478. Tytgat, H.L. and S. Lebeer, *The sweet tooth of bacteria: common themes in bacterial glycoconjugates.* Microbiol Mol Biol Rev, 2014. **78**(3): p. 372-417.

479. Giaever, G., et al., *Functional profiling of the Saccharomyces cerevisiae genome.* Nature, 2002. **418**(6896): p. 387-391.

480. Nickerson, D.P., C.L. Brett, and A.J. Merz, *Vps-C complexes: gatekeepers of endolysosomal traffic.* 2009. **21**(4): p. 543-551.

481. Koike, S. and R. Jahn, *SNAREs define targeting specificity of trafficking vesicles by combinatorial interaction with tethering factors.* Nature Communications, 2019. **10**(1).

482. Austin, C.D., et al., *Oxidizing potential of endosomes and lysosomes limits intracellular cleavage of disulfide-based antibody–drug conjugates.* Proceedings of the National Academy of Sciences of the United States of America, 2005. **102**(50): p. 17987-17992.

483. Nevo, O., et al., *Identification of Legionella pneumophila effectors regulated by the LetAS-RsmYZ-CsrA regulatory cascade, many of which modulate vesicular trafficking.* J Bacteriol, 2014. **196**(3): p. 681-92.

484. Lee, S., W.A. Lim, and K.S. Thorn, *Improved blue, green, and red fluorescent protein tagging vectors for S. cerevisiae.* PLoS One, 2013. **8**(7): p. e67902.

485. Ma, H., et al., *Plasmid construction by homologous recombination in yeast.* Gene, 1987. **58**(2-3): p. 201-16.

486. Schindelin, J., et al., *Fiji: an open-source platform for biological-image analysis.* Nat Methods, 2012. **9**(7): p. 676-82.

487. Schneider, C.A., W.S. Rasband, and K.W. Eliceiri, *NIH Image to ImageJ: 25 years of image analysis.* Nat Methods, 2012. **9**(7): p. 671-5.

488. Fasshauer, D., et al., *Conserved structural features of the synaptic fusion complex: SNARE proteins reclassified as Q- and R-SNAREs.* Proc Natl Acad Sci U S A, 1998. **95**(26): p. 15781-6.

489. Flanagan, J.J., I. Mukherjee, and C. Barlowe, *Examination of Sec22 Homodimer Formation and Role in SNARE-dependent Membrane Fusion.* The Journal of biological chemistry, 2015. **290**(17): p. 10657-10666.

490. Mascia, L. and D. Langosch, *Evidence that late-endosomal SNARE multimerization complex is promoted by transmembrane segments.* Biochimica et Biophysica Acta (BBA) - Biomembranes, 2007. **1768**(3): p. 457-466.

491. Roy, R., et al., *Role of the Vam3p Transmembrane Segment in Homodimerization and SNARE Complex Formation.* Biochemistry, 2006. **45**(24): p. 7654-7660.

492. Malhotra, J.D. and R.J. Kaufman, *Endoplasmic Reticulum Stress and Oxidative Stress: A Vicious Cycle or a Double-Edged Sword?* Antioxidants & Redox Signaling, 2007. **9**(12): p. 2277-2294.

493. Thibault, G. and D.T.W. Ng, *The Endoplasmic Reticulum-Associated Degradation Pathways of Budding Yeast.* Cold Spring Harbor Perspectives in Biology, 2012. **4**(12): p. a013193-a013193.

494. Vembar, S.S. and J.L. Brodsky, *One step at a time: endoplasmic reticulum-associated degradation.* Nature Reviews Molecular Cell Biology, 2008. **9**(12): p. 944-957.